Chemistry of Cyclodiphosph(III and V)azane Transition Metal Complexes: Synthesis, Activation with $B(C_6F_5)_3$ and Reactivity Toward Olefins

Kirill V. Axenov

Laboratory of Inorganic Chemistry
Department of Chemistry
Faculty of Science
University of Helsinki
Finland

Academic Dissertation

To be presented with the permission of the Faculty of Science of the University of Helsinki, for public criticism in the auditorium A110 of Chemicum, A.I. Virtasen Aukio 1, on 25th of November, 2005 at 12 noon.

Supervisors

Professor Markku Leskelä
and
Docent Timo Repo
Laboratory of Inorganic Chemistry
Department of Chemistry
University of Helsinki
Finland

Reviewers

Professor Reko Leino
Department of Organic Chemistry
Åbo Akademi University
Finland

Professor Robert Franzén
Department of Chemistry
Institute of Materials Chemistry
Tampere University of Technology
Finland

Opponent

Professor Dr. Hans-Herbert Brintzinger
Department of Chemistry
University of Konstanz
Germany

ISBN 952-91-9640-7 (printed version)
ISBN 952-10-2824-6 (PDF)
http://ethesis.helsinki.fi
Yliopistopaino
Helsinki 2005

Abstract

New diaminocyclodiphosph(III)azanes bearing bulky aryl substituents were prepared and their structures were investigated by NMR methods and X-ray single crystal diffraction studies. The synthesized compounds were used as ligand precursors for the coordination of group 4 metals. The corresponding dichloro Ti, Zr, and Hf complexes were synthesized and, after MAO activation, were used as catalysts in homogeneous ethene polymerization. Depending on the metal and ligand, moderate to high catalytic activities (up to 1×10^4 kg of PE/($mol_{cat}\times h$) were achieved. The complexes were converted into corresponding alkyl (methyl and benzyl) derivatives. The structures of these new alkyl derivatives, amido and chloro group 4 metal complexes based on the bis(amido)cyclodiphosph(III)azane ligand framework were studied by NMR and X-ray single crystal diffraction methods.

As a means to explore the nature of the catalytically active species in ethene polymerization, activation of the alkyl complexes with $B(C_6F_5)_3$ was investigated. ^1H NMR studies showed that $B(C_6F_5)_3$ abstracted one alkyl group from the metal atom, which led to the formation of cationic complexes and corresponding borate counter anions. This finding was supported by X-ray single crystal structural investigations. Depending on the nature of the metal and alkyl group, partial or full alkyl group abstraction was obtained in solid state, which defined the activated complexes as either thight contacted or fully dissociated cation - anion pairs. From ^{31}P NMR measurements it was found that Lewis acidity of the central atom in these cationic species is defined solely by the size and nature of the ligand substitution. The coordinated metal in the cations based on $[(t\text{-BuN})(t\text{-BuNP})]_2^{2-}$ ligand revealed high electropositive character, and after MAO activation the corresponding neutral chloro and alkyl complexes displayed high catalytic activity. Upon $B(C_6F_5)_3$ activation the complexes bearing bulky aryl substituents showed no visible change in the electrophilicity of the central atom and exhibited low or moderate ethene polymerization activity.

With a view to expanding the coordination chemistry of cyclodiphosphazanes, new ligands with chelate phosphoimino groups were prepared and used for the coordination of third row late transition metals. New dichloro Fe, Co, and dibromo Ni bis(imino)cyclodiphosph(V)azanes were synthesized and characterized by elemental analysis and mass spectrometry, and some of them by ^1H, ^{13}C, and ^{31}P NMR. It was found that, upon MAO activation, depending on the coordinated atom, they catalyze, with high activity, homogeneous ethene oligomerization or selective dimerization as well as selective propene dimerization. Mechanistic studies were performed by GC-MS and NMR methods. It was concluded that, in propene dimerization in the case of the Co complexes, 1,2-2,1 propene insertion prevails for the formation of propene dimers. In contrast to the

Co catalysts, in the propene dimerization process provided by Ni catalysts, the two propene insertion pathways (1,2-2,1 and 1,2-1,2) occur with equal probability, which is reflected in the composition of the produced hexene mixtures.

Preface

This work was done in the Laboratory of Inorganic Chemistry, University of Helsinki, Finland between 2000 and 2005. Financial support from University of Helsinki, Academy of Finland, TEKES, and CIMO foundation is gratefully acknowledged.

I would like to show here my deepest gratitude to Professor Markku Leskelä and Docent Timo Repo for their continuous support for my work at their research group and, especially, providing me the opportunity to work in Finland at University of Helsinki. I would also like to thank Docent Timo Repo for a lot of friendly advice and helpful discussions.

I am also grateful to Docent Victor P. Dyadchenko, who taught me how to work in laboratory and make scientific experiments. The working experience and knowledge obtained under his supervision during my undergraduate studies at Moscow State University helped much to perform my PhD work. Special thanks to Dr. Vasily Kotov, who proposed the cyclodiphosph(III)azane chemistry as a subject for my PhD work and helped me in the beginning of work. Docent Galina S. Zaitseva and Dr. Sergey Karlov are also gratefully acknowledged.

I want to thank my friends and coworkers from Catlab. First of all, I would like to express my gratitude to Mr. Antti Pärssinen for his undoubtedly great help to resolve problems and difficulties appeared all time. Also, my warm thanks to Arto Puranen and Pertti Elo ("Padawan") for their friendship and help. I am grateful to all Catlab members, as they always were ready to help and solve appeared questions. In particular, I would like to thank Dr. Pascal Castro, Katariina Yliheikkilä, Mikko Lankinen, Mikko Kalmi, Dr. Petro Lahtinen, Dr. Kristian Lappalainen and Ahlam Siubaouih. Separate thanks to Professor Mohammed Lancini and my coworker Vasilij Kozlov.

I would like to thank Kay Ahonen for her correction of my manuscript language and Sirpa Pirttiperä for help in printing of present book.

I am most thankful to my friends in Russia: Madina and Tanja, and, especially, Elmira and Tolik Lermontov's for their friendship and hospitality.

I would like to express my warm gratitude to my mother for always encouraging and supporting me in all my life. I would like to thank her for everything she has done for me.

Special thanks to the group 4 metals taking part in my work. In particular, I would like to acknowledge Hf and Zr complexes to being cooperative. I would like to show warm gratitude to the phosphorous compounds, NMR and, especially, $B(C_6F_5)_3$. Grateful thanks to the glass equipment which, unexpectedly, was not breaking very often.

Helsinki, November 2005

List of original publications

This thesis is based on the following original publications:

I. Axenov, K. V.; Kotov, V. V; Klinga, M.; Leskelä, M.; Repo, T. ”New Bulky Bis(amino)cyclodiphosph(III)azanes and Their Titanium(IV) Complexes: Synthesis, Structures and Ethene Polymerization Studies” *Eur. J. Inorg. Chem.*, **2004**, 695.

II. Axenov, K. V.; Klinga, M.; Leskelä, M.; Kotov, V. V; Repo, T. ”[Bis(amido)cyclodiphosph(III)azane]dichlorozirconium Complexes for Ethene Polymerization” *Eur. J. Inorg. Chem.*, **2004**, 4702.

III. Axenov, K. V.; Klinga, M.; Leskelä, M.; Repo, T. ”Bis(amido)cyclodiphosph(III)azane Hafnium Complexes and Their Activation by Tris(perfluorophenyl)borane” *Organometallics*, **2005**, *24*, 1336.

IV. Axenov, K. V.; Kilpeläinen, I.; Klinga, M.; Leskelä, M.; Repo, T. ”Ti and Zr Benzyl Complexes Bearing Bulky Bis(amido)cyclodiphosph(III)azanes: Synthesis, Structure, Activation and Ethene Polymerization Studies” *Organometallics*, **2005**, *accepted*.

V. Axenov, K. V.; Leskelä, M.; Repo, T. ” Bis(imino)cyclodiphosph(V)azane Complexes of Late Transition Metals: Efficient Catalyst Precursors for Ethene and Propene Oligomerization and Dimerization” *Journal of Catalysis*, **2005**, *submitted*.

Abbreviations

Ad	1-Adamantyl
BDMA	Benzyldimethylamine
CG (complex)	Constrained geometry (complex)
Cp	Cyclopentadienyl
DBE	Dibutyl ether
DME	Dimethoxyethane
DFT	Density functional theory
Fc	Ferrocenyl
Flu	Fluorenyl
GC	Gas chromatography
GPC	Gel permeation chromatography
HDPE	High density polyethene
i-Bu	Isobutyl
Ind	Indenyl
i-Pr	Isopropyl
LDPE	Low density polyethene
LLDPE	Linear low density polyethene
MAO	Methylaluminoxane
Me	Methyl
Mes	Mesityl
MS	Mass spectrometry
NMR	Nuclear magnetic resonance
Ph	Phenyl
t-Bu	Tertbutyl
THF	Tetrahydofurane
TMS	Trimethylsilyl
ΔH_{dr}	Reaction enthalpy

Table of Contents

1 Introduction

In 1953, Karl Ziegler discovered that the activation of certain transition metal halides with aluminum alkyls leads to the formation of organometallic complexes capable of polymerizing and oligomerizing ethene.[1] About 80 million tons of polyolefins per year were produced worldwide in 2003, 60% of those with Ziegler-Natta catalysts.[2] Number one in plastic production and utilization is polyethene - nearly 64 million tons per year is required for world industry.

Ziegler-Natta catalysts polymerize ethene to highly linear polymers (high density polyethene, HDPE) at room temperature and atmospheric pressure. HDPE exhibits increased hardness, melting point, and chemical resistance compared with LDPE (low density polyethene). Short-chain branching polymers (linear low density polyethene, LLDPE) are now produced by controlled incorporation of higher α-olefins, e.g. 1-hexene, into ethene polymerization.[3]

Depending on the presence or absence of a detectable border between catalyst and substrate phases catalysis is said to be homogeneous or heterogeneous. The classical Ziegler-Natta catalysts are heterogeneous - materials formed by titanium(III) chloride and aluminum alkyls, or by titanium tetrachloride on $MgCl_2$ and triethylaluminum.[1]

A primary advantage of homogeneous catalysts is that high activity and selectivity can usually be achieved under mild conditions.[4] Variation of the steric and electronic properties of homogeneous catalysts makes it possible, after adjustment of the process conditions, to obtain the desired product with high productivity.

The development of the homogeneous olefin polymerization catalysts was initiated by the discovery of Breslow and Newburg[5] and Natta[6] that titanocene derivatives could be activated for ethene polymerization by aluminum alkyls. In 1975, Sinn and Kaminsky observed the enormous and unexpected increase in the polymerization activity of titanocene dichloride complexes when activated with Me_3Al in the presence of a substantial amount of water.[7] The *in situ* formation of methylaluminoxane (MAO) was proposed, and this was supported by its direct synthesis and the activation of titanocenes and zirconocenes with preformed MAO.[8] Polymerization activity was exceedingly high under these conditions. This discovery ushered in the metallocene era. During the last 20 years, tremendous advances have tacken place in the design and application of metallocenes in α-olefin polymerization.[9]

At the same time, nonmetallocene complexes of the early and late transition metals have attracted growing attention as potential catalysts for homogeneous ethene polymerization. First introduced in the 1980s, this part of organometallic chemistry is now under rapid development (about five articles in 1990 and over 120 in 2001). Many organic and organometallic ligands now being exploited in this area: amines, imines, phosphines and many others.[10] The broad expansion in choice means that electronic character, geometry, and steric hindrance of the active center in the catalyst can easily be controlled through rational design of the ligand environment.

Recently, group 4 metal *cis*-bis(*t*-butylamido) complexes bearing cyclodiphosph(III)azane bridge have attracted attention as catalyst precursors for homogeneous ethene polymerization.[11] In these studies, only preliminary ethene polymerization studies were made however, and since only one ligand was tested no insight was gained into the factors defining the catalytic behavior of such complexes.

It is in this context that the present detailed study on ethene polymerization with cyclodiphosph(III and V)azane-based complexes was undertaken. Special attention was paid to factors, affecting the catalytic activity and properties of the product polymers.

2 Scope of Research

Ever since the first synthesis of cyclodiphosphazane in 1894, these compounds containing four member phosphorus-nitrogen ring have been the attractive subjects for scientific investigation. Because of unique combination of the inorganic rigid P-N framework with organic substituents, cyclodiphosphazanes exhibit properties of inorganic as well as organic substances. They have found wide use in different applications as result: from the synthesis of fireproof polymers to their application as ligands in coordination chemistry. Easy synthesis and rigid structure make cyclodiphosphazanes containing amino or imino functions desirable chelating agents for coordination of main group and transition elements, as well as promising ligands for the synthesis of single site olefin polymerization catalysts having metallocene-like structure.

The goal of the work was to exploit the cyclodiphosph(III and V)azane coordination chemistry with early and late transition metals. As the main emphasis in our work it was to investigate the bis(amido)cyclodiphosph(III)azane group 4 metal complexes as catalysts for ethene polymerization, and to study the structure of the activated complex species in order to explain the catalytic behavior of the complexes.

3 Background

The one of the main subjects in the present work are bis(amido)cyclodiphosph(III)azane group 4 metal complexes in ethene polymerization, and the first part of this chapter is describing the application of amido group 4 metal complexes in olefin polymerization. In present studies, the investigations concerning the activation of bis(amido)cyclodiphosph(III)azane complexes with $B(C_6F_5)_3$ have been made, and the second part of this chapter is the literature review about borane and borate activation of the group 4 metal complexes (includes the activation process, structure of the activated species in solution and solid state as well as the activation of the nonmetallocene complexes). To prevent the increase of the size of these thesis over considerable limits, another main topic in the present studies – the oligomerization of olefins with late transition metal complexes was discussed in short overview in the Results and Discussion chapter.

3.1 Nonmetallocene transition metal complexes in ethene polymerization.

3.1.1 Mechanism of the ethene polymerization

Knowledge of the polymerization mechanism is important for good catalyst design and in the search for new catalyst precursors. Kinetic studies and the application of analytical methods can provide fundamental information about the polymerization process.[12a]

The transition metal complexes used for olefin polymerizations are alone catalytically inactive. They are simply catalyst precursors and need activation. One of the best activators is MAO, discovered by Sinn and Kaminsky in 1975.[7] The cocatalyst acts in two important ways: it alkylates the catalyst precursor and it provides the formation of the active species through abstraction of one alkyl group (Scheme 1).[8]

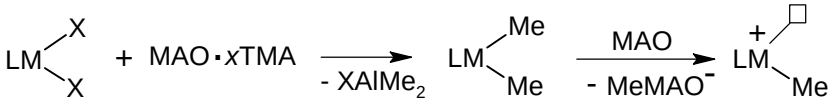

MAO - methylaluminoxane; TMA - Me_3Al

Scheme 1. Activation of complexes by MAO

The bulkiness of the ligand and the chemical nature of the labile groups X at the metal center define the rate of alkylation of the catalyst precursor. Complexes, in which X is amido or, more especially, alkoxy substituent, reveal high resistance in this step and alkylation is often incomplete.[12b,c] The efficiency of the alkyl abstraction is highly depended on the activator and the metal.

The catalytically active cationic species are formed through alkyl group abstraction. They are strong Lewis acids with a vacant site, that can coordinate olefin. The coordinated olefin molecule is inserted into the metal alkyl bond so that structurally similar metal cation with a longer alkyl chain is formed. This cation is able to coordinate the next olefin molecule and propagate the polymer chain and so on (Scheme 2).[13]

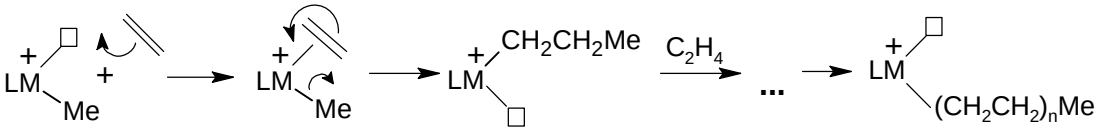

Scheme 2. Propagation step in olefin polymerization

The polymer chain can be terminated by β-hydrogen transfer to monomer or the chain transfer to the aluminum or β-hydrogen elimination may take place.[14] The M-H cation formed as a result of β-hydrogen elimination can be reactivated by olefin insertion into M-H bond (Scheme 3).

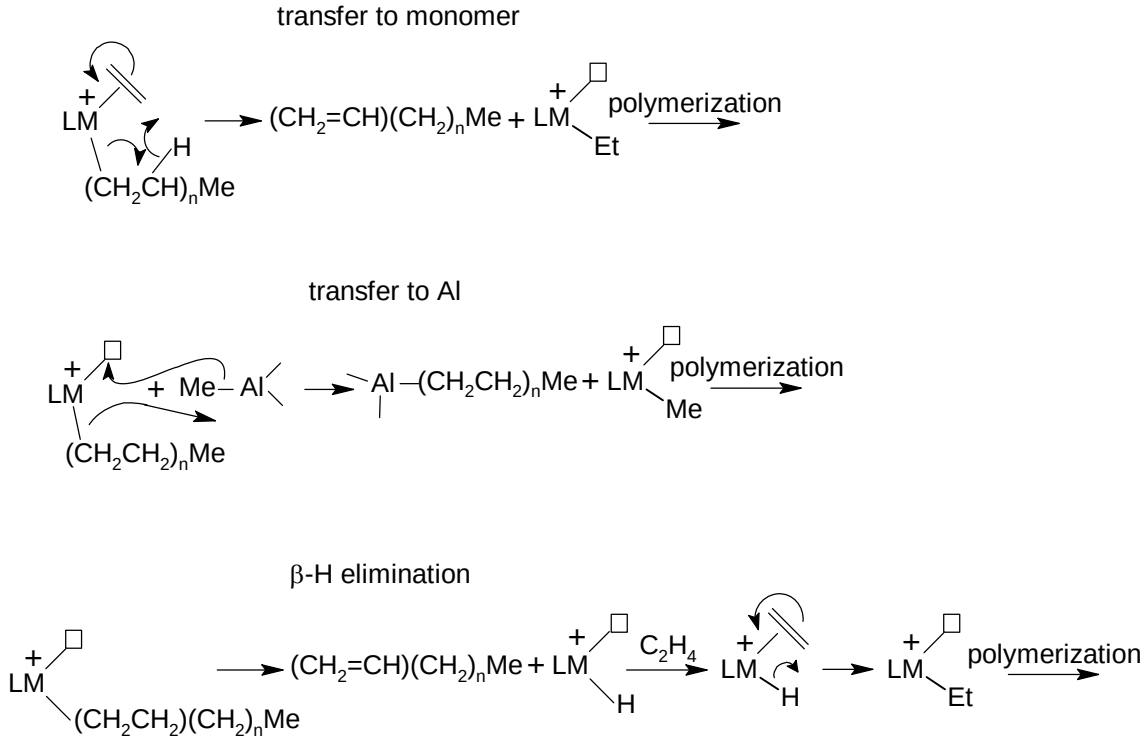

Scheme 3. Termination mechanisms for polymer chain growth

As a consequence of the mechanism of the catalytic ethene polymerization, the complex serving as a catalyst for homogeneous olefin polymerization should fulfill following requirements:

1) There should be at least two labile X groups in *cis*-orientation (halogens and alkyls are preferred), one providing a site for the olefin coordination and the other a site for bonding of the growing polymer chain.
2) The catalytic center should be effectively shielded, with a bulky ligand, from deactivation processes capable of breaking the metal-ligand bond. At the same time the metal center should be open enough to provide fast alkylation and alkyl abstraction.
3) For fast and strong olefin coordination, the metal atom in catalytically active species should have high positive charge. This means that the ligands should not donate too much electron density to the metal and diminish the Lewis acidity of the catalytic center.

3.1.2 Complexes of group 4 metals based on chelate amide ligands

The amido complexes of the group 4 metals have received growing attention in the last 15 years as catalysts for homogeneous Ziegler-Natta olefin polymerization. High electron deficiency on the metal atom in these 12 electron compounds makes them highly electrophilic and therefore potentially active in olefin polymerization.[10] The first highly active chelate bisamido catalysts based on Zr and Ti were reported in 1996 (**1**, Figure 1).[15] Later, analogous Ti alkyl complexes were found to cause living α-olefin polymerization upon $(C_6F_5)_3B$ borane activation.[16] The chain transfer to aluminum was identified as the main form of chain termination in the complex/MAO system. In the absence of aluminum alkyls or MAO, chain termination does not occur, which makes there the α-olefin polymerization living. [17] The substitution at propane bridge (as in compound **2** in Figure 1) led to a drop in the polymerization activity, possibly due to deactivation of the active species by toluene coordination to the cationic metal atom. The multi-site character of the ethene polymerization was supported by the broad molar mass distribution of the resulting polymers.[18] Further modification of the bridge or nitrogen substituents did not lead to an increase in polymerization activity but allowed fine tuning of the properties of the polyethene.[19] Only low catalytic activity was observed for ethylene and analogous Si-Si or B-B bridged bis(amido)complexes (**3**-**5**, Figure 1), although strong dependence on the activation type was evident for Si-Si type catalysts.[20,21,22] Much higher activity (up to 300 kg/(mol×h×bar, triphenylmethylborate as activator) was recorded for Zr complexes containing an electron-rich naphthalene bridge (**6**, Figure 1). Activated with MAO these complexes converted into amido aluminum species, which led to a drop in polymer productivity.[23] The Ti catalysts appeared to be even more active than that Zr analogues (up to 2800 kg/(mol×h×bar).[24] Biphenyl-bridged

bis(amido) Zr catalysts showed low activity in ethene and propene polymerization (**7**, Scheme 4).[25] The first macrocyclic bis(amido) catalyst (**8**, Figure 1) was reported in 1999. Although it exhibited low polymerization activity the product polymers had high (up to 2×10^6 g/mol) molar mass.[26]

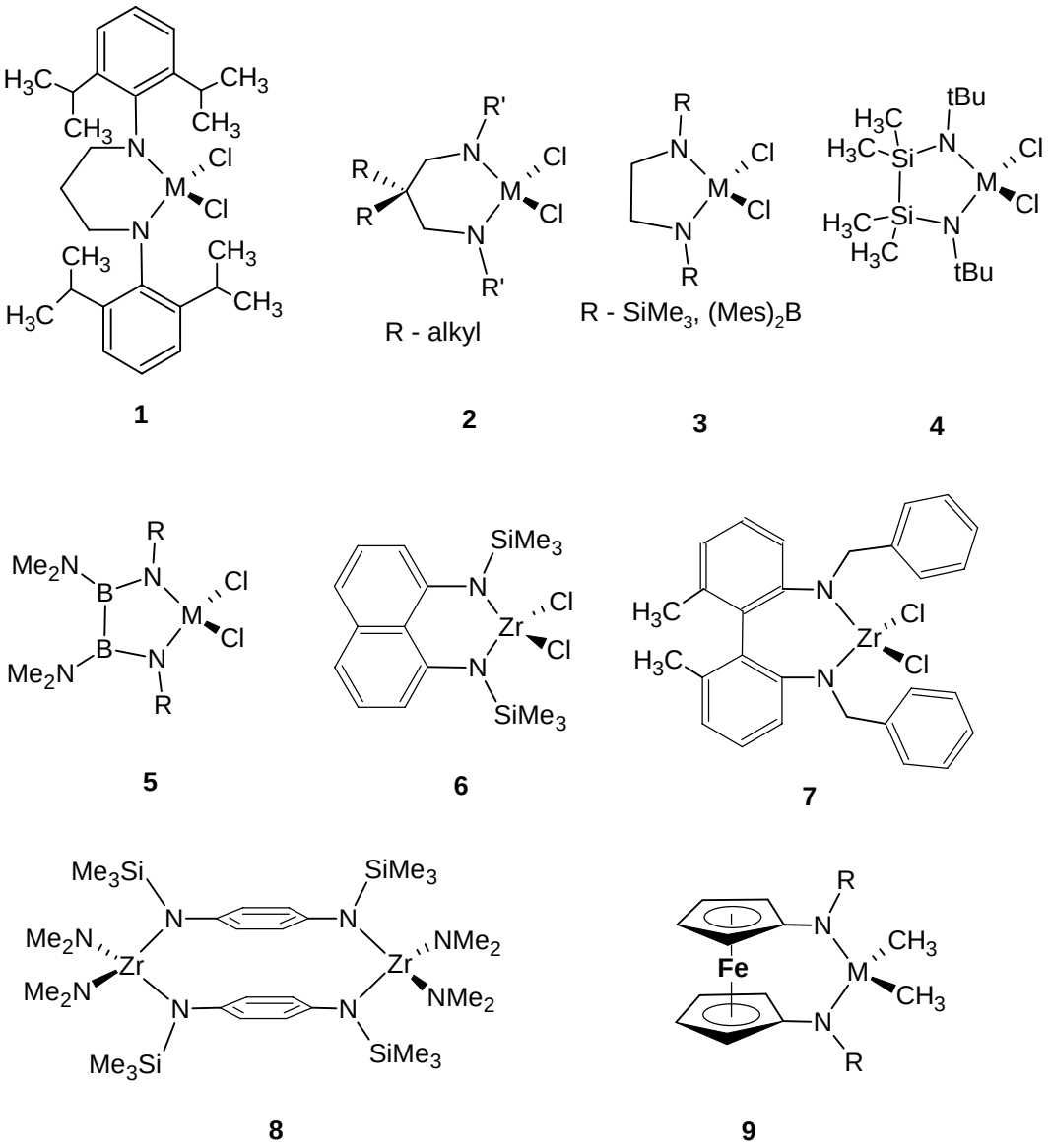

Figure 1. Bis(amido)complexes of group 4 metals that have been studied as catalysts in olefin polymerization

The additional interaction of ferrocenyl bridge with the central metal in complex **9** (Figure 1) probably stabilizes the active species in ethene polymerization, and the polymer productivity of these catalysts reached 100 kg/(mol×h×bar).[27]

Additional ligand-metal coordination can be provided by the introduction of electron-pair donor groups, such as N, O, P, and pyridyl (compounds **10** – **15,** Figure 2). After activation, stabile, four-coordinated cations may be formed and afford improvements in catalytic activity. High productivity

(up to 6000 kg/(mol×h)) was observed for complexes **10** (Figure 2) with pyridine group incorporated into the ligand bridge.[19a,28] Extended Hückel MO calculations showed that the pyridine-diamido ligand system has similar coordination behavior at the Zr atom to Cp_2ZrX_2, which served after activation with MAO as a highly active catalyst for ethene polymerization.[28] The analogous Ti complexes exhibited very low activity in ethene polymerization, probably due to reduction to Ti(III) species by MAO.[29] Replacement of the pyridine group with N, O, S, or P makes the ligand backbone flexible. Such nonrigid complexes adopt two isomeric forms: trigonal (*fac*) and planar (*mer*) (Scheme 4). It is believed that, in solution, they interconvert rapidly and their ratio depends only on the nature of the donor group and the steric influence of amido substituents.[30]

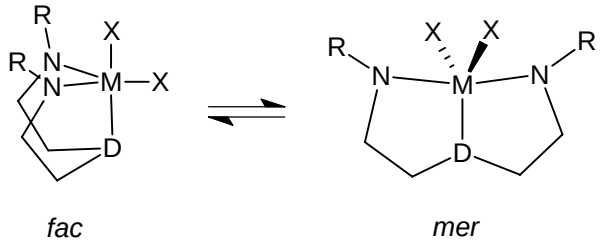

Scheme 4. Isomeric structures of nonrigid bis(amido)complexes having an additional donor group

In 1996, Horton and co-workers[31] showed that incorporation of the amino function into the ligand frame (**11**, D = $NSiMe_3$, R = $SiMe_3$, Figure 2) markedly increases the ethene polymerization activity of the Zr bis(amido) complexes (observed activity was up to 300 kg/(mol×h)). In recent report of the bis(amido)amino Zr complexes with bulky mesityl substituents (**11**, D = NMe, R = Mes) it was established that, in solid state, such compounds have *mer* geometry, but after activation the *fac* configuration dominates, in both solid state and in solution.[32] Sufficient catalytic activity was observed in the 1-hexene polymerization, but the living character of the process was discouraged by the aggregation (dimerization) of the active cationic species and C-H bond activation in the ligand framework.[33] The living character in 1-hexene polymerization can be achieved by the substitution of the mesityls to 2,6-dichlorophenyl groups, but catalytic activity then decreases markedly.[34] The analogous Hf complexes became prone to β-hydrogen elimination.[35]

The Zr complexes with NPyN ligand framework were staggered in *fac* configuration (**12**, Figure 2) and exhibited dramatic "initiator effect" in 1-hexene polymerization.[36] The 1,2 (propagation step) as well as 2,1 hexene insertions followed by β hydrogen elimination were observed.[37] The application of 2,6-dichlorophenyl groups as ligand substituents was detrimental to realizing the living character of the 1-hexene polymerization and improving the catalytic activity.[38] Complexes with different "arms" in the diamido/donor bridge (**11a**, Figure 2) did not provide living 1-hexene polymerization,

and only atactic polyhexenes were obtained.[39] In another approach (**13**, Figure 2), the asymmetric ligands were applied for catalyst synthesis; however, it was concluded that ligand to metal donor-acceptor coordination is then too labile and the introduced ligand asymmetry is insufficient to provide precise stereocontrol of the formed polymer.[40]

Bis(amido)oxo Zr complexes (**11**, D = O, Figure 2) have *mer* geometry in solid state and are active in 1-hexene polymerization.[41] However, the *fac* orientation of the ligand prevails in the similar but inactive Ti derivatives.[30] It was recently shown that isomeric forms are so close in energy that analogous complexes with only small difference in ligand substitution can adopt either *fac* or *mer* configurations.[42] Zr diamido/O-donor complexes with arylated bridge (**14**, Figure 2) were active in ethene polymerization (up to 800 kg/(mol×h)) and polymerized 1-hexene in living fashion.[43] It was proposed that, in solution, such Zr compounds have twisted *fac* geometry, while the geometry of the analogous Ti and Hf complexes is changing rapidly between *fac* and *mer*. *Fac* orientation of the ligand in solution is also preferred for the activated Zr and Hf compounds, but in solid state the ligand framework adopts the *mer* configuration around the Zr cationic center.[44] Use of ligands with restricted geometry (**15**, Scheme 6) did little to improve the catalytic behavior of diamido/O-donor complexes.[45]

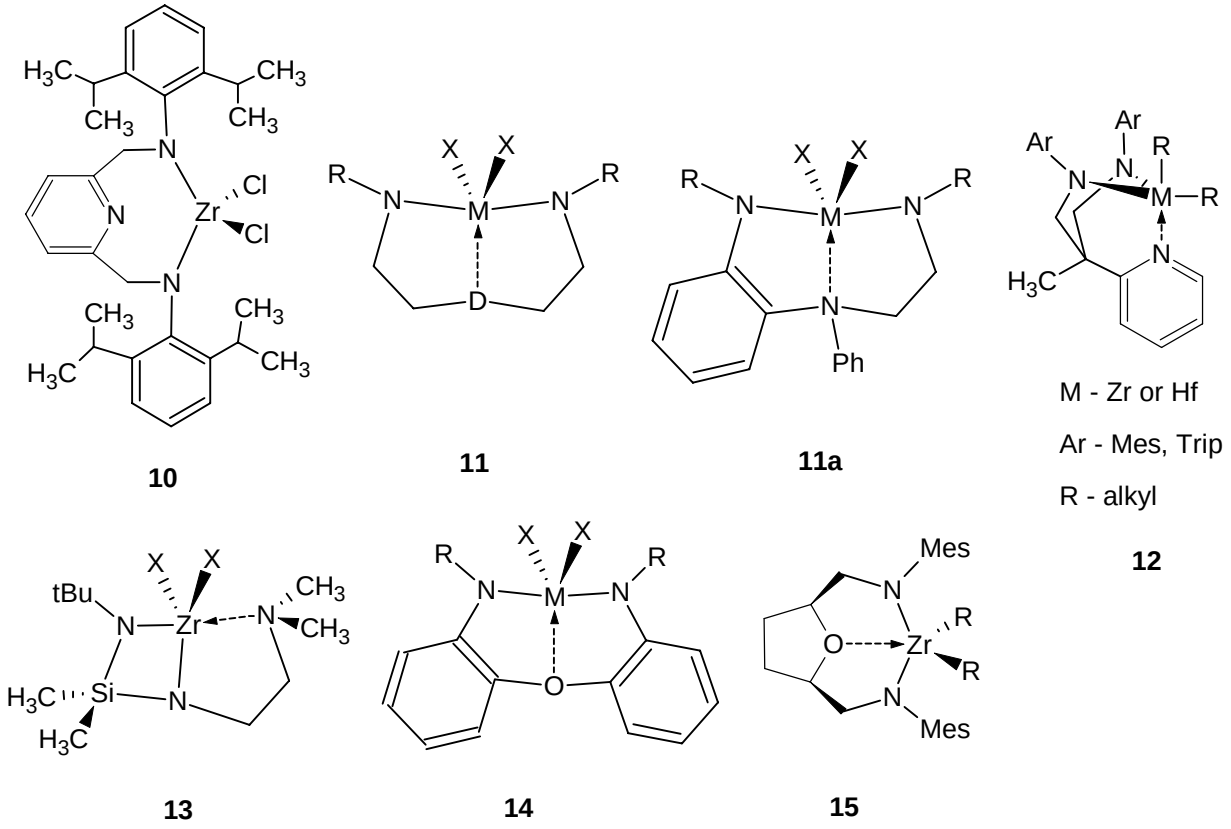

10 **11** **11a** **12** **13** **14** **15**

Figure 2. Bis(amido)complexes of the group 4 metals having an additional donor substituent, used for olefin polymerization

Bis(amido) Zr complexes having $Me_2SiOSiMe_2$ bridge adopt *mer* geometry in solid state and show moderate activity in ethene polymerization (up to 50 kg/(mol×h×bar)).[46] Polymers with high molar mass and modest molar mass distribution (2.8) are produced at low ethene pressure (1 bar).

3.2 Borane and borate activation of catalyst precursors

Ever since that the discovery that MAO-activated group 4 metallocenes display very high olefin polymerization activity, MAO has been the major cocatalyst for metal-catalyzed olefin polymerization. The function of MAO in the activation process is fairly well established and involves alkylation of the catalyst precursor followed by the formation of a cationic metal center by alkyl abstraction.[8] Detailed structural information about catalytically active species can not be obtained, however, due to the complicated and often variable composition of MAO.[47] Application of the single-site borane and borate activators, in turn, provides isolable and characterizable catalytically active species and plentiful data about the nature and structure of the catalytic species.[48]

In the first activation studies performed by Jordan *et al.*, Cp_2ZrMe_2 was reacted with $Ag[PF_6]$ or $Tl[PF_6]$ in acetonitrile, and the reaction led to the cationic $Cp_2ZrMe(MeCN)^+$ $[PF_6]^-$ complex, which is stable in MeCN (Scheme 5). However, this compound decomposed instantaneously in THF or CH_2Cl_2 to $Cp_2Zr(Me)F$ via F^- abstraction from $[PF_6]^-$ anion. Use of the $[BPh_4]^-$ anion provided a more stable cationic $Cp_2ZrMe(THF)^+[BPh_4]^-$ complex.[49] This complex was capable of polymerizing ethene. However, the presence of a donor ligand like THF slowed the polymerization rate dramatically owing to the competition between ethene and THF in coordination to the metal atom.[50]

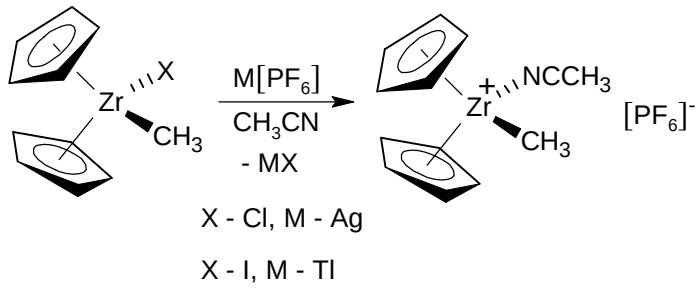

Scheme 5. Synthesis of the first Zr metallocene cationic complex

The benzyl analogue of $Cp_2ZrMe(THF)^+[BPh_4]^-$ showed similar behavior in ethene polymerization.[51] Bulky carborane anions were used to avoid the coordination of additional donor,

and the cationic complexes exhibited high polymerization activity; but also strong cation-anion interaction was observed, indicating the electron deficient character of such cationic complexes.[52]

In 1991 $[B(C_6F_5)_4]^-$ was proposed as an alternative noncoordinating anion. $[HNBu_3]^+[B(C_6F_5)_4]^-$ [53] and $[Ph_3C]^+[B(C_6F_5)_4]^-$ [54] were used to generate the corresponding cationic systems (Scheme 6). These cationic species in toluene exhibited similar catalytic activity and stereospecificity in propene polymerization to the parent neutral complexes after MAO activation.[54]

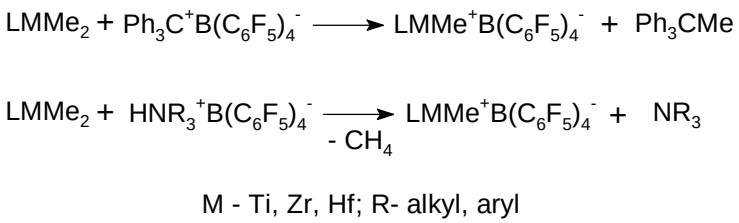

Scheme 6. Activation of the complexes with $[HNR_3]^+[B(C_6F_5)_4]^-$ or $[Ph_3C]^+[B(C_6F_5)_4]^-$

At the same time, a report[55] appeared of the ability of $B(C_6F_5)_3$ to abstract one of the alkyl groups from dialkylsubstituted group 4 metallocenes and produce the similar cationic like complexes (Scheme 7). Recently the abstraction of two Me groups from metal center was successfully achieved.[56]

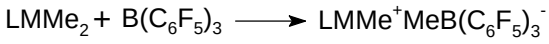

Scheme 7. Activation of the complexes with $B(C_6F_5)_3$

With these species the ethene and propene polymerizations proceeded rapidly under ambient conditions, and linear polymers with Ziegler-Natta mass distribution were obtained.[54,55] Since 1991 the last two methods have been widely used to activate various catalyst precursors: metallocenes, metallocenes with constrained geometry, and nonmetallocene complexes.[48]

3.2.1 Complex activation and ion-pair reorganization processes in solution

It is believed that borane or borate activator abstracts one of the alkyl substituents from the metal center.[48] Detailed studies have been carried out to obtain insight into this reaction. In *in situ* NMR investigations[57] of the reaction between $Me_2Si(Ind)_2MMe_2$ (M – Zr, Hf) and $[Ph_3C]^+[B(C_6F_5)_4]^-$, dimeric μ-Me cationic species were observed (Scheme 8). It was shown that, regardless of the nature of the central atom and ligand framework, such dimeric cations are initially formed in the activation reaction and then converted to the monomeric cationic species.

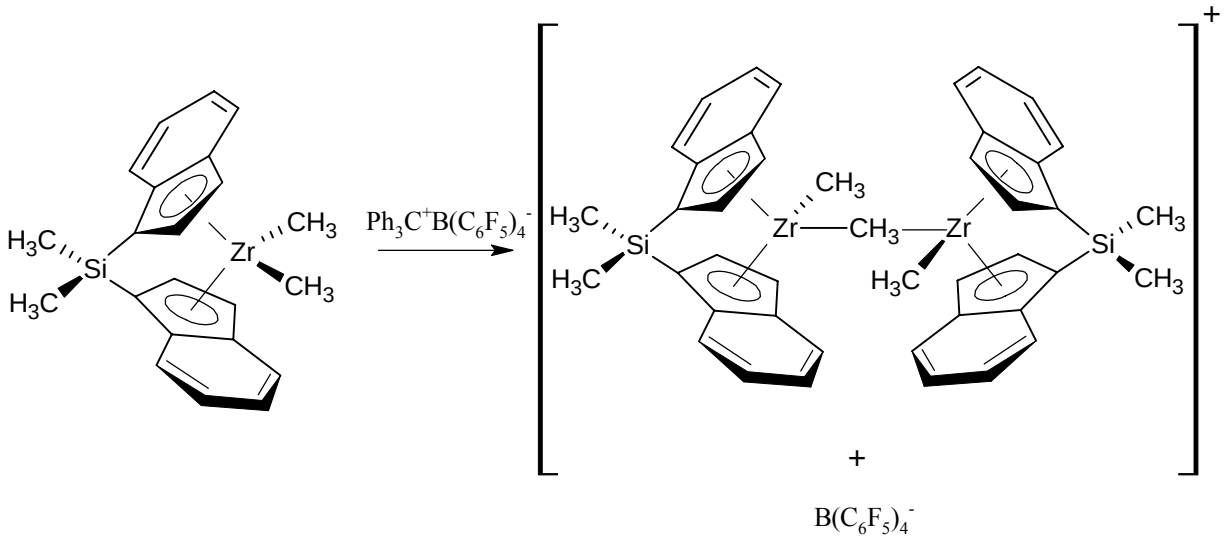

Scheme 8. Formation of dimeric cationic complexes

Depending on the steric bulk of the activator and complex molecules, as well as the solvent and the activator/complex ratio the "monomerization" of these dimeric species may be blocked or slowed down, leaving the dimeric cations as the major species in solution and in solid state.[58] Upon $[Ph_3C]^+[B(C_6F_5)_4]^-$ activation of Zr and Hf bis(amido)complexes with additional donor atoms (**11,** D = NMe, Figure 2), similar dimeric complexes were detected and characterized by NMR, elemental analysis, and X-ray diffractometry (Figure 3).[32] In the case of the bisphenolate complexes, the connection between the metal centers in dimeric cationic complex is realized via μ-O bridges.[59]

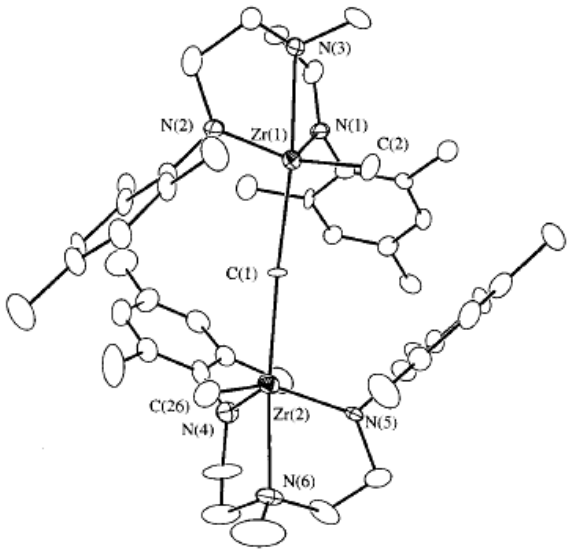

Figure 3. The solid-state structure of the dimeric cationic species from complex **11** (reprinted with permission from *Organometallics,* **2000**, *19*, 5325. Copyright 2000 Am. Chem. Soc.).

The dynamic NMR investigations showed the coexistence of two exchange processes in solution: complex activation/$B(C_6F_5)_3$ dissociation (k_{dr}) and cation-anion symmetrization (k_{ips}, Scheme 9).[60]

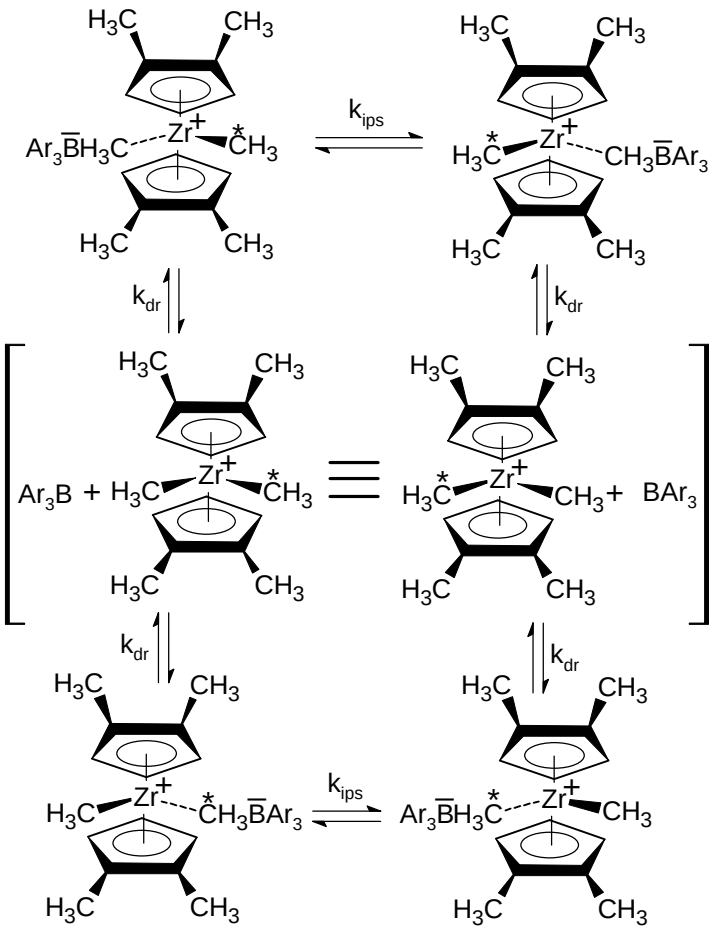

Scheme 9. Exchange processes in the alkyl group 4 metal complex/$B(C_6F_5)_3$ system (reprinted with permission from *J. Am. Chem. Soc.,* **1995**, *117*, 6128. Copyright 1995 Am. Chem. Soc.).

Cation-anion pair dissociation was found to be unimolecular, which was consistent with the rate-limiting $B(C_6F_5)_3$ abstraction followed by fast recombination.[61] As proposed for cation-anion symmetrization, the process proceeded predominantly *via* ionic quadruples or higher order ionic aggregates, and there was no evidence that it occurred *via* dissociative unimolecular reaction paths.[62]

Several Zr and Hf metallocenes were included in the kinetic studies.[60,61] It was discovered that complex activation/$B(C_6F_5)_3$ dissociation (k_{dr}) is much less sensitive to the ancillary coordination environment around the metal center than the cation-anion symmetrization process (k_{ips}). k_{dr} and k_{ips} showed significant sensitivity to the nature of metal.[61] It was also noticed that, in polar solvent, the cation-anion dissociation/reassociation reaction was very much accelerated, probably because of solvent assistance in the ion pair separation process.[62,63] The calorimetric data showed that the complex activation was an exothermic reaction (ΔH_{dr} was from -8.9 for $(Me_2Cp)_2HfMe_2$ to -22.6

kcal/mol for (Cp'$SiMe_2$N*t*-Bu)$TiMe_2$) and the use of high Lewis acidic boron activators was thermodynamically favored. As well the ion-pair reorganization barrier was found to grow in the order Zr<Ti<Hf, but to decrease sharply in the presence of the polar solvent or sterically bulky sized and crowded metal alkyl substituents.[62] In later studies were made of the influence of the complex activation/activator dissociation and mainly cation-anion symmetrization processes on the catalytic activity, chain transfer, and stereoselectivity in single-site olefin polymerization.[64]

The metal center in the cationic species has greater electrophilic character than in the parent dialkyl complexes, and, due to the abstraction of one alkyl group, there is no effective shielding. Such complexes are much more reactive and sensitive to the conditions therefore. The decomposition of the cationic species in solution has been studied and three main reaction pathways have been identified.[48]

As was observed by Marks and co-workers,[60] the 1,3-$(Me_3Si)_2$Cp substituted zirconocene undergoes the decomposition via C_6F_5 group abstraction (Scheme 10).[60]

$$(TMS_2Cp)_2ZrMe^+MeB(C_6F_5)_3^- \longrightarrow (TMS_2Cp)_2ZrMe(C_6F_5) + MeB(C_6F_5)_2$$

$$TMS = SiMe_3$$

Scheme 10. Cationic complex decomposition *via* C_6F_5 group abstraction

With $B(C_6F_4SiMe_3)_4^-$ as a counteranion even relatively stable $[Cp_2ZrMe]^+$ decomposes in the manner shown in the scheme, with formation of $Cp_2ZrMe(C_6F_4SiMe_3)$.[65] The formation of the unusual $(ArNC_3H_6NAr)Ti(C_6F_5)CH_2B(C_6F_5)_2$ was observed in the case of borane activation of the corresponding Ti bis(amido)complex. It was proposed that this is a result of $B(C_6F_5)_3$ addition to the intermediate carbene complex.[66]

Another commonly observed type of decomposition is abstraction of the fluorine atoms from counteranions by complex cations, which results in products having F-M (M = Ti, Zr) bonds.[60] In a few cases the formed $[(L_2ZrX)_2(\mu\text{-}F)]^+$ $[BR_4]^-$ (X = Me or F) were isolated and characterized.[60,65b,67] In the case of $Me_2C(Flu)(Cp)ZrMe_2$ activated with $B(C_6F_5)_3$, the $[Me_2C(Flu)(Cp)Zr(C_6F_5)]_2(\mu\text{-}F)]^+[MeB(C_6F_5)_3]^-$ complex was obtained as a result of the combination of the C_6F_5 group and F abstractions.[58]

Very often the decomposition of the cationic complex involves C-H bond activation of the ligand. This process was first recognized in the generation of 1,3-di-*t*-Bu substituted zirconocene cation (Figure 4),[60] and seems to be fairly common in the activation of CG (constrained geometry)-type[68]

or bis(amido) complexes (Scheme 11).[69] In some systems, C-H activation is facilitated by a nearby metal center[70] or additional chelating groups in the ligand.[71]

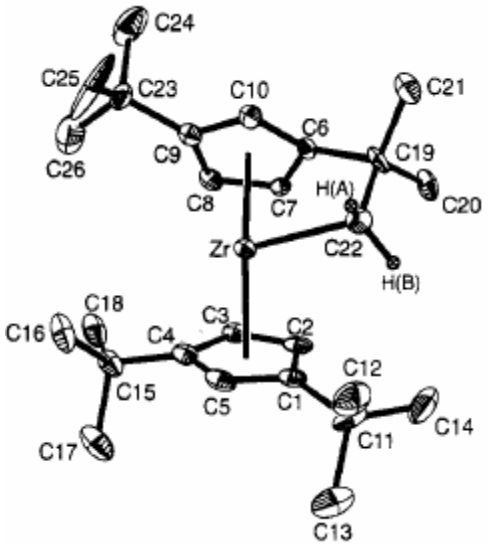

Figure 4. Solid-state structure of the1,3-di- *t*-Bu substituted zirconocene cation after intramolecular C-H activation (reprinted with permission from *J. Am. Chem. Soc.,* **1994**, *116*, 10015. Copyright 1994 Am. Chem. Soc.).

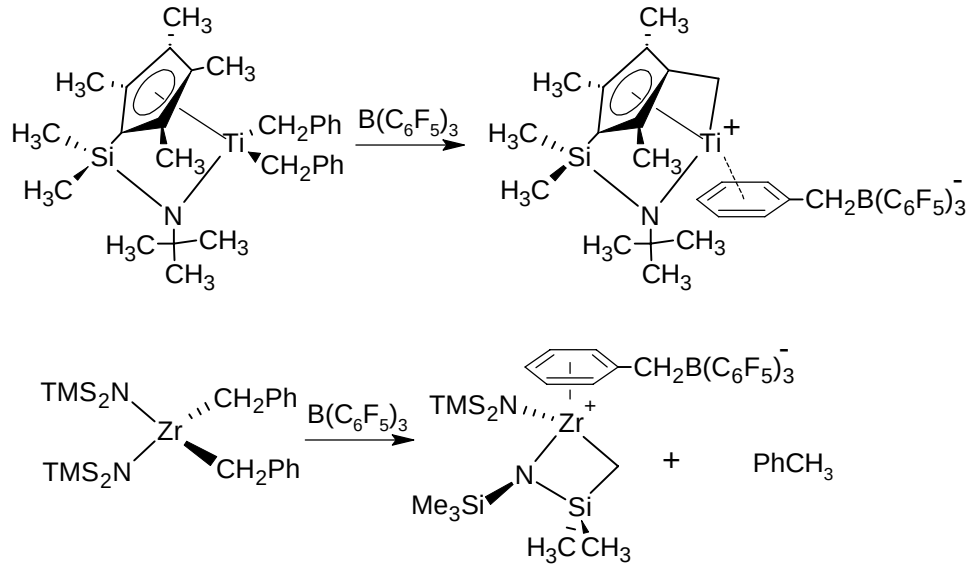

Scheme 11. The C-H activation in cationic CG and nonmetallocene group 4 metal complexes

Intermolecular C-H bond activation was observed upon activation of di(*i*-propyl) Hf NPyN complex by $[PhNHMe_2]^+[B(C_6F_5)_4]^-$ (Scheme 12).[37]

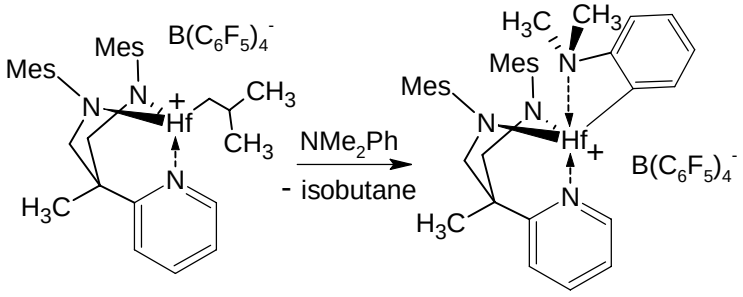

Scheme 12. Intermolecular C-H activation observed for NPyN-type complexes

In halogenated solvents the decomposition of cations often involves the formation of chloro complexes.[48] For example, $[Cl(Fc(NSiMe_3)_2TiCl)_2]^+$ (Fc – ferrocene) was isolated from the reaction of $Fc(NSiMe_3)_2TiMe_2$ with $B(C_6F_5)_3$ in CD_2Cl_2.[72]

In the reaction of $B(C_6F_5)_3$ with a Me_3SiCH_2-substituted CpTi alkoxy complex, methyl abstraction from the Me_3SiCH_2 group was observed instead of generation of the corresponding Ti cation (Scheme 13).[73]

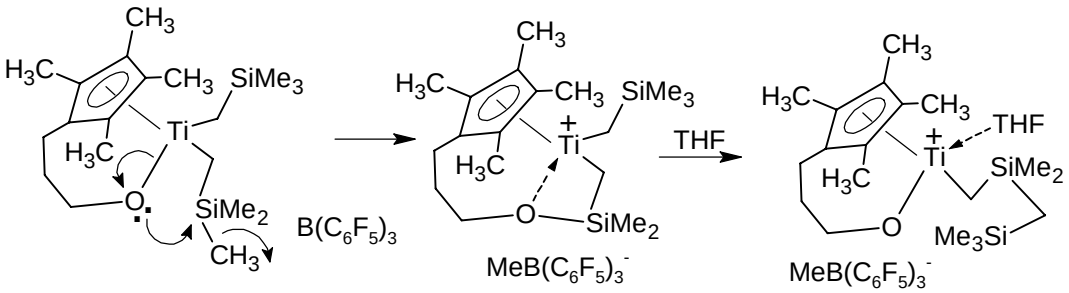

Scheme13. Activation of CpTi alkoxy complex

3.2.2 Structure of cationic complexes in solution and solid state

NMR spectroscopy is an important tool for investigating the structure of activated complexes in solution; in particular the character of the cation-anion coordination can be studied.[48] In practice, the activation is often carried out *in situ* in the NMR tube. ^1H and ^{13}C NMR were successfully applied by Bochmann *et al.*[74] to the structural study of $[Cp_2TiMe]^+BPh_4^-$ in solution. Five possible structures were suggested (A-E, Figure 5). From ^1H and ^{13}C NMR data (nonequivalence of cyclopentadienyl protons, absence of recognizable M-H agostic interactions, and bonding between metal center and BPh_4^- or amine ligands), they concluded that the Ti cation was pseudotetrahedral in solution and was stabilized by solvent coordination (Structure E, Figure 5). Analogous Zr complexes revealed the η^3 Zr-$PhBPh_3^-$ coordination (structure D, Figure 5).[75]

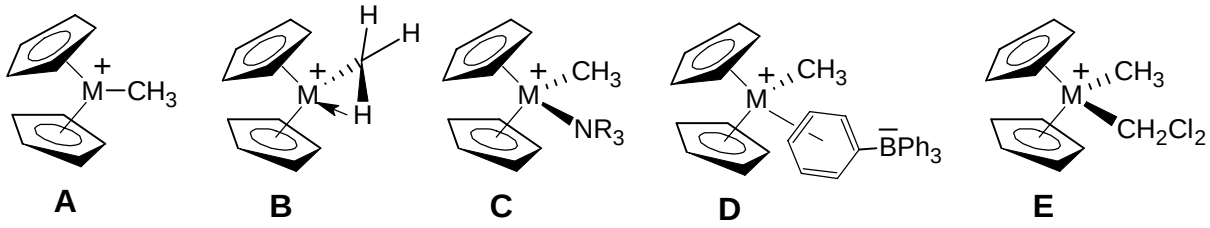

Figure 5. Possible structures of activated metallocene complex in dichloromethane solution

In ^{1}H and ^{13}C NMR spectra of zirconocenes activated with $B(C_6F_5)_3$, Marks and co-workers[60] found the broad MeB group and low-field (^{13}C NMR) Zr-Me (indicating the cation like character) signals. On the basis of ^{19}F NMR measurements, they concluded that in $MeB(C_6F_5)_3^-$ derived ion pairs the cation-anion coordination "is largely through Zr^+-Me-B^- contact". They and others detected direct metal-fluorine interactions between the cations and $B(C_6F_5)_4^-$, $B(C_6F_4i\text{-}Pr_3Si)_4^-$or $B(C_6F_4Bu_3Si)_4^-$.[60,61,67] Comparison of ^{19}F NMR spectra of ion pairs and the corresponding pure borate anions from their salts allowed a describtion of their relative cation coordination abilities.[60] It was found that $B(C_6F_5)_4^-$ is a much more "noncoordinating" anion than $MeB(C_6F_5)_3^-$.

As was mentioned above, owing to high electrophilicity the complex cations were also able to coordinate with solvent molecules or donor ligands, which freed the counteranion from the cation. One particular but important case is the interaction of the cationic species with aromatic solvents, which are widely used media in homogeneous olefin polymerization. The strong coordination of η^6-toluene to positively charged Zr(IV) was first observed in activated $CpZrMe_3$ complexes in 1993.[76] Similar Zr-toluene interactions have been found in "constrained geometry" Zr complex, together with dynamic cation symmetrization process, above 80 °C.[65b] Brintzinger *et al.*[77] investigated anion/added ligand exchange reaction with a set of hard and soft donors for various zirconocene cations. As was expected, the coordination ability of the donor ligands decreased with increasing steric bulk and decreasing basicity of the Lewis base. It was shown that the $MeB(C_6F_5)_3^-$/BDMA or DBE (BDMA = benzyldimethylamine, DBE = dibutyl ether) displacements were first-order reactions for zirconocene as well as for Lewis bases (Eq 1), while pseudo-first-order rate constants were obtained for Si-bridged complexes and N,N-dimethylaniline.[77]

$$v = k[Zr][BDMA] \qquad \text{(Equation 1)}$$

DFT (PM3-tm) calculations identified the pentacoordinated zirconocene species as a intermediates or transition states for the anion/donor ligand exchange reaction.[77]

Several coordination modes between cation and anion can be observed in solid state, varying with the metal, activator and ligand. The first solid-state structure of a metallocene activated by $B(C_6F_5)_3$ was presented in 1991 (Figure 6).[55]

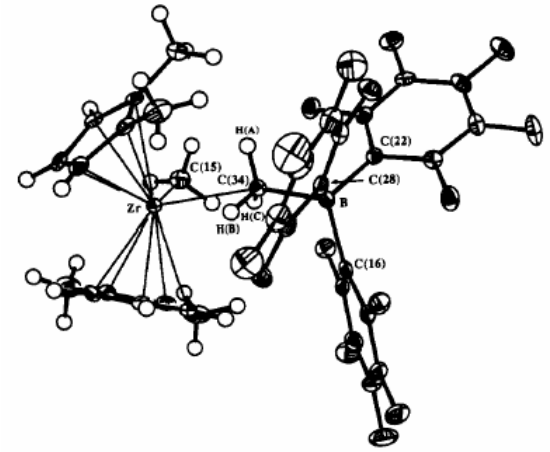

Figure 6. Solid-state structure of the 1,2-*t*-Bu_2Cp substituted zirconocene cation (reprinted with permission from *J. Am. Chem. Soc.,* **1991**, *113*, 3623. Copyright 1991 Am. Chem. Soc.).

The overall geometry of the metallocene moiety resembles the structure of the parent complex, but the marked difference between the two Zr-Me bond lengths (Zr-Me(terminal) 2.252(4) Å *vs.* Zr-Me(bridged) 2.549 (3) Å) shows that the methyl group abstraction by $B(C_6F_5)_3$ is really taking place. This is further supported by the tetrahedral configuration of the boron atom and short B-Me(bridged) distance (1.663(5) Å).[55] In the obtained cationic structures, the electrophilicity of the central atom has a noticeable influence on the lengths of the Me(bridged)-B, Zr-Me(terminal) and Zr-Me(bridged) bonds. It is believed that anion-cation coordination is provided "principally through the hydrogen atoms of the bridging group".[60]

A second cation-anion coordination mode is illustrated by the metal-fluorine contacts, which can also be seen in solution (see above). In solid state this interaction has been found in only a few activated complexes, like $Cp_2ZrH^+HB(C_6F_5)_3^-$.[60] The structure of cationic thorium complex (Figure 7) is another example of such coordination between metal and $MeB(C_6F_5)_3^-$ anion. The Th-F distances in this compound are 2.675(5) Å and 2.757(4) Å, which are quite short tough still longer than sums of the Th^{4+} and F^- ionic radii.[78]

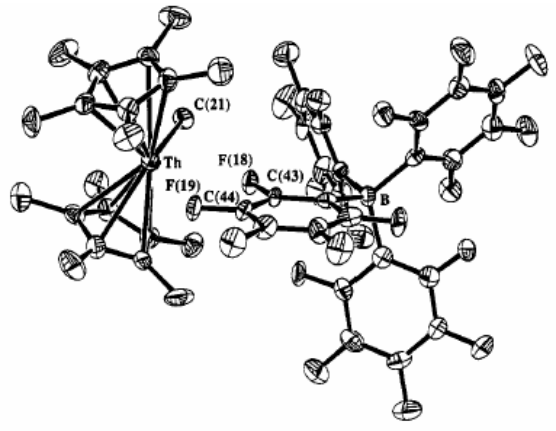

Figure 7. Solid-state structure of the decamethylthorocene cation- $MeB(C_6F_5)_3^-$ anion pair bonded *via* Th-F interactions (reprinted with permission from *Organometallics,* **1991**, *10*, 840. Copyright 1991 Am. Chem. Soc.).

As in solution, the additional coordination of the solvent molecule or the donor ligand to the cationic center has been observed in solid state. Such contacts were already ascertained in the first solved solid-state structures of the activated complexes. For example, the cationic Zr metallocene crystallized from THF had a solvent molecule coordinated to the Zr atom (Figure 8) with Zr-O bond length 2.122(14) Å showing tight Zr-THF coordination.[50]

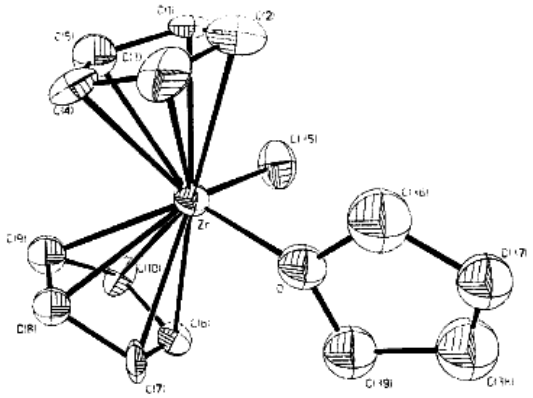

Figure 8. Solid state structure of the $Cp_2ZrMe(THF)^+$ cation (reprinted with permission from *J. Am. Chem. Soc.,* **1986**, *108*, 7410. Copyright 1986 Am. Chem. Soc.).

Relatively stable Hf cationic arene complexes were obtained in the presence of toluene the and investigated in solid state (Figure 9).[76b,c] The complex geometry and similarity of the Hf-Cp and Hf-arene distances (approx. 2.480 Å *vs.* 2.669-2.689 Å) established the η^6-toluene coordination.[76c]

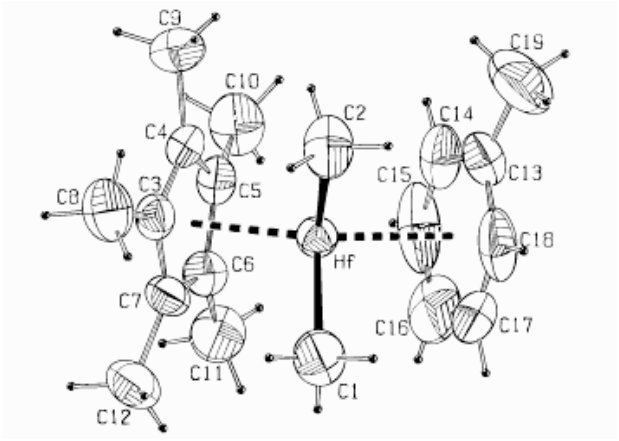

Figure 9. Solid state structure of the $CpZrMe_2(\eta^6\text{-toluene})^+$ cation (reprinted with permission from *Organometallics,* **1996**, *15*, 3600. Copyright 1996 Am. Chem. Soc.).

Another structural feature of the cationic complexes having additional ligand in solution and solid state is that the donor molecule forces the counteranion out from the internal coordination sphere.[77]

The cationic benzyl species have a more diverse structural chemistry than their methyl substituted analogues owing to the presence of the electron-rich phenyl ring, which can also interact with positively charged metal center. The first benzyl cationic complex was isolated and characterized by Jordan *et al.*[51a] (Scheme 14). In solid state the benzyl group was bonded to Zr in η^2 fashion through methylene carbon and *ipso* carbon atom (Zr-C bond lengths 2.344(8) and 2.648(6) Å, respectively). The significant up field shift of the *ortho* protons in ^{1}H NMR and the signals of the methylene and *ipso* carbons in ^{13}C NMR indicated that this structure was maintained in solution. The BPh_4^- anion was shifted to outer coordination sphere by acetonitrile coordination.[51]

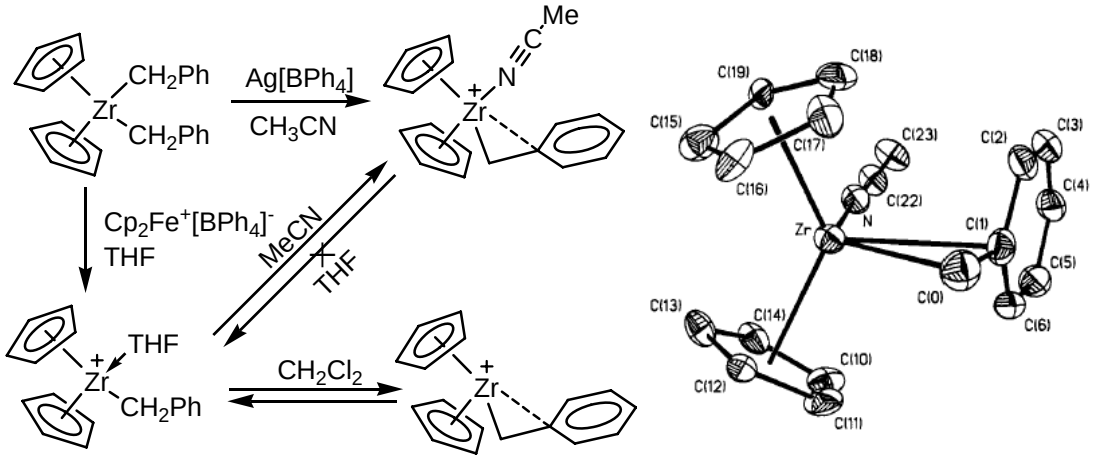

Scheme 14. Synthesis of the benzyl zirconocene cationic complex, the solid state structure was reprinted with permission from *J. Am. Chem. Soc.,* **1987**, *109*, 4111. Copyright 1987 Am. Chem. Soc.

Later the activation of $(PhCH_2)_4Zr$ by $B(C_6F_5)_3$ was studied.[79] ^1H and ^{13}C NMR measurements showed that, in solution, the cationic complex had one η^2-benzyl substituent (and two η^1- $PhCH_2$ groups) and was strongly coordinated with $PhCH_2B(C_6F_5)_3^-$ counteranion *via* the benzyl group. Solid-state data supported these results. The $PhCH_2B(C_6F_5)_3^-$ anion was bonded with Zr atom in η^6-fashion, and also η^2-benzyl-Zr coordination was present (Figure 10).[79]

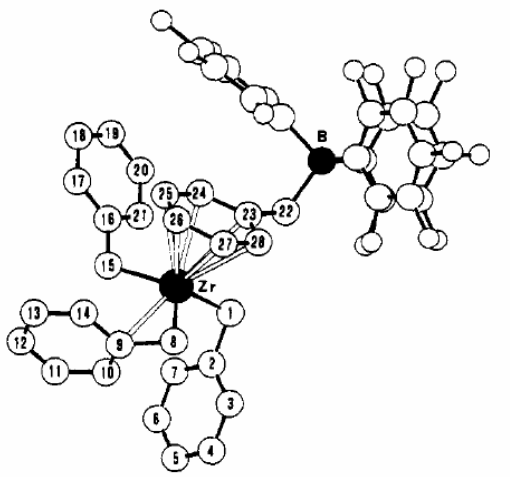

Figure 10. Solid-state structure of $Zr(CH_2Ph)_4$ activated with $B(C_6F_5)_3$ (reprinted with permission from *J. Am. Chem. Soc.,* **1993**, *115*, 1160. Copyright 1993 Am. Chem. Soc.).

In activation studies of the benzyl complexes it was concluded that η^2-coordination to the metal center of the remaining benzyl group and the cation-anion interactions through a multihapto arene bridge are common in solution.[51b,76a] Unusual solid-state structures were obtained for activated mono Cp-substituted benzyl Zr complexes. In the case of $[(C_5H_5)Zr(CH_2Ph)_2]^+[PhCH_2B(C_6F_5)_3]^-$, the absence of η^2-bonded CH_2Ph and the presence of "η^5"(idealized η^6)-$PhCH_2B(C_6F_5)_3^-$ coordination of the anion to the Zr atom were found, which indicates lower unsaturation of the cation than in $[Zr(CH_2Ph)_3]^+[PhCH_2B(C_6F_5)_3]^-$.[80] In solid state, the related $[(C_5Me_5)Zr(CH_2Ph)_2]^+[PhCH_2B(C_6F_5)_3]^-$ complex consisted of discrete ions without noticeable cation-anion interactions. The highly electrophilic Zr cation was bonded with two remaining benzyl groups which behaved as η^7 and η^3 ligands (Figure 11). MO calculations showed that the η^3 benzyl group interacted with Zr mainly through methylene carbon atom and, to a lesser extent, trough *ipso* and one of the *ortho* carbon atoms; in the η^7 ligands, all carbon atoms were participating in bonding to the same extent. The likely driving force for the observed benzyl group arrangements was the relieving of the electron deficiency of Zr, resulting in the formation of a formally 18-electron complex.[81]

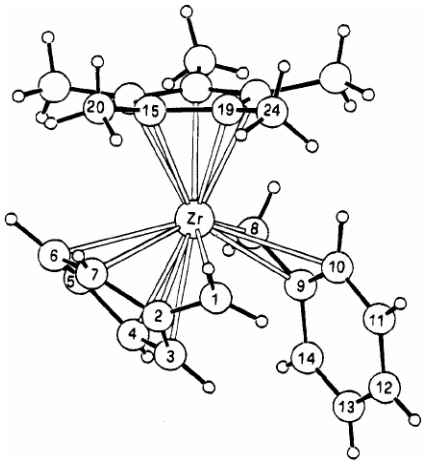

Figure 11. Solid-state structure of $[(C_5Me_5)Zr(CH_2Ph)_2]^+$ (reprinted with permission from *Organometallics,* **1994**, *13*, 3773. Copyright 1994 Am. Chem. Soc.).

3.2.3 Activation of nonmetallocene alkyl complexes

The metal center in nonmetallocene cations is usually less saturated and potentially more electrophilic than that in activated metallocenes. Thus, different chemical and structural behavior can be expected for the nonmetallocene cationic complexes.

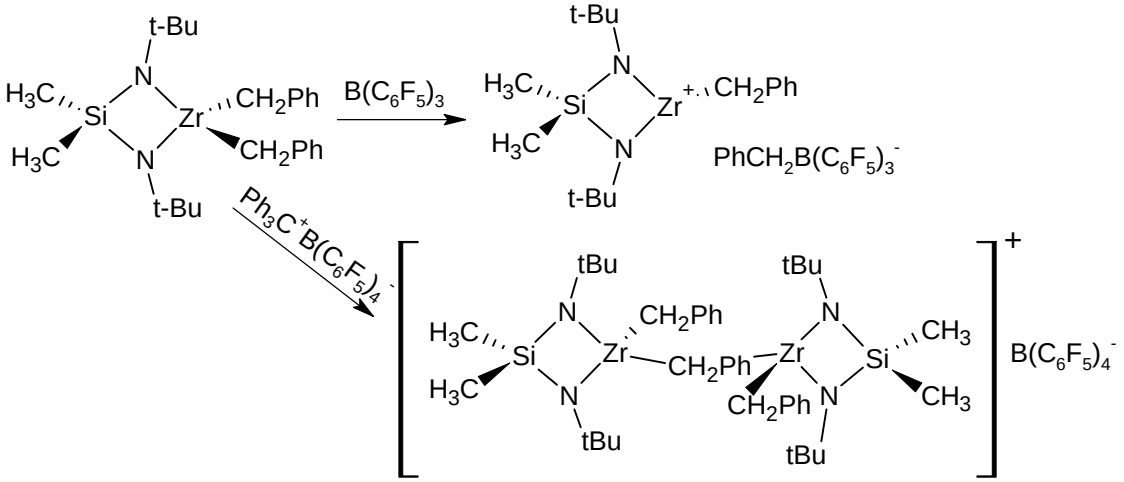

Scheme 15. Activation of Si-bridged bis(amido) Zr complex

Studies of activation of the amido Zr complexes were initiated by Horton and de With.[69] Upon reaction of the open $[(Me_3Si)_2N]_2Zr(CH_2Ph)_2$ with $B(C_6F_5)_3$ they observed C-H activation. NMR studies showed that the $PhCH_2B(C_6F_5)_3]^-$ anion that formed was bonded with the cation via η^6-benzyl-Zr interaction. In contrast to this, Horton *at al.* observed the activation of bridged $[Me_2Si(N\textit{t}\text{-}Bu)_2]Zr(CH_2Ph)_2$ to proceed in a common way (Scheme 15), but according to ^1H, ^{13}C

and ^{19}F NMR measurements the borate counteranion was still coordinated to highly electrophilic Zr.[31] Reaction of the same complex with $Ph_3C^+B(C_6F_5)_4^-$ gave a product containing two kinds of benzyl groups in ratio 2:1, which indicated the formation of the dimeric cationic complex (Scheme 15).[82]

The activation of $[RN(CH_2)_3NR]TiMe_2$, which served as catalyst precursors for living α-olefin polymerization, led to the highly unstable cationic species, which slowly converted to Ti-C_6F_5 derivative (see above).[66] The analogous Zr cations also revealed high instability. Surprisingly, the cationic complexes showed better stability in CD_2Cl_2 than in benzene, probably due to additional coordination of CD_2Cl_2. The NMR spectra displayed strong anion-cation contacts in solution.[83] From NMR investigations of the generated $[R_2BN(CH_2)_3NBR_2]MMe^+MeB(C_6F_5)_3^-$ (M – Ti, Zr) strong cation-anion interactions were also established in dichloromethane, which was presumably a reason for the low polymerization activity of these complexes in CD_2Cl_2. In aromatic solvents (toluene or chlorobenzene), cationic complexes may have been stabilized by the cation-solvent coordination.[20c,d] The ferrocene-bridged bis(amido)Ti methyl cation $\{[(\eta^5\text{-}C_5H_4NSiMe_3)_2Fe]TiMe\}^+$ (generated from complex **9**) showed marked stability in solution due to intramolecular Ti-Fe interaction. No significant direct metal-metal contacts were found in the solid state (Fe-Ti distance 3.32 Å) (Figure 12). The abstraction of one methyl group was also supported by differences in the Ti-Me bond lengths (2.297(4) vs. 2.080(5) Å) and tetrahedral configuration of the boron atom. Unlike the $\{[(\eta^5\text{-}C_5H_4NSiMe_3)_2Fe]TiMe\}^+$ cation in the dimeric chloro Ti cationic complex, $\{[(\eta^5\text{-}C_5H_4NSiMe_3)_2Fe]TiCl\}_2Cl^+$, the Ti-Fe distance was extremely short (2.49 Å).[72] The Zr benzyl substituted cation, $\{[(\eta^5\text{-}C_5H_4NSiMe_3)_2Fe]ZrCH_2Ph\}^+$, displayed similar structural features to the analogous Ti complex: absence of the recognizable Zr-Fe interactions (Zr-Fe distance 3.1981(7) Å) and the presence of strong cation-anion contacts, which were provided via η^6-$PhCH_2B(C_6F_5)_3^-$ coordination (Zr-Ph_{centr} 2.385(4) Å).[84]

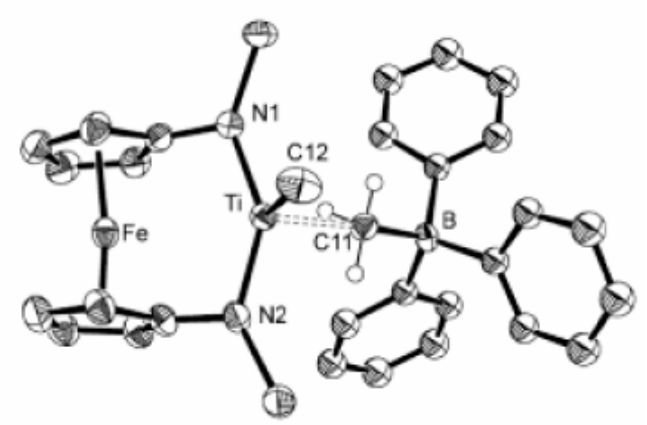

Figure 12. Solid-state structure of the ferrocene-bridged bis(amido)Ti methyl cation (reprinted with permission from *J. Am. Chem. Soc.,* **2001**, *123*, 9212. Copyright 2001 Am. Chem. Soc.).

With the aim of obtaining more stable, four-coordinated alkyl cations, chelating diamide complexes with additional donor were investigated by Schrock and co-workers.[43,44] The perfluorophenylborane activation of the dimethyl Zr[NON] derivative ([NON] - [((*t*-Bu-*d*6)N-*o*-$C_6H_4)_2O]^{2-}$) led to the unstable [NON]$ZrMe^+MeB(C_6F_5)_3^-$ complex, in which the methyl groups appeared to be nonequivalent.[43b] Analogously to the activated metallocenes in solid state, [NON]$ZrMe^+MeB(C_6F_5)_3^-$ revealed "zwitterionic" structure, where borane had partially abstracted one of the methyl groups (Figure 13).[43a]

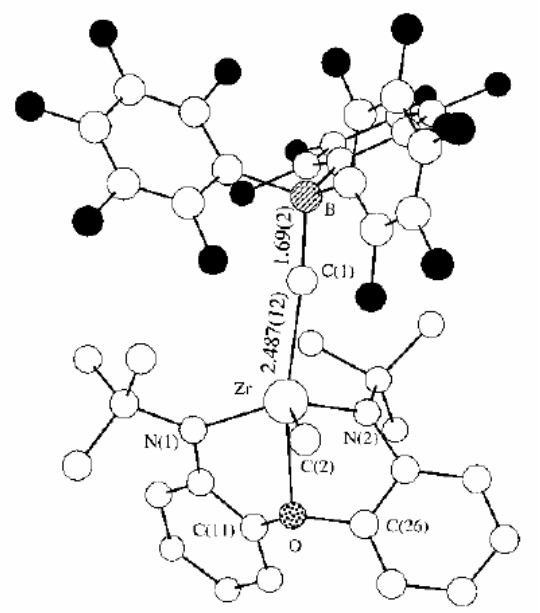

Figure 13. Solid-state structure of [NON]$ZrMe^+MeB(C_6F_5)_3^-$ (reprinted with permission from *J. Am. Chem. Soc.,* **1997**, *119*, 3830. Copyright 1997 Am. Chem. Soc.).

Addition of $PhNMe_2H^+B(C_6F_5)_4^-$ to [NON]$ZrMe_2$ also generates the corresponding cationic species, where dimethyl aniline coordinates with the metal center.[44] Similar structure and aniline coordination were found for $PhNMe_2H^+B(C_6F_5)_4^-$ activated [RN-$CH_2CH_2)_2O$]MMe_2 (M – Zr, Hf). The cations generated from [RN-$CH_2CH_2)_2S$]MMe_2 (M – Zr, Hf) were not formed so cleanly and were not as stable as those obtained for oxygen donor systems.[42]

The complexes having an additional donor in ligand bridge revealed structural lability. Depending on the conditions (ligand framework *etc.*), they adopt either *mer* or *fac* geometry (see above). In the presence of external donor (like Et_2O or NMe_2Ph), five-coordinated cationic species obtained from [NON]$ZrMe_2$ or [NNHN]$ZrMe_2$ complexes exhibited *fac* geometry, and the additional Lewis base ligand was bound in apical position *trans* to the O or N atoms of the bridge.[32,43,44] In contrast to this, the pseudooctahedral [NON]$ZrMe(THF)_2^+$ contains the [NON] ligand in *mer* configuration with

two THF molecules *trans* to each other. However, when the possibility to occupy the *trans* positions is excluded for Lewis donor, the *fac* geometry is essential, *e.g.* for [NON]ZrMe(DME)$^+$.[85] In all these compounds where the cation was coordinated with additional Lewis bases, the counteranion remained "noncoordinated".

The generated [MesNNMeNMes]ZrMe$^+$ (Mes – mesityl) is rather unstable and undergoes intramolecular C-H activation, which can be eliminated by replacement of the Mes substituents with 2,6-$Cl_2C_6H_3$ groups.[33,34] A cationic dimer was formed in the reaction of [MesNNMeNMes]ZrMe$_2$ (**11**, D = NMe, Figure 2) with 0.5 eq. of $Ph_3C^+B(C_6F_5)_4^-$. In solution, Zr-Me groups were involved in dynamic exchange, probably occurring *via* the dimeric intermediate, containing three bridged Me groups between Zr atoms. The dissociation-recombination process was established from NMR investigations.[34]

The diamido pyridine derivatives PyC(Me)($CH_2NHR)_2$ ([RNPy]H_2, Py – 2-pyridyl) were employed as relatively rigid [NNN]-type ligands for synthesis of the alkyl Zr and Hf complexes (see above). Upon activation of [MesNPy]Zr(alkyl)$_2$ complex by $Ph_3C^+B(C_6F_5)_4^-$, either cationic dimer (alkyl = Me) or monomeric cation (alkyl – *i*-Bu) unstable towards β-hydrogen elimination ($t_{1/2}$ = 40 min) was formed depending on the alkyl group.[86] Under the same conditions the analogous Hf species (alkyl = *i*-Bu, *i*-Pr, or Et) appeared to be moderately stable towards β-hydrogen elimination. In the case of the Hf-Et or *i*-Pr substituted complexes, two different monomeric cations can be distinguished from the NMR data. The first is formed *via* a direct alkyl group abstraction, while the second is due to insertion of the eliminated alkene (C_2H_4 or C_3H_6) into Hf-alkyl bond (Scheme 16).[37] The structure and catalytic behavior of the activated complexes bearing electron-withdrawing 2,6-$X_2C_6H_3$ (X – Cl or F) have also been investigated.[38]

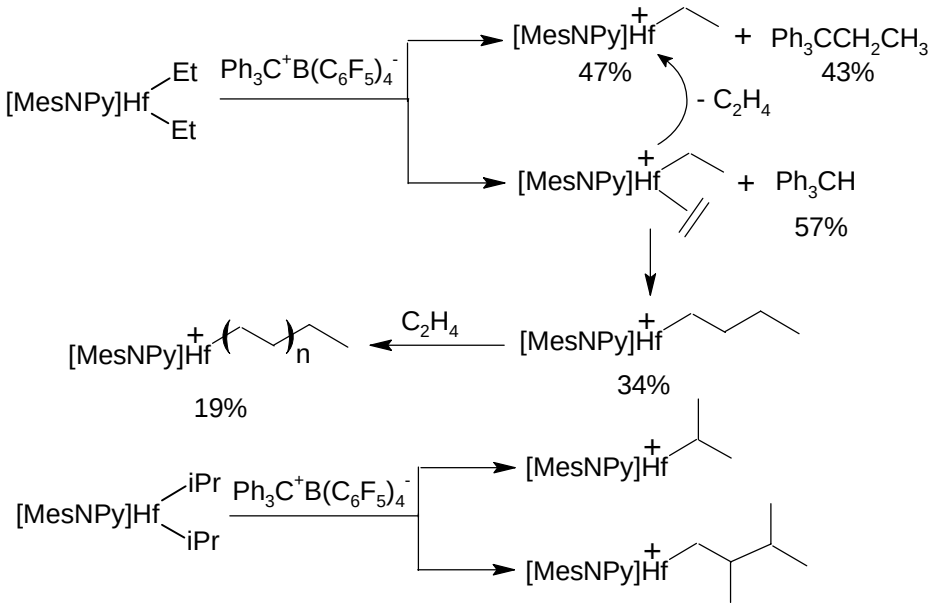

Scheme 16. Actvation of the RNPy type Hf alkyl complexes

The addition of $B(C_6F_5)_3$ to $(t\text{-}Bu_3PN)_{4-x}TiR_x$ (R-Me, CH_2Ph; x – 2,3) gave the corresponding "zwitterionic" systems, while activation by $PhNMe_2H^+B(C_6F_5)_4^-$ generated several kinds of cationic species. These cationic species can be transformed to a single cationic complex by coordination with PMe_3.[87] The product of the abstraction of two Me groups was isolated and characterized by X-ray studies.[88]

Recently there was a report of the $B(C_6F_5)_3$ activation of bis(phenolato) complexes. The reaction occurred rapidly, and cationic species with strong cation-anion interactions were formed.[59,89] In some cases this was followed by intramolecular C-H activation. The solid-state structures of bulky $(2,6\text{-}Ph_2C_6H_3O)_2M(CH_2Ph)^+PhCH_2B(C_6F_5)_3^-$ (M – Ti, Zr) were determined, and strong cation-anion bonding via M-η^6-CH_2Ph connection was established (Ti-arene bond 2.538(7)-2.627(6) Å; Zr-arene distance 2.653(4)-2.821(4) Å).[90] Similar M-η^6-CH_2Ph coordination in solution was found for other bis(phenolato) cationic complexes.[91]

The bis(phenolato) derivatives with donor group in the ligand bridge often show structural lability. In solid state, for example, the cationic bis(8-quinolinato) Zr benzyl complex has a different configuration than the parent complex. The structural transformation can be presented as the initial formation of five-coordinated cationic species followed by the shift of one of the quinolinato moieties (Scheme 17). The remaining benzyl group is connected with the metal center in η^2-fashion.[92]

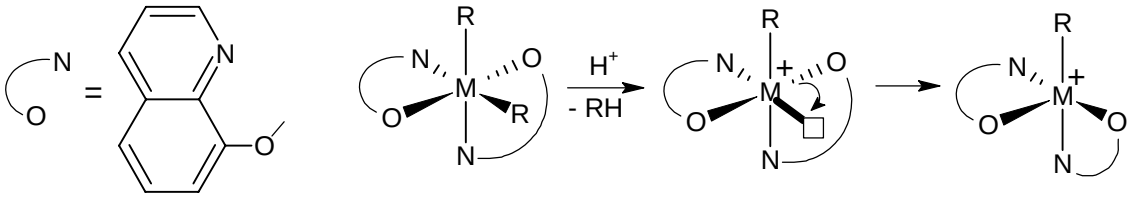

Scheme 17. Configuration transformation in the cationic complex formation

The neutral acene benzyl Zr complexes can be converted into corresponding cations by protonolysis with $PhNMe_2H^+B(C_6F_5)_4^-$. The coordination of the side-formed $PhNMe_2$ is observed both in solution and in solid state (Figure 14). The Zr-N_{donor} distance was 2.441(4) and comparable to Zr-N bond lengths in related Zr complexes containing neutral N-donor ligands. The chemical behavior of these acene cationic complexes in solution was also investigated by NMR methods.[93]

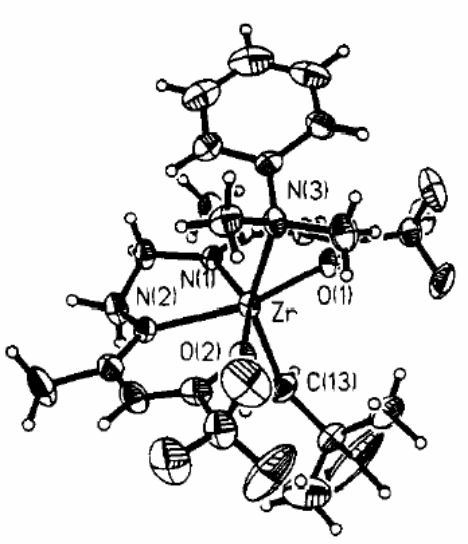

Figure 14. Solid-state structure of (F6-acen)Zr(CH_2CMe_3)(NMe_2Ph)$^+$ cation (reprinted with permission from *Organometallics,* **1995**, *14*, 371. Copyright 1995 Am. Chem. Soc.).

4 Results and Discussion

4.1 Experimental notes

The ligands and complexes were prepared and handled under inert argon atmosphere using standard Schlenk technique and a glovebox. All solvents, including the ones for preparation of NMR samples, were dried with appropriate drying agents. Detailed descriptions of the solvent purification, complex synthesis, analyses, and polymerization procedures can be found in the experimental parts of the attached original publications. The synthesis and structures of the different ligands and metal complexes and their activated forms are presented in the following. The polymerization activity of each complex is described in connection with its synthesis and structure.

4.2 Bis(amino)cyclodiphosph(III)azane ligands

4.2.1 Ligand preparation[I]

Phosphazanes, both cyclic and acyclic, are an established class of P-N compounds known for their stability and ease of synthesis. Cyclodiphosph(III)azanes (containing a P_2N_2 moiety) were first reported by Michaelis and Schroeter in 1894[94] but were fully characterized only in the 1970s.[95] It

was found for bis(amino)cyclodiphosph(III)azanes that the greater bulkiness of the substituents at nitrogen atoms increases the thermodynamic stability of both the P_2N_2 cycle and the *cis* configuration of the amino groups at the ring (Figure 15).[96] Study by ^{31}P NMR helps to distinguish the *cis* and *trans* isomers from each other and to define the absolute configuration of the investigated cylodiphosph(III)azane.[95b,97] Because the *cis* orientation of the amino substituents favors the coordination of metals and complex formation, the coordination chemistry of *cis*-bis(amino)cyclodiphosph(III)azanes has been well studied.[98]

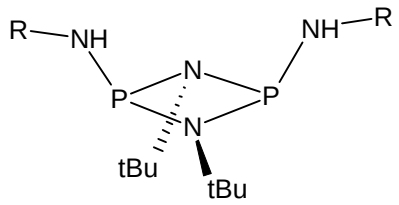

Figure 15. Bis(amino)cyclophosph(III)azanes with *cis* configuration of the amino groups

Homosubstituted bis(amino)cyclodiphosph(III)azanes, (*i.e.* having identical organic substituents at all four nitrogen atoms) are synthesized by condensation reaction of the appropriate amine with PCl_3.[95b] Heterosubstituted ligands are prepared by a two-step route. First the dichlorosubstituted cyclodiphosph(III)azane (**16**) is obtained,[94,95b,99] and this is reacted with certain lithium amides, or with the excess of a free amine. Both these alternatives lead to diamines in good yields.[98, 100] And both were investigated here as a means to access new, bulky bis(amino)cyclodiphosph(III)azanes.

The homosubstituted *cis*-di-*t*-butylaminocyclodiphosph(III)azane (**17**) was obtained by the reaction of *t*-butylamine and PCl_3 (Scheme 18). The modified literature procedure was used.[95b] New aryl-substituted ligands, in turn, were prepared from the *cis*-dichlorocyclodiphosph(III)azane (**16**). Because of the bulky amines employed, modifications in the general procedure were required to make substitution to P-Cl bonds. The attempts to use strong nucleophiles (amido lithium salts) failed because the substitution reaction occurred unselectively and the P_2N_2 ring was partially destroyed in the course of the reaction. Direct substitution in the presence of amine excess did not lead to the desired products even in harsh conditions. The application of Et_3N, which is a more active base and less bulky than aryl amines and can serve as a P-Cl bond activator and as base for the utilization of forming HCl, led to the desired results. Still, relatively harsh conditions (at least fourfold excess of Et_3N and 4 days of reflux in THF) were required to achieve full disubstitution at the P_2N_2 ring. This procedure was applied to synthesize new *cis*-bis(amino)cyclodiphosph(III)azanes bearing bulky substituents (**18**-**24**, Scheme 18).[I-II]

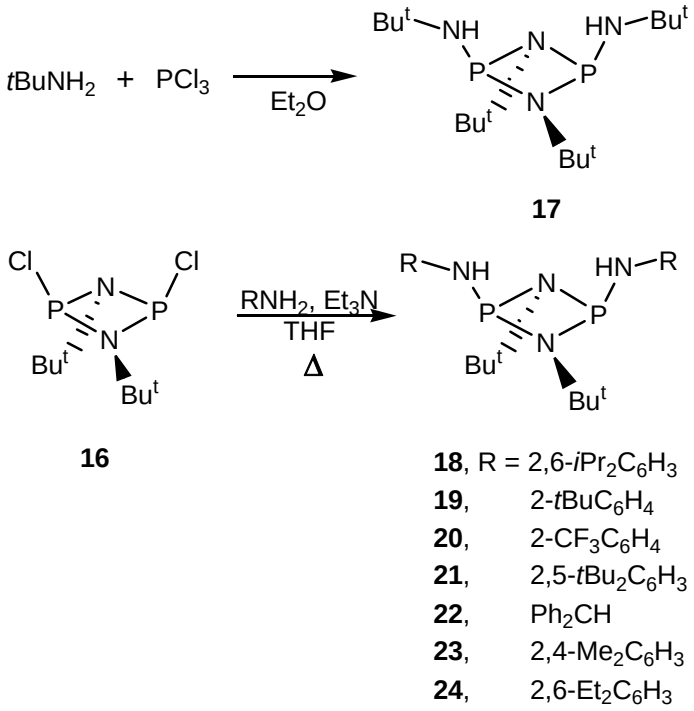

Scheme 18. Preparation of bulky bis(amino)cyclodiphosph(III)azane ligands[I-II]

4.2.2 Structure of bulky cis-bis(amino)cyclodiphosph(III)azans[I-II]

The cyclodiphosph(III)azane ligands **17-24** are air- and moisture-sensitive oils or sticky solids. ^{31}P NMR showed that they all adopt the *cis* configuration. Single crystal X-ray diffraction analysis was undertaken for a series of four of new cyclodiph(III)azanes (Figure 16). Like ^{31}P NMR, the measurements supported the exclusive presence of the *cis* isomer. The data showed that, despite the sterically bulky aryl or alkyl substituents, the basic structural features (bond lengths and angles) of the ligand backbone are more or less the same as earlier reported for nonbulky ones.[98,100,101] In **19-21** in solid state the P_2N_2 ring was bent, in agreement with previously reported theoretical calculations. The bending could be a result of the repulsive lone pair - bond pair electronic interactions.[96]

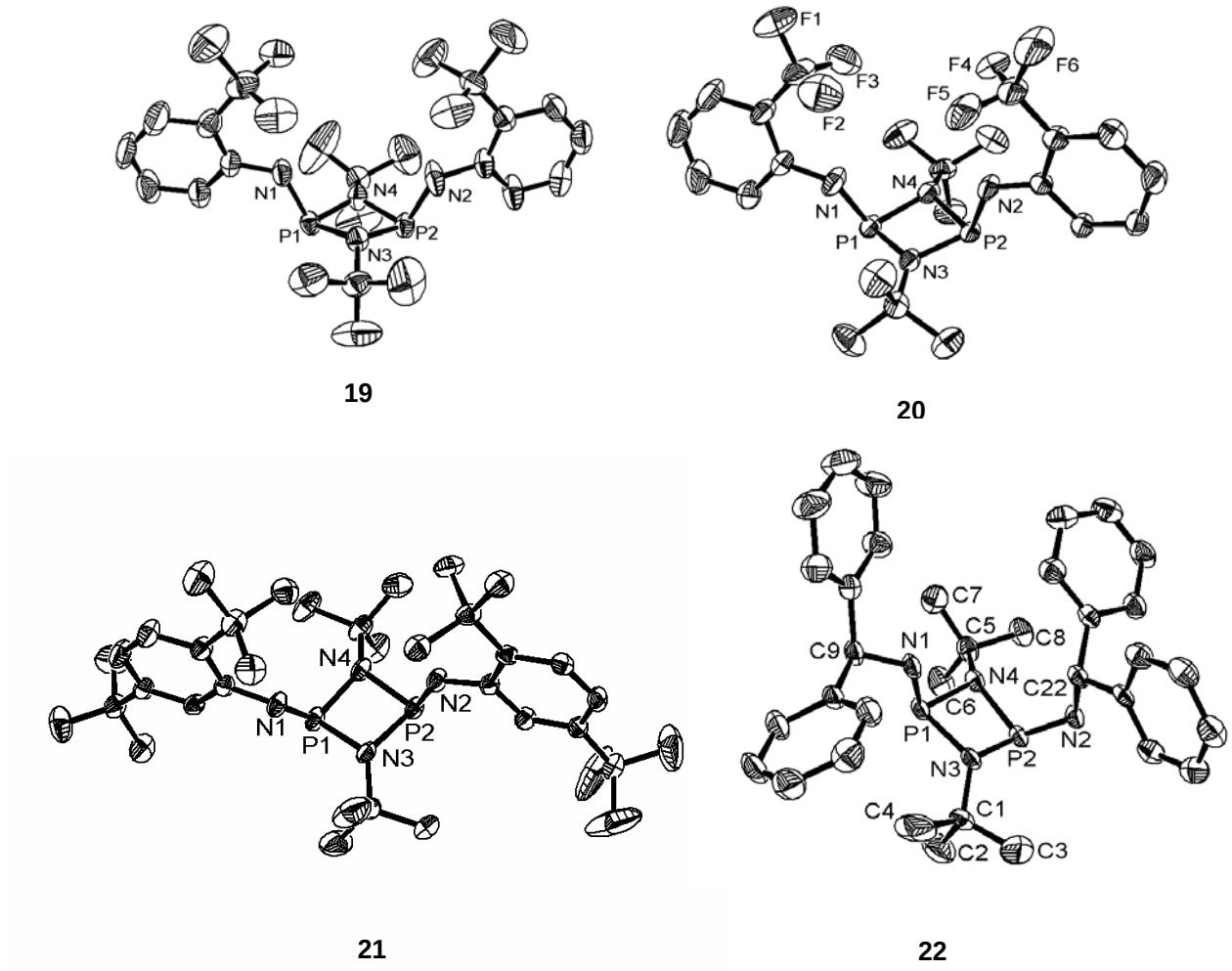

Figure 16. Solid state structures of the synthesized *cis*-bis(amino)cyclodiphosph(III)azans. **19** - *cis*-[(2-*t*-BuC_6H_4NH)(*t*BuNP)]$_2$; **20** - *cis*-[(2-$CF_3C_6H_4$NH)(*t*BuNP)]$_2$; **21** - *cis*-[(2,5-di-*t*-$Bu_2C_6H_3$NH)(*t*BuNP)]$_2$; **22** - *cis*-[(Ph_2CHNH)(*t*BuNP)]$_2$[I-II]

The structures of **19** and **20** are similar.[I] The orientation of the aniline groups and their substituents gives the molecules overall C_{2v} symmetry. The influence of the electron-withdrawing CF_3 substituents is seen only in the elongation of the exocyclic PN bonds. Owing to the presence of a second *tert*-butyl substituent at the aniline moieties, **21** has lost superfacial C_{2v} symmetry. The bond distances and angles in the P_2N_2 ring in **21** are nevertheless similar to those in **19** and **20** (Figure 16).[I]

The solid state structure of compound **22** bearing very bulky diphenylmethyl groups differs sharply from the previously described structures. According to X-ray crystallographic data, the NH groups in all other known cyclodiphosph(III)azans adopt the *endo* orientation relative to the P_2N_2 ring,

[98,100,101] (*e.g.* compounds **19-21** in Figure 16), while in **22** these substituents have the *exo-endo* orientation. Such an unusual structural feature has earlier been reported only for *cis*-[(*t*BuNH)(*t*BuNPS)]$_2$ with P(V).[95b] Furthermore, the distortion of the P_2N_2 ring is diminished as indicated by the P-N bond distances and the planarity of the ring. This may be mostly a consequence of the unique *exo-endo* orientation.[II]

4.2.3 Coordination chemistry of bulky cis-bis(amino)cyclodiphosph(III)azans

The coordination chemistry of the bis(amino)cyclodiphosph(III)azanes has attracted significant attention because the *cis* ligand structure favors the complexation of various main group elements.[98] Although the detailed investigations in this area were beyond the scope of this study, but the chemistry of the Li and Mg compounds were prepared and preliminarily investigated as potential sources for transition metal complexes. The reactions of **18** and **23** with *n*BuLi and **23** with Bu_2Mg occurred selectively according to ^{31}P, ^{1}H, and ^{13}C NMR, but because of the bulky substituents in the ligand framework, a long time was required to complete the reaction (Scheme 19).[I]

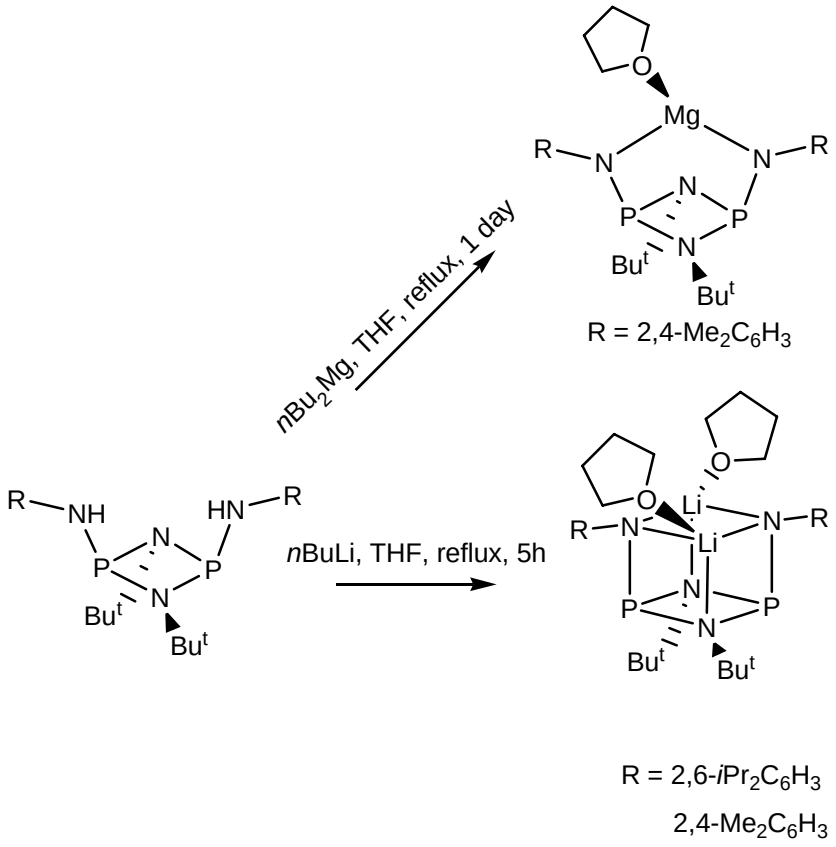

Scheme 19. Preparation of Li and Mg derivatives of bulky bis(amino)cyclodiphosph(III)azanes [I]

The structure of the Li salt, *cis*-[(2,4-di-MeC_6H_3N)(PN-*t*Bu)]$_2$$Li_2(THF)_2$ (**25**), was resolved by X-ray single crystal diffraction analysis. In solid state the P_2N_2 ring, exocyclic N, and both Li atoms form an inorganic heterocube that is surrounded by the aniline groups of the ligand and two coordinated THF molecules (Figure 17). The P_2N_2 ring is almost planar, which is also related to the symmetry of the molecule and the equal bond distances in the ring. The exocyclic P-N bonds are shorter than the endocyclic ones (1.674(3) Å vs. 1.768(3) Å). The bond lengths between Li and the exocyclic nitrogen atoms are almost equal (from 2.071(6)Å to 2.095(6)Å) and similar to those found in related lithium amides.[102] Thus, the solid-state structure of compound **25** has similar structural features to those described for *cis*-[(*t*BuN)(PN-*t*Bu)]$_2$$Li_2(THF)_2$.[101b] Relative to the structure of *cis*-[(*t*BuN)(PN-*t*Bu)]$_2$$Li_2(THF)_2$, however, the distances between the lithium atom and the endocyclic nitrogen atoms are lengthened (2.133(6) Å vs 2.104(5) Å) and they can be considered typical for bonds between a coordinated lithium cation and a donor nitrogen atom.[I]

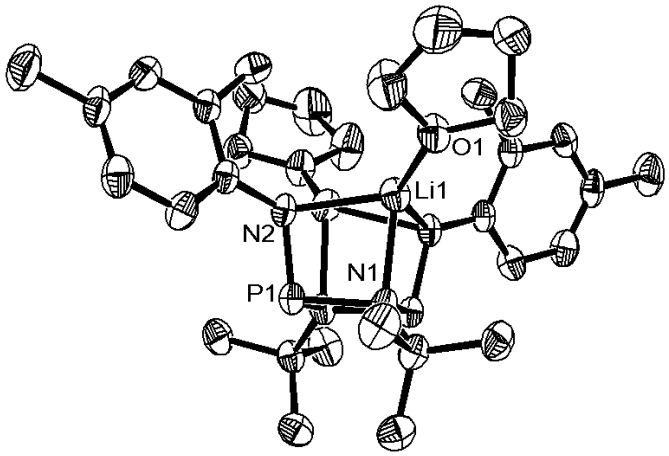

Figure 17. Solid-state structure of Li bis(amido)cyclodiphosph(III)azane salt (**25**).[I]

4.3 Group 4 metals complexes of bis(amido)cyclodiph(III)azanes

First bis(amido)cyclodiphosph(III)azane complexes were prepared in 1997.[11a] From preliminary ethene polymerization experiments the poor stability of Ti and Zr complexes in the presence of MAO was claimed.[11] One of goals of the present studies was to investigate the influence of the ligand substitution on the catalytic behavior of bis(amido)cyclodiphosph(III)azane group 4 metal complexes in ethene polymerization and to find stable enough and active catalysts. Also the investigations how the ligand substitution is affecting on the structure of the activated species have been made.

4.3.1 Synthesis of bis(amido) group 4 metal dichloro derivatives[I-III]

One of the general synthetic routes to the bis(amido)complexes of transition metals is the transmetallation reaction between metal halides and alkali or alkaline earth metal salts of the ligand.[103] The known bis(amido)cyclodiph(III)azane Ti, Zr and Hf complexes based on *cis*-[(*t*BuN$^-$)(PN-*t*Bu)]$_2$ ligand framework were obtained by this route.[11,100] Our attempts to obtain group 4 metal complexes bearing bulky amido substituents *via* corresponding lithium or magnesium salts failed. The explanation might be the steric demand of these lithium salts, which slows down the reaction; or Ti, Zr, and Hf tetrachlorides, which are strong Lewis acids, may attack the phosphorus lone pair more readily than the N-Li or N-Mg bond.

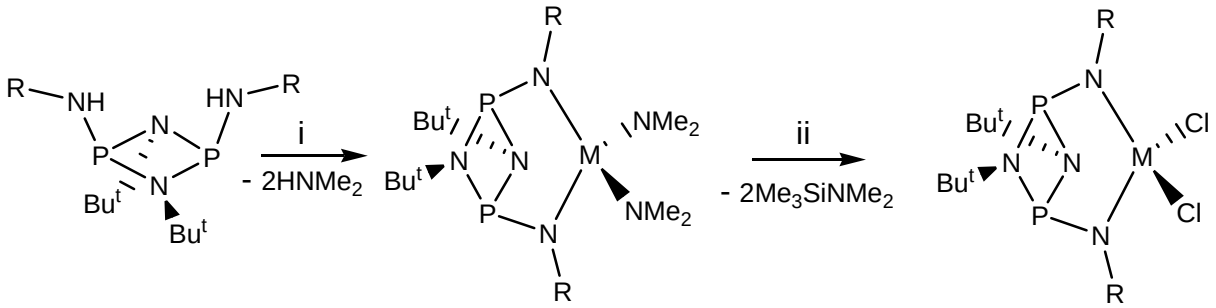

R	M - Ti [I]		M -Zr [II]		M - Hf [III]	
	NMe_2	Cl	NMe_2	Cl	NMe_2	Cl
Ph	**26a**	**-**	**31a**	**31**	**-**	**-**
Ph_2CH	**27a**	**27**	**32a**	**32**	**-**	**-**
2,6-$Et_2C_6H_3$	**28a**	**28**	**33a**	**33**	**-**	**-**
2,6-*i*$Pr_2C_6H_3$	**29a**	**29**	**34a**	**34**	**36a**	**36**
2,5-*t*$Bu_2C_6H_3$	**30a**	**30**	**35a**	**35**	**37a**	**37**

i - $M(NMe_2)_4$, toluene, reflux; ii - excess of Me_3SiCl

Scheme 20. Preparation of cyclodiphosph(III)azane group 4 metal complexes

An alternative approach, direct ligand metallation by Ti, Zr and Hf amides, was found to be efficient. The reaction of the less Lewis-acidic $M(NMe_2)_4$ (M = Ti, Zr, Hf) with [(RNH)(*t*BuNP)]$_2$ occurred selectively, and the bis-amido complexes [(RN)(*t*BuNP)]$_2$M(NMe$_2$)$_2$ were formed in high yield (Scheme 20).[I-III] The M-NMe$_2$ bonds are stronger and more resistant against substitution than M-Cl bonds because NMe$_2$ groups are stronger π donors (the free electron pair on N is more accessible for a metal) than Cl atoms.[104] This slows down the activation of the NMe$_2$-substituted complexes and makes the M-Cl derivatives more attractive candidates for application in

homogeneous olefin polymerization. The prepared amido complexes were converted into $[(RNH)(t\text{BuNP})]_2MCl_2$ with high yields by reaction with excess of Me_3SiCl (Scheme 20).[I-III]

4.3.2 Preparation of Ti, Zr, and Hf alkyl complexes[III,IV]

The known complex $[(t\text{BuNH})(t\text{BuNP})]_2TiCl_2$ (**38**) and three new complexes **28**- **30** were allowed to react with $PhCH_2MgCl$ in Et_2O. Phosph(III)azane derivatives **29** and **30** bearing bulky 2,6-*i*-$Pr_2C_6H_3$ and 2,5-*t*-$Bu_2C_6H_3$ groups, respectively, were directly converted into benzyl-disubstituted complexes $[(RN)(t\text{-BuNP})]_2Ti(CH_2Ph)_2$ (**39**, R = 2,6-*i*-$Pr_2C_6H_3$; **40**, R = 2,5-*t*-$Bu_2C_6H_3$), while **28** and **38** gave only $[(RN)(t\text{-BuNP})]_2Ti(CH_2Ph)Cl$ (**41**, R = *t*-Bu; **42**, R = 2,6-$Et_2C_6H_3$) (Scheme 21). Later attempts to introduce a second benzyl group to **41** and **42** by treatment with additional $PhCH_2MgCl$ led to the desired dibenzyl substituted derivatives in low yields. In this case it appeared that the preferable reaction was decomposition of the complex with the formation of large quantities of dibenzyl.[IV]

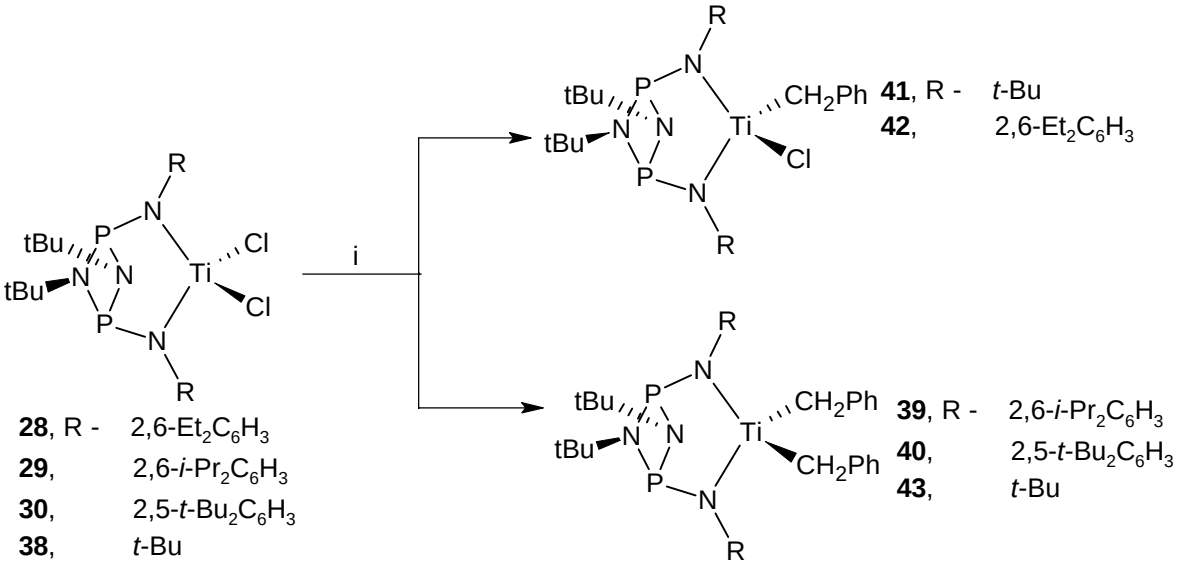

Scheme 21. Preparation of cyclodiphosph(III)azane Ti benzyl complexes[IV]

Pure $[(t\text{BuN})(t\text{-BuNP})]_2Ti(CH_2Ph)_2$ (**43**) was obtained in a moderate yield *via* treatment of **38** in Et_2O and $PhCH_2MgCl$ solution in THF (Scheme 25). The benzylidene derivative,$[(t\text{-BuN})(t\text{-BuNP})]_2TiCHPh(THF)$ (**44**), was isolated as side-product from the reaction mixture. These two Ti complexes can be separated from each other because of their different solubility in alkane solvents. In the proposed mechanism, deprotonation of the initially formed **41** by $PhCH_2MgCl$ followed by

Cl^- abstraction leads to the carbene complex **44**, which is stabilized by coordination with THF (Scheme 22).[IV]

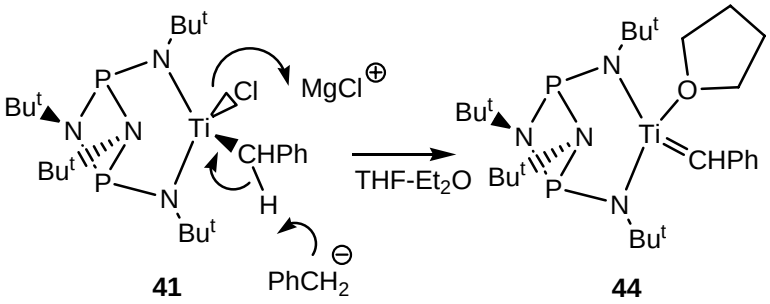

Scheme 22. Proposed mechanism for formation of Ti carbene complex **44**

The benzylation of Zr complexes $[(RN)(t\text{-BuNP})]_2ZrCl_2$ (**34**, **35**, and **45**, R = *t*-Bu) was carried out under similar conditions as used for Ti derivatives. Bulky $[(RN)(t\text{-BuNP})]_2ZrCl_2$ (**34**, R = 2,6-*i*-$Pr_2C_6H_3$ and **35**, R = 2,5-*t*-$Bu_2C_6H_3$) were converted into monobenzyl $[(RN)(t\text{-BuNP})]_2Zr(CH_2Ph)Cl$ (**46** and **47**, respectively) (Scheme 23), while less sterically crowded $[(t\text{BuN})(t\text{-BuNP})]_2ZrCl_2$ (**45**) was directly transformed into corresponding dibenzyl complex **48** (Scheme 23). In efforts to get dibenzyl Zr derivatives from **34** and **35,** only complex decomposition was observed.[IV]

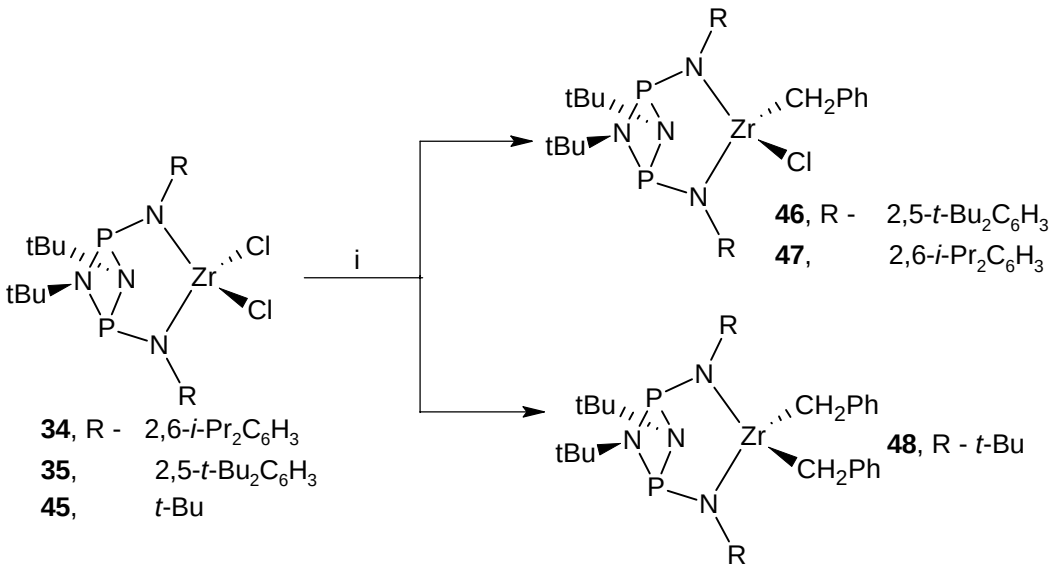

i $PhCH_2MgCl$ in Et_2O; solvent Et_2O; temperature - 50 °C

Scheme 23. Preparation of cyclodiphosph(III)azane Zr benzyl complexes.[IV]

The benzyl Ti and Zr complexes exhibited modest thermal instability and high air and moisture sensitivity.

The dimethyl Hf complexes **49-51** were prepared by the reaction of corresponding dichloro Hf derivatives with MeMgBr in Et_2O (Scheme 24). They exhibited high thermal stability but were extremely air and moisture sensitive.[III]

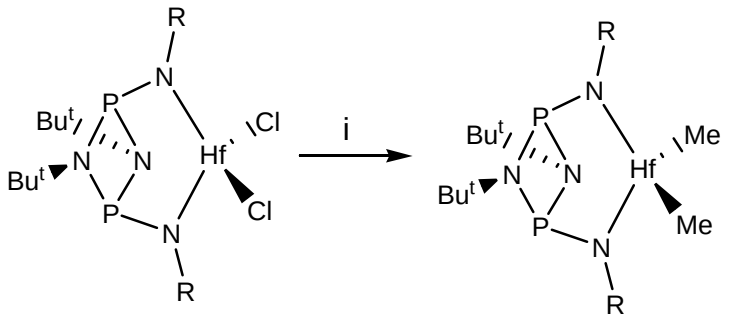

49, R = *t*Bu
50, 2,6-*i*Pr$_2$C$_6$H$_3$
51, 2,5-*t*Bu$_2$C$_6$H$_3$

i - MeMgBr in Et_2O

Scheme 24. Synthesis of the dimethyl hafnium cyclodiphosph(III)azane complexes[III]

4.3.3 Structure of the group 4 metal complexes[I-IV]

The synthesized group 4 metal derivatives were isolated as oils or solids depending on the substitutions at the amido nitrogen. Colors of the obtained material were defined by the coordinated metal: Ti derivatives were red to brown, Zr derivatives – white to orange, and Hf derivatives – white or pale-yellow.

In ^{1}H and ^{13}C NMR spectra the complexes exhibited C_2 molecular symmetry, since *t*-butyl substituents at the P_2N_2 ring, as well as alkylaryl groups, were chemically equivalent. In the case of the unsymmetrically substituted [(*t*-BuN)(*t*-BuNP)]$_2$Ti(CH$_2$Ph)Cl (**41**), ^{1}H NMR showed chemical nonequivalence of *t*-butyls at the P_2N_2 ring and C_s molecular symmetry can be proposed.[IV]

Single-crystal X-ray analyses of *cis*-bis(amido)cyclodiphosph(III)azane transition metal derivatives are few; only solid state structures of a few complexes based on the *cis*-[(*t*BuN$^-$)(PN-*t*Bu)]$_2$ framework are described in the literature.[100,104] In this work investigation was made of the solid-state structures of group 4 metal *cis*-bis(amido)cyclodiphosph(III)azane complexes. The structures of the Zr and Hf alkyls are described below in connection with activation studies (Section 4.3.5).

Here the structural features of (PhN)(*t*BuNP)]$_2$Ti(NMe$_2$)$_2$ (**26a**) and [(Ph$_2$CHN)(*t*BuNP)]$_2$Zr(NMe$_2$)$_2$ (**32a**) are presented.[I,II] The two structures are similar (Figure 18). The four amido-metal bonds, and an additional coordination of the cyclodiphosph(III)azane ring nitrogen atom to the metal, define a rather distorted trigonal bipyramidal configuration of the

coordination center. The presence in solid state of an the additional donor acceptor bond between the P_2N_2 ring and metal changes the molecular symmetry from C_2 in solution to C_s in solid state. The Ti-N_{amido} bond lengths in **26a** are not equal and vary from 1.884(4) Å to 2.020(3) Å. All Zr-N_{amido} bonds in **32a** are equidistant with average length 2.110 Å. The donor-acceptor bond M-N_{P2N2} is longer in the Zr complex **32a** than in the Ti complex **26a** (2.325(4) Å *vs*. 2.448(7) Å) and in both complexes the M-N_{P2N2} interaction is weaker than normal covalent metal-amido nitrogen bonds. The elongation of the Zr-N_{P2N2} bond length relative to Ti-N_{P2N2} may be related to the larger radius of the Zr atom or it may be a consequence of the weaker Lewis acidity of Zr(IV) than Ti(IV). The $[(PhN)(t\text{BuNP})]_2TiCl_2$ complex, the dichloro substituted analogue of complex **26a**, has been described in the literature.[100] The Ti-N_{P2N2} distance was given there as 2.1588(7) Å, which is much shorter than in **26a**. This difference can be explained by stronger π-donor character of NMe_2 substituents than of Cl groups, or by the donation of additional electron density from the sp^2-hybridized amido nitrogen atoms to the metal center in complex **26a**, which decreases the Lewis acidity of titanium and thereby the strength of the Ti-N_{P2N2} interaction. In the complex **26a,** and also **32a**, the amido nitrogen atoms are in a pseudo-tetrahedral environment around the metal center with angles between two M-N_{ligand} bonds 111.80(1) º in Ti compound and 108.5(2) º in the Zr derivative. The Me_2N-M-NMe_2 angle increased from 98.66(2) º in structure **26a** to 100.0(3) º in **32a**.[I,II]

In the Zr complex **32a**, the geometry of the ligand framework (compare structure **22**, Figure 16) is altered by the zirconium coordination, and the P-N(amido) bonds adopt *endo-endo* orientation relative to the cyclodiphosph(III)azane ring.[II]

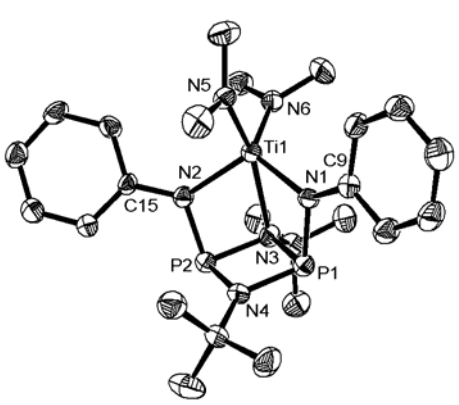

26a

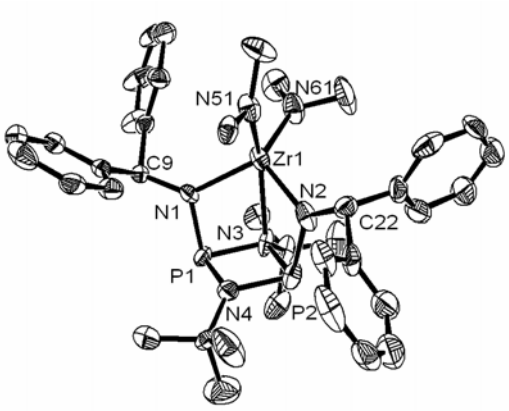

32a

Figure 18. Solid-state structures of group 4 metal cyclodiphosph(III)azane complexes: **26a** - *cis*-$[(PhN)(t\text{BuNP})]_2Ti(NMe_2)_2$, **32a** - $[(Ph_2CHN)(t\text{BuNP})]_2Zr(NMe_2)_2$.[I,II]

[(*t*-BuN)(*t*-BuNP)]$_2$TiCHPh(THF) (**44**) (Figure 19) is distinguished from other group 4 metal cyclodiphosph(III)azane derivatives by the presence of Ti-C double bond.[IV] The first indication of the carbene character of **44** was obtained from ^{1}H and ^{13}C NMR data. In ^{1}H NMR the proton signal of the TiCH group is downfield shifted (4.05 ppm *vs*. 3.22 ppm for $TiCH_2$ peak of **43**) and in ^{13}C NMR a low-field carbene signal of the TiCH moiety (221.93 ppm with J_{CH} = 162.85 Hz) is detected. The structural data from the single crystal X-ray studies are in a good agreement with the observed NMR spectra.

In solid state, [(*t*-BuN)(*t*-BuNP)]$_2$TiCHPh(THF) (**44**) is highly unsymmetrical. The titanium atom adopts a distorted trigonal bipyramidal configuration, defined by two Ti-N_{amido}, Ti=CH, Ti-O, and donor-acceptor Ti-N(from P_2N_2 cycle) connections (Figure 19). The double Ti=CH bond is short (1.901(4) Å) and distinguished from the single (in range 2.1-2.2 Å) Ti-CH_2Ph bond[105] in normal benzyl Ti bis(amido)complexes. Because the electron density has moved from metal center to the benzylidene ligand, titanium acquires a high Lewis acid character, as seen in the shortening of the Ti-N_{P2N2} bond (2.205(3) Å *vs*. 2.267(2) Å in [(*t*-BuN)(*t*-BuNP)]$_2$$TiCl_2$). The configuration of the carbene atom with the angle between the Ti=C bond and Ph substituent 161.3(4)° is highly distorted from the sp^2 defined geometry, which may be due to the presence of significant agostic interactions between C61-H61a and titanium. The C61-C62 bond is 1.445(6) Å, which consists with the length of standard C(sp2)-C(sp2) bond (1.48 Å).[IV]

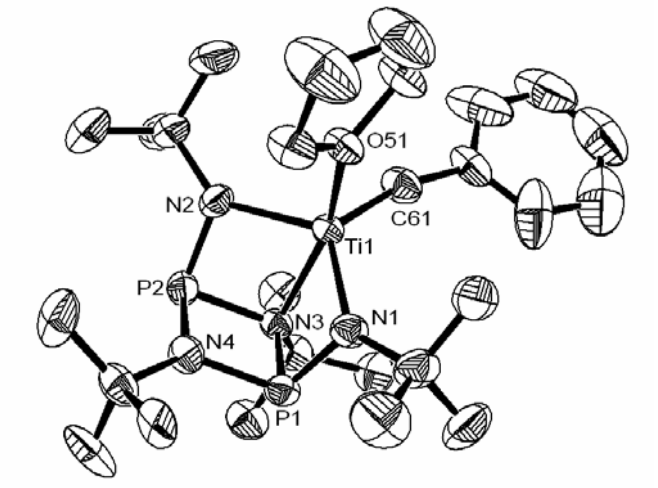

Figure 19. Solid-state structure of the cyclodiphosph(III)azane Ti carbene complex *cis*-[(PhN)(*t*BuNP)]$_2$TiCHPh(THF) **44**.[IV]

4.3.4 Results of ethene polymerization [I-IV]

Despite the clear interest in *cis*-bis(amido)cyclodiphosph(III)azane-based group 4 metal complexes, only a few preliminary reports have described their behavior in olefin polymerization.[11b,100] Unfortunately, neither exact values of polymerization activity nor the properties of the produced polymers were reported. Here. in order to study in detail the catalytic behavior of *cis*-bis(amido)cyclodiphosph(III)azane derivatives, polymerization experiments with known and novel Ti, Zr, and Hf complexes were carried out after activation with MAO, and investigations were made of the properties of the produced polymers.

Under the same polymerization conditions, the Zr based catalysts exhibited the highest activities among the group 4 metal complexes (Figure 20).[II]

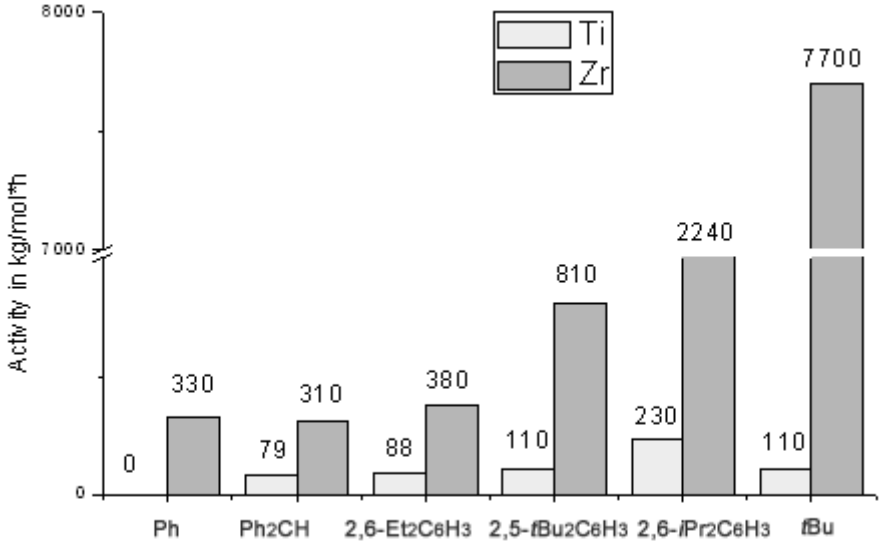

Figure 20. Catalytic activity of $[(RN)(t\text{BuNP})]_2MCl_2$ (M = Ti, Zr) in ethene polymerization. Conditions: 200 ml of toluene, ethene pressure 3.8 bar, Al/M (M = Ti or Zr) ratio 1000, polymerization temperature 50 ºC[I,II]

The experimental data showed the catalytic activity and properties of the resulting polymers to depend on the substitution at the ligand framework (Figure 20). Most active were Ti and Zr complexes bearing *cis*-$[(t\text{BuN}^-)(\text{PN-}t\text{Bu})]_2$. The relatively small *t*-butyl groups at amido nitrogen atoms leave the metal center open for activation and polymer chain propagation, but at the same time the catalyst appears to be susceptible to side reactions and deactivation. This may explain the good polymerization activity of these catalysts and the fast deactivation of *cis*-$[(t\text{BuN})(\text{PN-}t\text{Bu})]_2TiCl_2$ (**38**) under the applied polymerization conditions. As a result, the overall productivity

of complex **38** in polymerization was not high. The labile character of **38** is also supported by the formation of polymer with bimodal molar mass distribution in the course of the reaction (Figure 21).[I] Although highly active, *cis*-[(*t*BuN)(PN-*t*Bu)]$_2$ZrCl$_2$ exhibited enchanced sensitivity to increase in the polymerization temperature and MAO concentration.[II]

The replacement of the *tert*-butylamido groups in the *cis*-[(*t*BuN)(PN-*t*Bu)]$_2$ZrCl$_2$ complex with diphenylmethylamido substituents led to dramatic change in the catalyst behavior (Figures 20 and 21).[I,II] The activity declined substantially and the produced polyethene had high M_w and bimodal molar mass distribution. Polyethene with narrow molecular mass distribution was obtained with the similar Ti complex **27**, which also showed rather low polymerization activity (Figure 20).

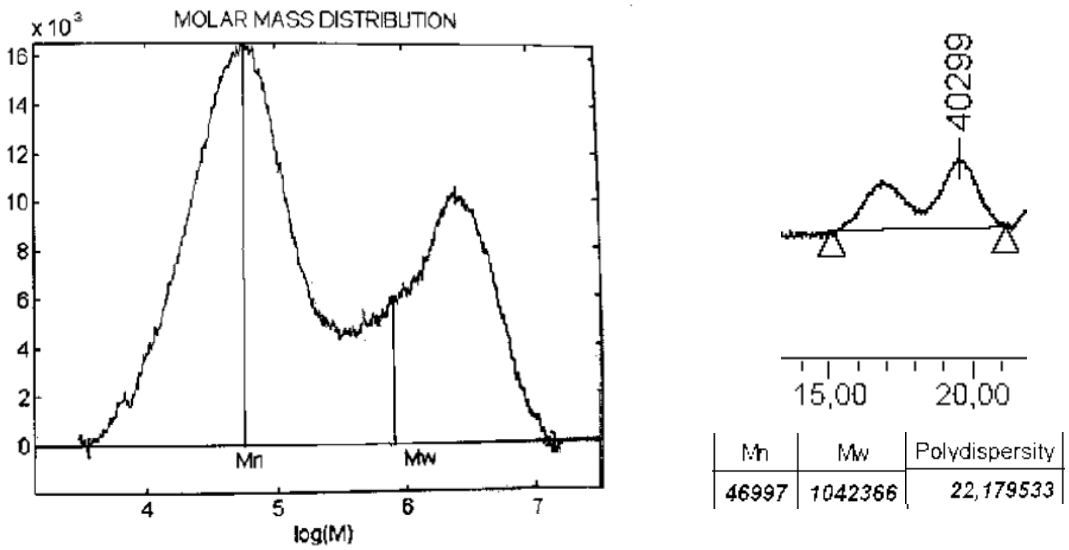

38 **32**

Figure 21. Bimodal molecular mass distribution in the polyethene obtained with catalysts **38** containing *t*-butylamido substituents and **32** bearing Ph_2CH groups.[I]

In the series of Ti and Zr catalysts bearing arylamido groups, the polymerization activity grows with the bulkiness of the ligand substitution in the order Ph < 2,6-$Et_2C_6H_3$ < 2,5-*t*-$Bu_2C_6H_3$ < 2,6- *i*-$Pr_2C_6H_3$.[I,II] These complexes produced very high molecular mass polyethene with relatively narrow polydispersity, the values lying in the range 2.1 – 6. The polyethylene obtained with Ti derivatives has higher M_w (more than 2×10^6 g/mol was achieved) than the polyethene obtained with Zr derivatives. The increased bulk of the arylamido substituents relative to the *t*-Bu group was still insufficient to efficiently protect the catalyst from decomposition under harsh conditions. Both Ti and Zr derivatives showed a decline in catalytic activity when polymerization temperature was elevated to 70 ºC and MAO concentration increased to Al/Zr ratio 2000:1.[I,II] Only Zr complex **34**

bearing very bulky 2,6- *i*-$Pr_2C_6H_3$ groups showed increased catalytic activity under such harsh conditions.[II]

The polymers produced with catalysts used had such high molecular mass that their solubility even in hot toluene was very low. At higher monomer concentration, due to enhanced polymer formation, the active complex quickly became embedded in the swollen gel-like polymer matrix, which led to diffusion-controlled reaction conditions (Figure 22).[II]

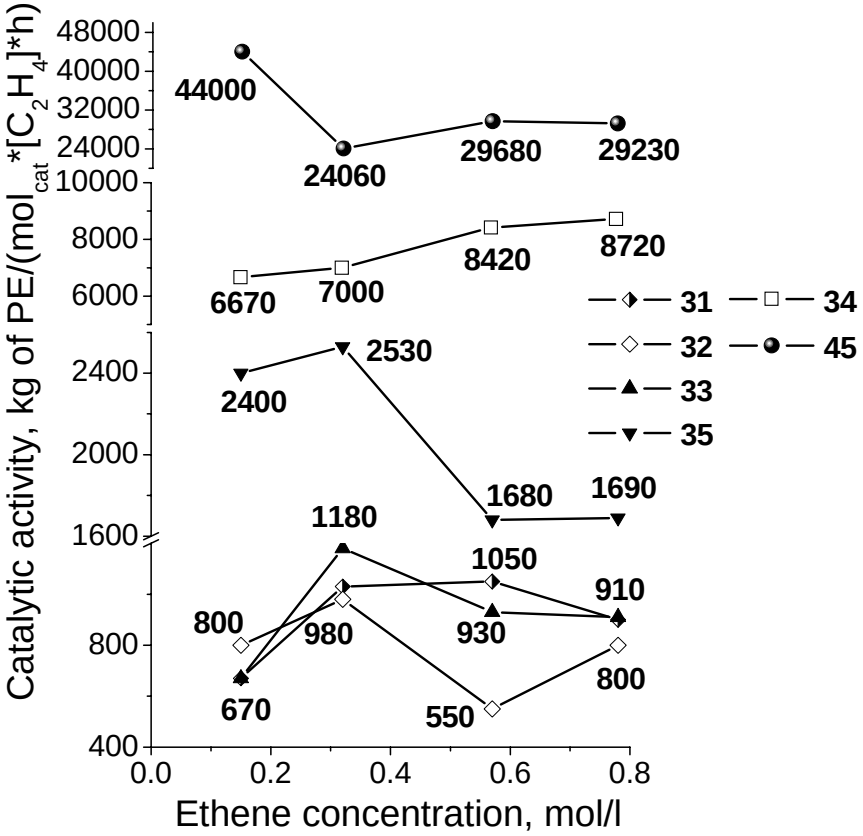

Figure 22. Catalytic activity of complexes as a function of ethene concentration for [(PhN)(*t*BuNP)]$_2$ZrCl$_2$ (**31**), [(Ph_2CHN)(*t*BuNP)]$_2$ZrCl$_2$ (**32**), [(2,6-$Et_2C_6H_3$N)(*t*BuNP)]$_2$ZrCl$_2$ (**33**), [(2,6-*i*$Pr_2C_6H_3$)(*t*BuNP)]$_2$ZrCl$_2$ (**34**), [(2,5-*t*$Bu_2C_6H_3$N)(*t*BuNP)]$_2$ZrCl$_2$ (**35**), [(*t*BuN)(*t*BuNP)]$_2$ZrCl$_2$ (**45**) as catalyst precursors. Experimental conditions: MAO (Al/M = 1000), polymerization temperature 50 ºC[II]

The benzyl Ti and Zr derivatives **39**-**43** and **46**-**48** were also studied as catalyst precursors for ethene polymerization. Unfortunately, the high air and moisture sensitivity and thermal instability of the parent complexes, as well as the species activated by $B(C_6F_5)_3$ or MAO, prevented the obtaining of high quality data. The complexes activated by $B(C_6F_5)_3$ showed very low catalytic activity. In further experiments, where MAO was the activator, polymerization activities were

moderate to high. However, in all experiments, some precatalyst decomposition was detected even before the start of polymerization. As a result, two or more kinds of catalytic species may have been present in the polymerization mixture. Indeed, according to GPC measurements, most of the polymers had bimodal molecular mass distribution and consisted of high and low molecular mass fractions (See example on Figure 23).[IV]

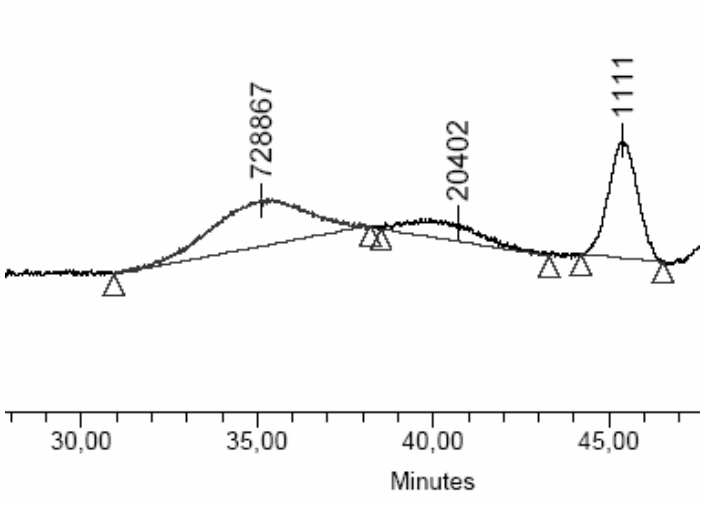

Figure 23. GPC of the polyethene produced with complex **39** ([(2,6-*i*-$Pr_2C_6H_3N$)(*t*-BuNP)]$_2$Ti(CH_2Ph)$_2$)[IV]

Heavier components had similar M_w values to those of the corresponding dichloro Ti and Zr complexes (**27-35**); lighter ones had low molecular masses (around 10000 kg/mol) and probably were produced by products of the original catalyst decomposition (Table 1).[IV]

Table 1. Ethene polymerization data for benzyl Ti and Zr complexes [a]

entry	catalyst	conc. (μmol)	reaction temp. (°C)	MAO/M	yield (g)	activity[b]	M_w (1)	M_w (2)
1	**39**	20	20	2000	1.1	110	1.45×10^6	6.9×10^4
2	**41**	20	20	2000	1.5	150	5.4×10^5	9.4×10^4
3	**42**	10	20	1000	0.46	92	9.7×10^5	1.6×10^4
4	**46**	10	20	1000	0.53	106	-[c]	-
5	**47**	20	40	2000	3	300	1.06×10^6	1.1×10^4
6	**48**	5	20	1000	11.5	4600	4.9×10^5	2.2×10^4

[a]200 ml of toluene, pressure of ethylene 4 bar, polymerization time 30 min; [b]kg PE/($mol_{cat}\times h$); [c]polymer stacked on the filters in Waters chromatograph.

t-Butyl-substituted Ti and Zr derivatives **41** and **48** showed highest polymerization activities in the series of benzyl complexes. In the case of the Ti catalyst **41**/MAO, fast decline in catalytic activity has observed during the polymerization. In the set of benzyl Ti and Zr cyclodiphosph(III)azane derivatives bearing bulky aryl groups the complexes **39** and **47**, having large 2,6-*i*-$Pr_2C_6H_3$ substituents, were the most catalytically active.[IV] Comparison of Ti and Zr catalysts with the same R substituent $[(RN)(t\text{-BuNP})]_2MX_2$ (X = Cl or CH_2Ph) shows them to have similar catalytic behavior in ethene polymerization regardless of the nature of the X groups. This means that the actual active species have the same or a closely related structure regardless of the X group. This finding is in accordance with largely accepted activation mechanism for the homogeneous catalytic ethene polymerization (see above).

Hf methyl and chloro complexes (**36**, **37**, **49**-**51**) showed poor ability to catalyze the polymerization of ethene. Also in this case the catalysts bearing *t*-Bu groups, $[(t\text{-BuN})(t\text{-BuNP})]_2HfX_2$ (X = Cl or Me), exhibited highest polymerization activity among Hf derivatives.[III]

On the basis of the experimental data it can be concluded that the nature and size of the amido substituents play a strong role in defining the catalytic activity of the group 4 metal *cis*-bis(amido)cyclodiphosph(III)azane derivatives as well as the properties of the polymers.

4.3.5 Activation studies[III,IV]

The presence of an electron-rich phosphorus-nitrogen ring in the vicinity of the metal center in *cis*-bis(amido)cyclodiphosph(III)azane complexes raises the question of the site for MAO coordination during the activation step. To understand the processes occurring during activation and the nature and structure of the true catalytic species involved in olefin polymerization, *cis*-bis(amido)cyclodiphosph(III)azane Ti, Zr, and Hf alkyl complexes were activated with $B(C_6F_5)_3$ and investigated by NMR and X-ray diffraction techniques.

The activated species were generated and NMR studies made in two different media: deuterobenzene and deuterodichloromethane. After activation of $[(t\text{-BuN})(t\text{-BuNP})]_2HfMe_2$ by $B(C_6F_5)_3$ in deuterobenzene, two different signals for Hf-Me protons were observed in ^1H NMR. One of these peaks was the same as before activation and the second could be ascribed to the Hf-Me-B group. The *t*-BuN_{imino} groups in the activated species appeared to be chemically nonequivalent, which may be due to the appearance of an additional donor-acceptor coordination between the P_2N_2 ring and Hf atom in solution. ^{19}F NMR showed the presence of coordinated $[MeB(C_6F_5)_3]^-$ anion in deuterobenzene, while the full dissociation to $LHfMe^+$ and $[MeB(C_6F_5)_3]^-$ was observed in CD_2Cl_2. Presumably, in CD_2Cl_2, according to ^{31}P NMR results, the intermolecular

coordination occurred between naked Hf cations and electron rich phosphorus(III) atoms from an other $LHfMe^+$ species.[III]

The activated Hf complexes **50**, **51** bearing aryl substituents were poorly solubile in benzene. Generated in CD_2Cl_2, however, they stayed in solution and could be investigated by NMR techniques. Unlike *cis*-[(*t*BuN)(PN-*t*Bu)]$_2$HfMe$^+$ dissolved in benzene, they had C_2 molecular symmetry in solution and full dissociation on Hf cation and boron anion.[III] On the basis of NMR investigations it can be proposed that aryl substituents play an important role in the delocalization of positive charge. The activation of the complexes is presented in Scheme 25.

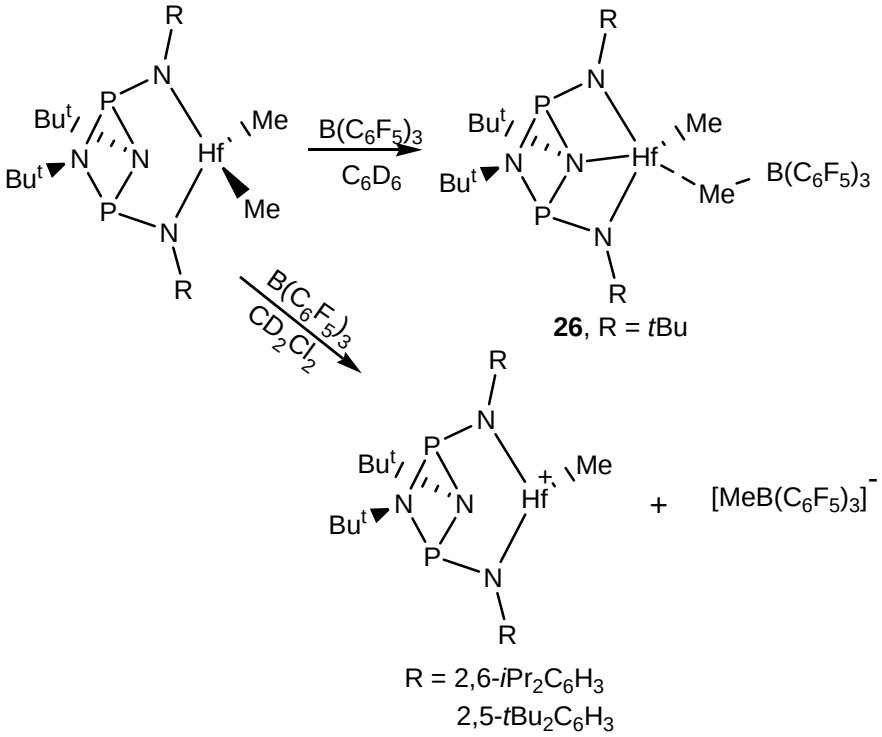

Scheme 25. Activation of Hf complexes bearing *t*-butylamido or bulky anilido groups [III]

The cationic nonmetallocene complexes are generally characterized by poor stability, and solid-state structures are few. The solid-state structures of {[(*t*-BuN)(*t*-BuNP)]$_2$HfMe$^+$[MeB(C$_6$F$_5$)$_3$]$^-$} (**52**) and its parent complex **49**, [(*t*-BuN)(*t*-BuNP)]$_2$HfMe$_2$, were successfully resolved by single-crystal X-ray analysis.[III]

In both complexes the central Hf atom has a distorted trigonal bipyramidal configuration defined by two amido-hafnium bonds, two hafnium-methyl bonds and an additional coordination of the metal with one of the imino nitrogen atoms in the cyclodiphosph(III)azane ring (Figure 24). In compound **49** the Hf-Me bonds are equidistant (2.254(5) Å), while in **52** the coordination of B(C$_6$F$_5$)$_3$ to one of the hafnium methyl groups causes significant elongation of the Hf-C61 bond (2.473(5) Å *vs.* 2.228(6) Å for Hf-C21). The C61-B bond is short (1.673(8) Å) and the configuration of the boron

atom is close to tetrahedral, as is common for anionic tetracoordinated boron species. As a result, **52** in solid state can be considered a tight ion pair ($[LHfMe]^+[MeB(C_6F_5)_3]^-$), where the hafnium cation is weakly associated with a borate anion.[III] This association may be provided *via* agostic Hf-H-B interactions.

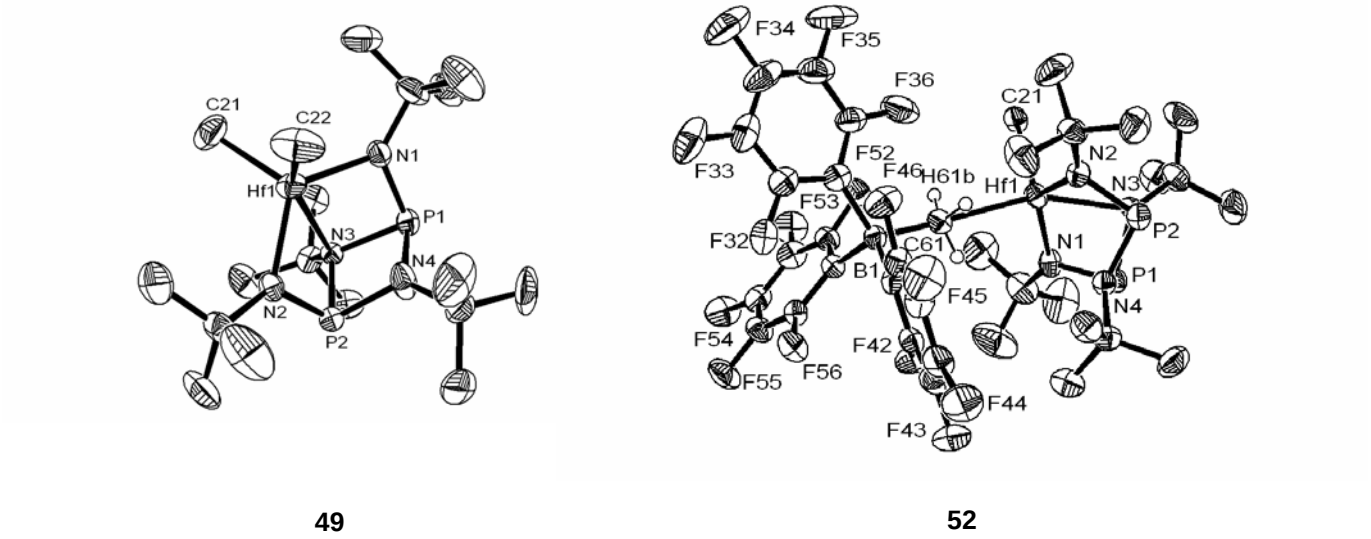

49 **52**

Figure 24. Solid-state structures of the cationic Hf bis(amido)cyclodiphosph(III)azane **52**, {[(*t*-BuN)(*t*-BuNP)]$_2$HfMe$^+$[MeB(C$_6$F$_5$)$_3$]$^-$}, and its parent complex **49**, [(*t*-BuN)(*t*-BuNP)]$_2$HfMe$_2$ [III]

The increased, relatively to the parent complex, Lewis acidity of the central atom in **52** is seen in the shortening of the donor-acceptor Hf-N$_{P2N2}$ coordination (2.315(4) Å *vs*. 2.428(3) Å in **49**). Also the uncoordinated second imino nitrogen in the P_2N_2 ring moves closer to Hf, causing puckering of the P_2N_2 ring (2.765(5) Å for Hf-N4 in **52** *vs.* 3.000(5) Å in **49**). The Me-Hf-Me angle is slightly diminished from 104.2(2)° in **49** to 100.4(2)° in **52**.

The B(C$_6$F$_5$)$_3$ activation of the Ti and Zr benzyl complexes was carried out in the same way as described for the Hf derivatives. In this case, however, [D$_6$]-benzene could not be used because of the poor solubility of the activated Ti and Zr species. The cation generation and NMR investigations were therefore performed in CD_2Cl_2 instead. In ^{1}H NMR study of [(*t*-BuN)(*t*-BuNP)]$_2$Zr(CH$_2$Ph)$_2$/B(C$_6$F$_5$)$_3$ and the analogous Ti derivative **43**/B(C$_6$F$_5$)$_3$, two kinds of benzyl groups were observed: B-CH$_2$Ph (broadened signal at 2.8 ppm, triplets at 6.84 and 6.96 ppm, and doublet at 6.71 ppm) and M-CH$_2$Ph (Ti-CH$_2$Ph sharp peak at 2.9 ppm, Zr-CH$_2$Ph sharp peak at 3.1 ppm, Ph group multiplet at 7.0-7.21 ppm). The proton signals of Zr-CH$_2$ were shifted downfield compared with those of the parent complex (3.10 ppm *vs.* 2.45 ppm). These data are consistent with the cleavage of one of the M-CH$_2$Ph bonds by B(C$_6$F$_5$)$_3$ followed by formation of the [(*t*-BuN)(*t*-

BuNP)]$_2$M(CH_2Ph)$^+$ cation and borate $PhCH_2B(C_6F_5)_3^-$ anion in the same was asfor the Hf complexes (Scheme 25).[IV] Comparable ^{1}H NMR spectra were obtained for the activated 2,5-$Bu_2C_6H_3$ substituted Ti dibenzyl and Zr monobenzyl derivatives **40** and **46** (with the exception of M-CH_2Ph signal). Activated Ti and Zr complexes **39** and **47** bearing 2,6-*i*-$Pr_2C_6H_3$ groups, in turn, appeared to be highly unstable in CD_2Cl_2 and rapidly (in a few minutes) decomposed to the corresponding phosph(III)azane ligand. The partial decomposition of the cation was also detected in the activation of **40**, **43**, **46**, **48.** The Ti and Zr cationic species are thus highly unstable in dichloromethane.

The ^{19}F NMR spectra showed that $PhCH_2B(C_6F_5)_3^-$ anion was not coordinated to the cationic metal center. Regardless of the ligand substitution, the positions of the $PhCH_2B(C_6F_5)_3^-$ peaks in ^{19}F NMR were about the same. The absence of recognizable cation-anion contacts means that the metal center is coordinatively unsaturated. The possibility to bind the additional ligands was shown in the experiments with trimethylphosphine. Despite the cation-Me_3P interactions observed in ^{31}P NMR, no changes were detected in ^{19}F NMR, which is consistent with the uncoordinated character of the $PhCH_2B(C_6F_5)_3^-$ anion.[IV] The unsaturation of the complex cations may be associated with their instability in CD_2Cl_2 solution. Decomposition of activated complexes can be initiated by the coordination of solvent to the metal center. The decomposition of [(*t*-BuN)(*t*-BuNP)]$_2$Ti(CH_2Ph)$_2$ (**43**)/$B(C_6F_5)_3$ occurred via phosph(III)azane ring degradation.[IV] Indeed, such lability of the P_2N_2 ring in **43**/$B(C_6F_5)_3$ may also be the reason for fast deactivation in the ethene polymerization of the Ti catalysts **38** and **41** bearing *t*-Bu groups.

The activity of the catalysts in ethene polymerization may be associated with the electrophilicity of the central atom in cationic species. In the case of the bis(amido)cyclodiphosph(III)azane group 4 metal derivatives, the relative electrophilicity of the metal center can be defined by the shift ($\Delta\delta_P$) of the ^{31}P NMR peak of the cationic species from the position of the ^{31}P NMR signal of parent alkyl complex. The largest $\Delta\delta_P$ were observed for the most active [(*t*-BuN)(*t*-BuNP)]$_2$$MX_2$ complexes, while $\Delta\delta_P$ close to zero were obtained for the much less active aryl-substituted [(ArN)(*t*-BuNP)]$_2$$MX_2$.[III,IV]

The solid-state structures of the activated [(*t*-BuN)(*t*-BuNP)]$_2$Zr(CH_2Ph)$_2$·Et_2O/$B(C_6F_5)_3$ (**53**), and of the parent complex **48,** were investigated by single-crystal X-ray diffraction methods. In both compounds the central zirconium atom has highly distorted trigonal bipyramidal configuration. In complex **48,** two amido nitrogens, two carbon atoms (from $PhCH_2$ groups), and one donor nitrogen of the P_2N_2 ring are located at the vertices of the coordination polyhedron, while in the related cation **53** the coordination sphere of the central atom is defined by two Zr-N_{amido}, one Zr-O_{Et2O}, one donor-acceptor Zr-N_{P2N2} bond and η^2-coordination to benzyl group (Figure 25).[IV] The presence of

the additional donor-acceptor interactions with phosph(III)azane ligand and Et_2O, as well as binding of the $PhCH_2$ substituent in η^2-fashion, define the positively charged complex **53** as a $16e^-$ species. The complex saturation despite the positive charge on the Zr atom appears in the only slightly shortened the donor-acceptor Zr-N_{P2N2} bond relative to that in the parent complex **48** (2.423(3) Å *vs.* 2.4755(16) Å),[IV] the opposite situation was observed for the highly electron deficient {[(*t*-BuN)(*t*-BuNP)]$_2$HfMe$^+$[MeB(C_6F_5)$_3$]$^-$} (see above).[III]

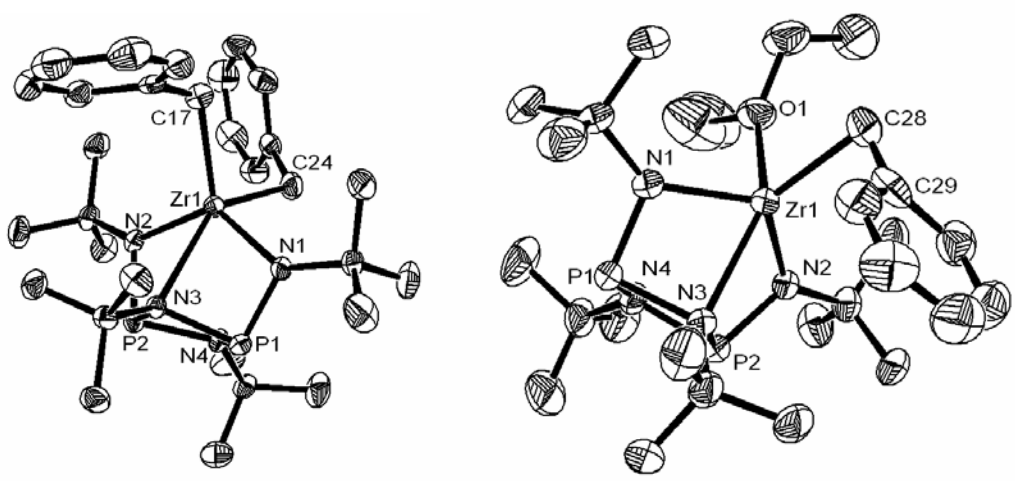

48 **53**

Figure 25. Solid-state structure of cationic Zr bis(amido)cyclodiphosph(III)azane **53**, {[(*t*-BuN)(*t*-BuNP)]$_2$Hf Zr(CH_2Ph)(Et_2O)$^+$[$PhCH_2B(C_6F_5)_3$]$^-$}, and its parent complex **48**, [(*t*-BuN)(*t*-BuNP)]$_2$Zr(CH_2Ph)$_2$[IV]

The Zr-CH_2Ph bonds in **48** and **53** are almost equidistant (2.278(2) Å and 2.248(4) Å, respectively). In cation **53** the benzyl substituent is connected with the central atom in η^2-fashion with Zr-C29 distance 2.697(4) Å, the same type of coordination type does not appear in the parent complex **48**.[IV]

The structures of the activated complex **48**/B(C_6F_5)$_3$ and **53** in solution were investigated by means of ^{1}H and ^{13}C NMR methods. The positions of the methylene protons as well as the aromatic protons (from BCH_2Ph and $ZrCH_2Ph$ groups) in ^{1}H NMR spectra of **53** (C_6D_5Br or CD_2Cl_2 were used as solvents) were similar to those observed for B(C_6F_5)$_3$ activated Ti and Zr complexes (see above). In ^{13}C NMR (C_6D_5Br) spectrum of **53,** the signal for methylene carbon of Zr-CH_2Ph group appears at 70.2 ppm, and the signal for C_{ipso} atom of Zr-CH_2Ph group was found at 148.6 ppm. Similar shifts for the carbon atoms of the benzyl group were found in ^{13}C NMR spectra of **48**/B(C_6F_5)$_3$. Despite of the Zr-η^2-CH_2Ph coordination displayed for **53** in solid state, it can be concluded then, that in solution the benzyl group coordinates to the central atom with η^1-fashion.

4.4 Bis(imino)cyclodiphosph(V)azane ligands

The coordination chemistry of multidentate cyclodiphosph(V)azanes has attracted considerable attention in recent years.[106] Prepared from the corresponding cyclodiphosph(III)azanes by oxidative addition, these ligands have two kinds of chelating groups: One an electron donor bonded with phosphorus(V) by single bond (usually amino group) and the other an electron donor connected with phosphorus(V) by double bonds (usually O, S etc.) (Figure 26 a). The goal of the work was to synthesize bidentate cyclodiphosph(V)azans capable of coordinating to a metal atom presumably at the facial site of the ligand (Figure 26 b).

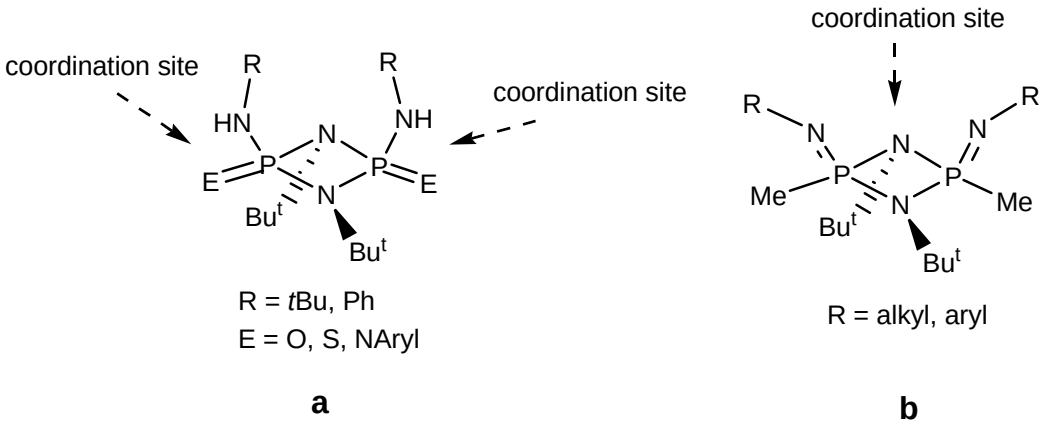

Figure 26. Structures of cyclodiphosph(V)azane complexes used for side coordination of the metal (a) and proposed for facile coordination of the central atom (b).

4.4.1 Ligand preparation[V]

Starting from the already known compound *cis*-[(*t*-BuNP)$_2$Cl$_2$] (**16**), a very labile methyl derivative **54**[107] was obtained (Scheme 26) in low, but reasonable yield for the ligand synthesis.[V] This compound was introduced into the Staudinger reaction with three different organic azides: Me_3SiN_3,[107] AdN_3 (Ad = 1-adamantyl), and 2,6-di-*i*-$Pr_2C_6H_3N_3$. The bis(imino)cyclodiphosph(V)azane ligands **55-57** formed selectively and in high yield. According to ^{31}P NMR, imino substitiuents had *cis* configuration, although admixtures of the *trans* isomers were also detected. The presence of small Me groups at phosphorus(V) stabilizes the desired *cis*-configuration of the molecules.[96]

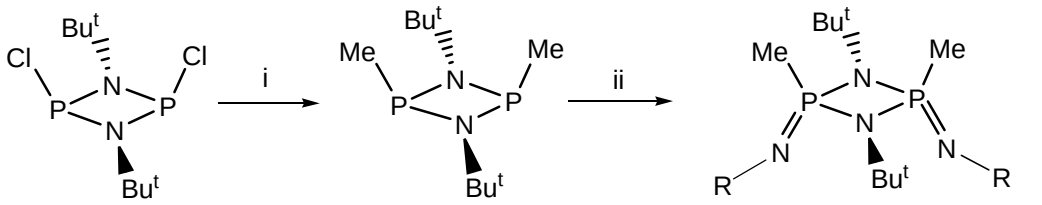

16 **54**

55, R - Me_3S i
56, R - 2,6-*i*-$Pr_2C_6H_3$
57, R - 1-adamantyl

i - MeLi, Et_2O, -50 ^{0}C; ii - RN_3, reflux in toluene

Scheme 26. Synthesis of the bis(imino)cyclodiphosph(V)azane ligands[V]

4.4.2 Ligand structure[V]

The solid-state structure of [($Bu^tNPMe)_2(Me_3SiN)_2$] (**55**) was resolved by single-crystal X-ray diffraction analysis. However, the crystals obtained for X-ray measurements represented the **55** in *trans* configuration. Evidently, the product was contaminated by the *trans* isomer (see above), which seems to crystallize better than the *cis* form (Figure 27). The molecule is highly symmetric and has a center of inversion. The P_2N_2 ring is almost planar and P-N bonds in the ring are of equal length. The exocyclic phosphorus-nitrogen groups have *exo* orientation relative to the phosphazane ring. The phosphoimino bonds are much shorter than P-N distances in the P_2N_2 ring (1.528 Å *vs.* 1.697 Å) which confirms the multiple PN connection in P=N$SiMe_3$ substituents. The lengths of the Si-N_{imino} bonds are also different from the classical Si-N_{amino} case. The shortening of Si-N bonds in **55** could be due to the donation of electron density from occupied π orbital of P=N double bonding to the empty d orbitals of Si atoms. This is supported by the differences in Si-N bond lengths in the solid structure of $(Me_3Si)_2NP(NSiMe_3)_2$, where there are two types of Me_3Si groups, bonded with either amino or imino nitrogens.[108] Yet another explanation is possible: in the imino nitrogen atom, sp^2 orbitals have more s character and the maximum of the electron density is closer to the nuclei compared with the electron density distribution at sp^3 hybridized amino nitrogen, and this leads to shortening of Me_3Si-N_{imino} bonds.[V]

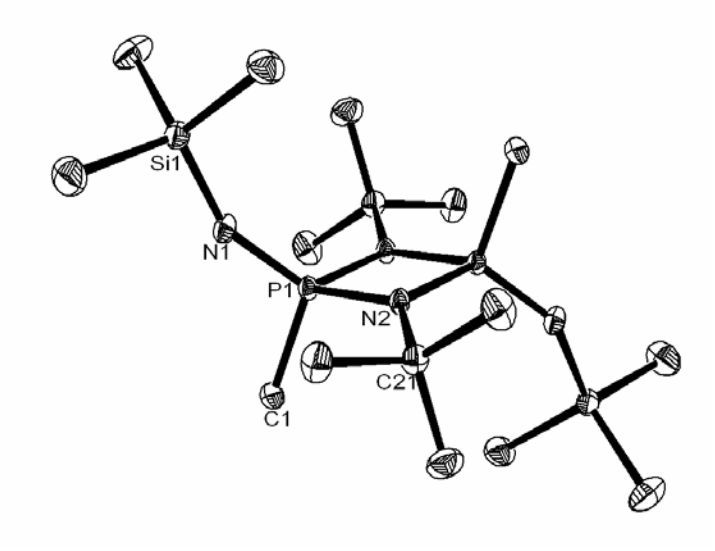

Figure 27. Solid-state structure of *trans*-[($Bu^tNPMe)_2(Me_3SiN)_2$] (**55**)[V]

4.5 Late transition metal complexes of bis(imino)cyclodiphosph(V)azanes

4.5.1 Synthesis[V]

The newly synthesized ligands **55-57** were reacted with $FeCl_2$, $CoCl_2$, and $NiBr_2$ (Scheme 27).[V]

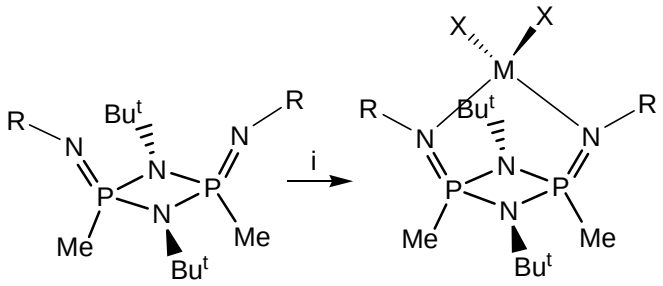

R	MX_2		
	$FeCl_2$	$CoCl_2$	$NiBr_2$
Me_3Si	green (**58**)	blue (**61**)	green (**64**)
2,6-di-*i*$Pr_2C_6H_3$	dark blue (**59**)	green (**62**)	olive (**65**)
1-adamantyl	brown (**60**)	blue (**63**)	-

i - MX_2, reflux in THF

Scheme 27. Preparation and color of bis(imino)cyclodiphosph(V)azane late transition metal complexes[V]

They displayed a mild ability to coordinate with the metals, and only moderate yields were achieved. To increase the yield, the reactions were carried out in polar aprotic coordinating solvents like THF, at elevated temperatures. Owing to its polymeric structure, $NiBr_2$ revealed the poorest complexation activity in the series $FeCl_2$, $CoCl_2$, and $NiBr_2$, and all attempts to obtain adamantly-substituted Ni complex failed.

4.5.2 Structure[V]

The Ni, Fe, and Co complexes were isolated as differently colored solids (Scheme 27). As was expected, they appeared to be paramagnetic, and their composition could be confirmed only by MS and elemental analysis. However, complexes bearing 2,6-*i*-$Pr_2C_6H_3$ groups provided reliable ^1H, ^{13}C, and ^{31}P NMR spectra. The NMR data revealed the coordination of metal to the ligand **56,** and C_{2v} symmetry was established for Fe, Co, and Ni complexes of **56** in solution.[V]

4.5.3 Ethene dimerization and oligomerization[V]

In the family of the late transition metal olefin polymerization catalysts, Fe, Co, and Ni complexes incorporating bulky diimino ligands have shown exceptionally high catalytic activity.[10] Compounds containing phosphoimino substituents display similar coordination properties to ketimines and aldimines, which have been used in the preparation of highly active late transition metal catalysts. Recently, it was reported that complexes bearing bulky phosph(V)imino ligands are capable of polymerizing ethene.[109] The bis(imino)cyclodiphosph(V)azane Ni, Fe, and Co complexes studied here can be considered as analogues of Brookhart's α-diimino Ni(II) and Pd(II) derivatives, which display high ethene polymerization activity.[110]

All synthesized late transition complexes **58** – **65** were assessed in ethene polymerization studies.[V] Polymerization experiments made in the presence of Ni or Co complexes activated by MAO revealed a high level of ethene consumption. Surprisingly, no polymer was found in the resulting product mixture. The GC-MS investigations showed that, instead of ethene polymerization, the phosph(V)azane-based catalysts **61** – **65** produced merely a mixture of olefins. The presence of C_4 to ~ C_{20} alkenes was detected.[V]

Iron bis(imino)cyclodiphosph(V)azane derivatives **58** - **60** displayed low catalytic activity. Activated with MAO, Ni catalysts **64**, **65** gave products with high (up to 95%) content of butene (the result of ethene dimerization), while the Co complexes **61** – **63** produced mixtures of low molecular mass C_4 – C_{20} oligomers (Table 2).[V]

Table 2. Ethylene dimerization and oligomerization results obtained for the complexes **61**-**65**.[a]

comp.	ethene cons. (l)	activity $kg/mol_{cat}*h$	C_4[b] (wt%)	C_6 (wt%)	C_{10} (wt%)	C_{12} (wt%)	C_{14} (wt%)	C_{16} (wt%)	C_{18} (wt%)
61	6.15	1550	14	15	14	13	12	10	7
62	5.98	1510	19	19	14	11	8	7	5
63	2.84	720	71	10	5	4	5	5	-
64	6.03	1590	89	10	1	-	-	-	-
65	4.44	1120	94	6	-	-	-	-	-

[a] Oligomerization conditions: toluene 200 ml, ethene pressure 8 bar, oligomerization temperature 30 ºC, Al/M ratio 1000.
[b] C_8(wt%) was calculated on the basis of α value: 15% for **61**, 17% for **62**.

Today, about one-half of the linear α-olefins are ethene oligomers produced by late transition metal catalysts.[111a] The most best-known commercial process for linear α-olefin production is SHOP (Shell High Olefin Process), in which the oligomerization reaction is carried out by Ni complexes bearing P∩O bidentate ligands.[112] Other types of late transition metal complexes, based on cyclopentadienyl,[113] bidentate diimine,[114] bis(imino)pyridyl,[115] phosphinopyridine,[116] and chelate P∩O ligands,[117] were recently tested for selective ethene dimerization and oligomerization.[118]

The ethene oligomerization activities of the bis(imino)cyclodiphosph(V)azane complexes are in the range of the values observed for the known olefin oligomerization catalysts (see Table 2 and references above).[V] Complexes **61** – **65** showed different stability in ethene oligomerization according to the central metal atom. At the beginning of the oligomerization process, the activity of the Co catalysts was higher than that of the Ni complexes, but Co catalysts were deactivated faster, as seen in the swift decline in ethene consumption. Despite these differences in catalytic behavior, Co and Ni complexes based on the same ligands displayed similar levels of productivity in ethene oligomerization (Table 2). The Co catalysts, as well as the Ni derivatives, showed high thermal sensitivity, and at 70 ºC no ethene consumption was observed. Despite the noticeable influence of temperature on the complex catalytic activity, the olefin distribution in the resulting products varied only slightly with temperature. In the case of the ethene dimerization catalyzed by Ni complexes, the yield of the C_4 fraction was slightly increased at elevated temperatures.[V]

In the ethene dimerization and oligomerization experiments, the bis(imino)cyclodiphosph(V)azane Co and Ni complexes **61** – **65** showed similar behavior to the late transition metal catalysts used in SHOP (Shell Higher Olefin Process).[111] Many new late transition metal complexes capable of ethene oligomerization have been reported in recent years. Species containing M-H bonds are largely accepted to be catalytically active sites for this process (Scheme 28).[111a] To draw full analogy with the postulated mechanism, the bis(imino)cyclodiphosph(V)azane Co or Ni hydride

species are proposed as catalytically active intermediates in ethene dimerization and oligomerization.

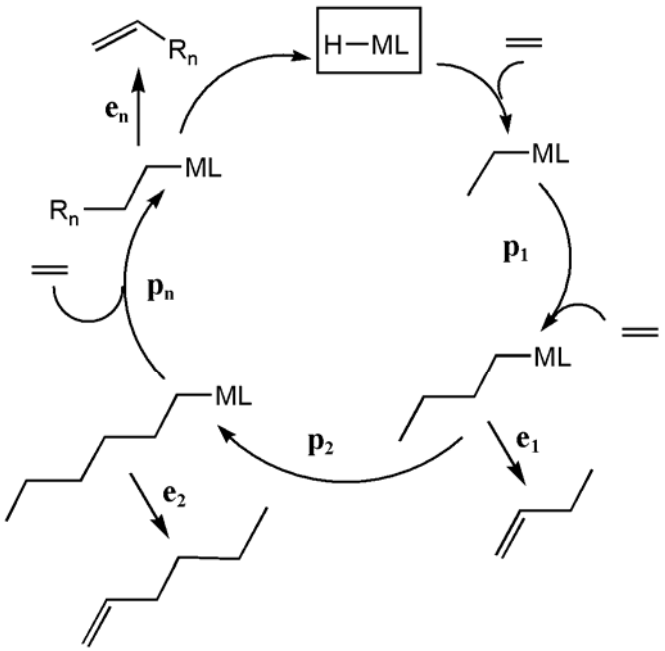

Scheme 28. The proposed catalytic cycle of olefin oligomerization[111a]

Several detailed ^{1}H NMR experiments with Ni complex **61** bearing Me_3Si groups were performed in deuterobenzene to explore the ethene dimerization. Signals of C_4 olefins, toluene (from MAO solution), and a small amount of C_6 fraction were found in the obtained spectra. According to the ^{1}H NMR data, the ratio of butenes-2 to butene-1 was 1.6-1.7:1 and the *trans*-butene-2 dominated in the mixture of the butenes-2 with ratio 1.4-1.7:1.[V] These results are in agreement with values of ΔH reported for formation of the different butenes. Such butene distribution may be a result of the fast isomerization process. It has been proposed that olefin isomerization is catalyzed by the same M-H species as are responsible for ethene oligomerization.[119]

4.5.4 Propene dimerization and ethene-propene codimerization[V]

Propene dimerization experiments were carried out with all synthesized Ni and Co complexes (**61** – **65**). Under the conditions used (polymerization temperature 20 °C and propene pressure 7 bar), Co catalysts **61** – **63** exhibited very low activity in propene dimerization, while the Ni bis(imino)cyclodiphosph(V)azane derivatives **64** and **65** showed high productivity (Figure 28). GC-

MS investigations indicated that both Ni and Co catalysts produce C_6 olefins. As well, the traces of C_9 and C_{12} olefin fractions were detected.[V]

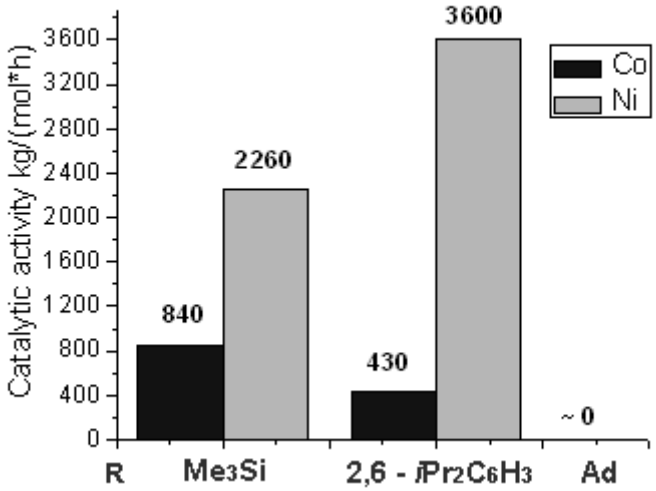

Figure 28. Catalytic activity of $[(Bu^tNPMe)_2(RN)_2]MX_2$ (M = Co, X = Cl; M = Ni, X = Br) in propene dimerization.

An analysis of all possible propene-propene combinations (Scheme 33), that could appear in the propene dimerization process, indicated nine hexenes (12 if *cis*/*trans* isomers are counted). Six different alkenes were found in ^1H and ^{13}C NMR spectra of the product mixtures obtained with Ni complex **65**: hexene-1, hexenes-2, hexenes-3, 4-methyl-1-pentene, 4-methyl-2-pentenes, and 2,3-dimethyl-1-butene. ^1H and ^{13}C NMR spectra of olefins (from Aldrich) measured in pure state and as mixtures confirmed the analysis. The products of the propene dimerization were also investigated by GC-MS, with the same results (Figure 29 and Table 3).[V]

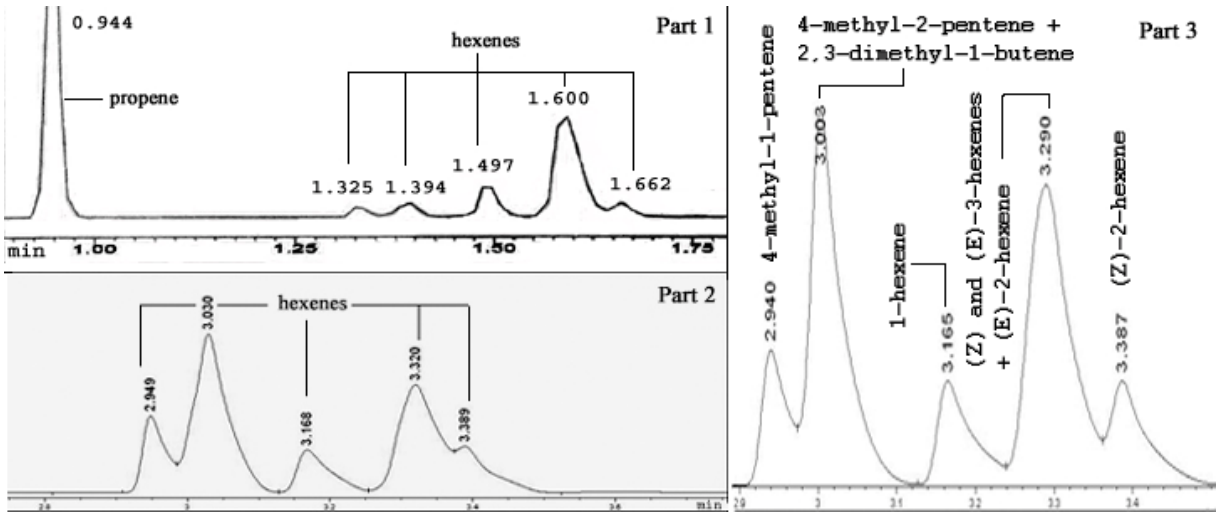

Figure 29. Gas chromatograms of products obtained with Co complex **61** (Part 1) and Ni complex **65** (Part 2). Comparison is made with the Gas chromatogram observed for mixture of pure 4-methyl-1-pentene, 4-methyl-2-pentene, 2,3-dimethyl-1-butene, 1-hexene, (Z) and (E) 2- and 3-hexenes (Part 3)[V]

Table 3. Comparison of product mixtures from propene dimerization experiments

catalyst	1-hexene (%)	2-hexene and 3-hexene (%)	4-methyl-1-pentene (%)	4-methyl-2-pentene and 2,3-dimethyl-1-butene (%)	C_6 total (wt%)	C_9 (wt%)	C_{12} (wt%)
61	13	71	7	9	83	13	4
62	20	65	5	10	65	24	11
64	5	42	10	43	~100	<1	<1
65	5	53	9	33	~100	<1	<1

According to Scheme 29, 1-hexene can form through 1,2-propene insertion into the M-H bond followed by 2,1-insertion, while 2-methyl-1-pentene is the result of the 1,2-1,2 insertion sequence. 2,3-Dimethyl-butene-1 can be formed by 1,2 insertion of propene into the M-*i*Pr cation, and 2-methyl-1-pentene, alternatively, by 2,1 insertion of propene into this M-*i*Pr cation (Scheme 29).

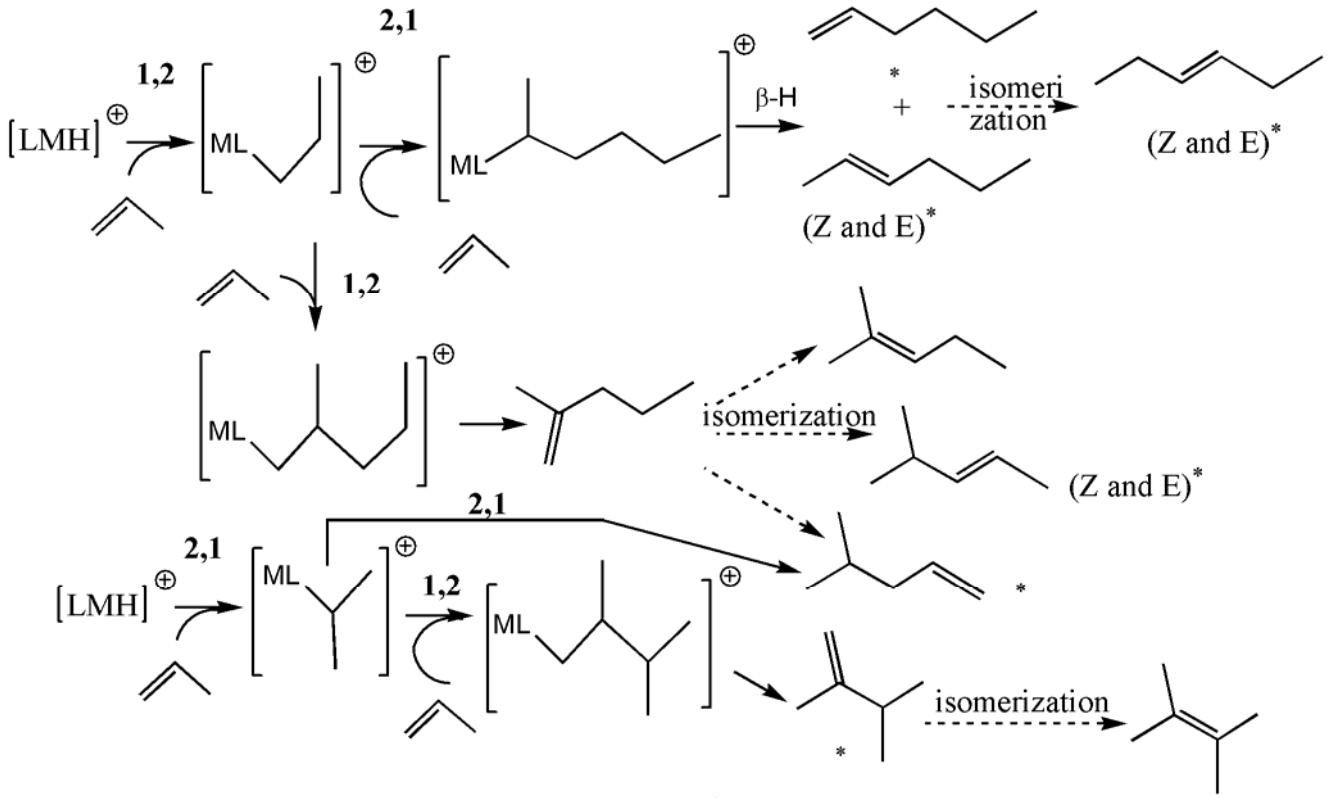

Scheme 29. Possible routes for formation of the different hexenes during the dimerization process[V]

The GC data (Table 3) indicates that the 1,2-2,1 propene insertion sequence prevails for the Co complexes **61** and **62**, and the content of the n-hexenes is high. In the propene dimerization process provided by Ni catalysts **64** and **65**, the two insertion pathways (1,2-2,1 and 1,2-1,2) are of equal probability and the content of the branched hexenes is increased in the product mixtures.[V]

Note, that 2-methyl-1-pentene was not present among the propene dimerization products. In addition, the content of 1-hexene was not high. This can be explained by the fast isomerization that was occurring. Hexene isomerization can be catalyzed by the same complex species that provides the propene dimerization, analogously to the butene isomerization occurring in ethene dimerization. The distribution of the alkenes in the series: 1-hexene, 2-hexenes, 3-hexenes, as well as in the products of 2-methyl-1-pentene isomerization, corresponds to the order of thermodynamic stability of hexenes. Absence or low content of the kinetic products, like 2-methyl-1-pentene or hexene-1, is consistent with low activation energy of the isomerization process.

Since the Ni bis(imino)cyclodiphosph(V)azane derivatives exhibited high activity in propene as well as ethene dimerization, ethene-propene codimerization with Ni catalysts was expected. The reaction was carried out in propene-ethene atmosphere. According to GC investigations of the products, a mixture of three fractions (C_4, C_6 and C_5 olefins) was obtained (Figure 30). The pentene

olefins were present as a result of the expected ethene-propene dimerization. The content of the pentenes in the dimerization product directly depended on the initial propene concentration (Figure 30). Such behavior may follow from the probably small energy difference between ethene and propene insertion into Ni-alkyl bond in the case of the bis(imino)cyclodiphosph(V)azane Ni catalysts.

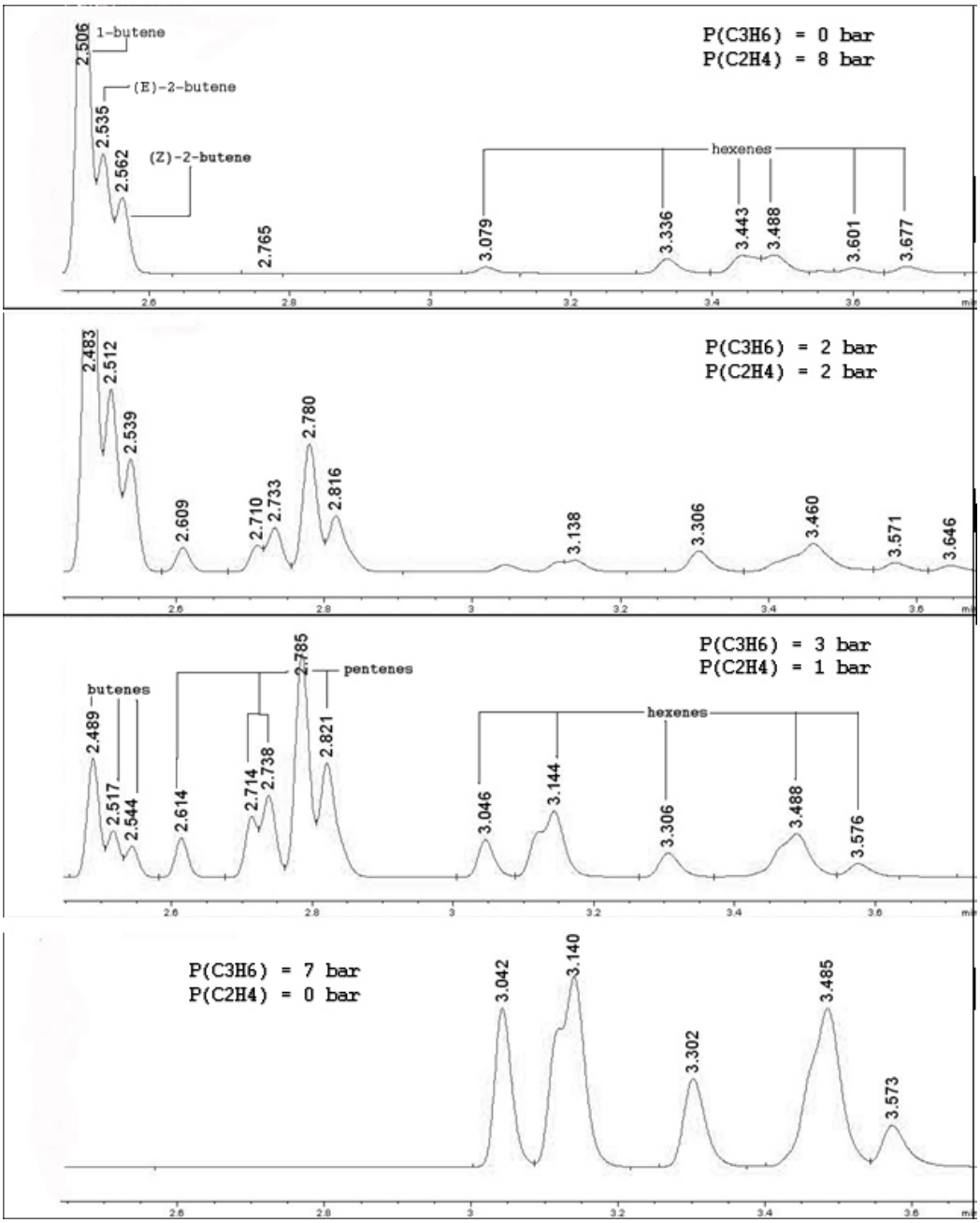

Figure 30. Analysis of the product mixtures of propene-ethene codimerization made with complex **65** by GC

Shielding of the metal center by bulky aryl may make the ethene coordination and subsequent insertion into Ni-ethyl or Ni-propyl bond preferable to the incorporation of propene. As a result of

this steric control, the formation of the ethene-ethene or ethene-propene co-dimers may be preferred to the formation of propene-propene dimers. Greater butene and pentene contents were observed in the alkene mixtures produced by Ni catalyst **65** bearing large 2,6-diisopropylphenyl groups, indicating that steric control really was occurring in the case of complex **65**.

5 Conclusions

New early and late transition metal complexes based on the cyclodiphosphazane ligand framework were synthesized and investigated. Cyclodiphosph(III)azane complexes of group 4 metals were obtained through direct ligand metallation with Ti, Zr or Hf tetrakis(dimethylamides). In solid state an additional donor-acceptor ligand-metal coordination was observed, while in solution the compounds revealed C_2 molecular symmetry. Direct alkylation with Grignard reagents led to the corresponding group 4 metal bis(amido)cyclodiphosph(III)azane alkyl complexes.

Chloro and alkyl Ti and Zr derivatives revealed moderate to high catalytic activity in ethene polymerization and produced high molecular mass polyethene. The size and nature of the ligand substitution plays a noticeable role in defining the catalytic behavior of these complexes. Irrespective of the nature of the X groups in $[(RN)(t\text{-BuNP})]_2MX_2$ (M = Ti, Zr; R = alkyl or bulky aryl), complexes bearing the same R substituents exhibited similar catalytic behavior in ethene polymerization. This means that, catalytic species active in ethene polymerization have same or closely related structure, whatever the X group is. This is consistent with the accepted activation mechanism of homogeneous olefin polymerization. The activation studies showed that, in spite of the presence of electron rich phosphorus(III) atoms, the Lewis acidic cocatalysts activate the metal center for ethene polymerization. The electrophilicity of the central atom in bis(amido)cyclodiphosph(III)azane group 4 metal catalytic species defines the catalyst behavior, in particular the catalytic activity of the complex. At the same time, too high electron deficiency on the metal atom leads to destabilization of the phosph(III)azane ring and its breakage in the course of the polymerization reaction, which results finally in catalyst deactivation.

The late transition metal complexes of the bis(imino)cyclodiphosph(V)azanes were obtained by the reaction of free ligands and corresponding metal salts. The nature of the central atom defined the behavior of the complex in ethene and propene oligomerization. After activation with MAO, the Co catalysts produced ethene oligomers with high activity and dimerized propene with low productivity. After MAO activation the Ni complexes dimerized ethene and propene with high

catalytic activity and selectivity. The selective alkene dimerization with Ni catalysts may be related to the high instability of the Ni-alkyl bond against β-hydrogen elimination. Both Co and Ni catalysts are sensitive to harsh conditions, but good catalytic activities can be achieved at mild temperatures and modest MAO concentrations. In propene dimerization catalyzed by Co catalysts, the 1,2-insertion followed by 2,1 propene insertion sequence is the main route for chain propagation. As a result, olefin mixtures with high content of the n-hexenes are produced. In the case of the Ni complexes, the probabilities of 1,2-1,2 and 1,2-2,1 propene insertion sequences seem to be about equal, as reflected in the ratio of the linear/branched hexenes in the products. It is reasonable to assume that bis(imido)cyclodiphosph(V)azane complex species containing M-H bonds are responsible for olefin oligomerization as well as for the observed olefin isomerization. The resulting olefin distribution is defined by thermodynamic rules, and consistent with low activation energy of the isomerization process. In the case of Ni catalysts, the ethene-propene codimerization occurred as a result of the small energy differences between ethene and propene insertion into Ni–alkyl bond.

As shown in this work the cyclodiphosphazane compounds are prospective ligands for the synthesis of new active catalysts for use in olefin poly- and oligomerization processes.

References

(1) (a) Ziegler, K.; Holzkamp, R.; Breil, H.; Martin, H. *Angew. Chem.* **1955**, *67*, 426. (b) Ziegler, K. GB 799823 (Application made in Germany Jan. 19, 1954; issued 1958). (c) Ziegler, K.; Breil, H.; Martin, H.; Holzcamp, E. US patent 3257332 (filled in Nov. 15, 1954; issued 1966). (d) Ziegler, K. *Angew. Chem.* **1964**, *76*, 545.

(2) Stevens, J. C. in *2nd Blue Sky Conference on Catalytic Olefin Polymerization*, 26-29 June 2005, Sorrento, Italy.

(3) (a) Steinert, R. B.; Trishman, C. A.; Santiago, B. G. DE 3317335, Ger. Offen. (1984). (b) Drögemüller, H.; Heiland, K.; Kaminsky, W. *Transition Metals and Organometallics as Catalysts for Olefin Polymerization*; Kaminsky, W.; Sinn, H., Eds.; Springer: Berlin, 1988; p.303.

(4) Kaminsky, W.; Arndt, M. *Applied Homogeneous Catalysis with Organometallic Compounds*; Cornils, B.; Herrmann, W. A., Eds.; VCH: Weinheim, New York, Basel, Cambridge, Tokyo, 1996; Vol. 1, p.5.

(5) (a) Breslow, D. S.; Newburg, N. R. *J. Am. Chem. Soc.* **1957**, *79*, 5072. (b) Breslow, D. S.; Newburg, N. R. *J. Am. Chem. Soc.* **1959**, *81*, 81.

(6) (a) Natta, G.; Pino, P.; Mazzanti, G.; Giannini, U.; Mantica, E.; Peraldo, M. *Chimica e'lIndustria* **1957**, *39*, 19. (b) Natta, G.; Pino, P.; Mazzanti, G.; Lanzo, R. *Chimica e'lIndustria* **1957**, *39*, 1032.

(7) (a) Andersen, A.; Cordes, H. G.; Herwig, J.; Kaminsky, W.; Merck, A.; Mottweiler, R.; Pein, J.; Sinn, H.; Vollmer, H. J. *Angew. Chem.* **1976**, *88*, 689.

(8) (a) Sinn, H.; Kaminsky, W.; Vollmer, H. J.; Woldt, R. *Angew. Chem.* **1980**, *92*, 346. (b) Kaminsky, W.; Miri, M.; Sinn, H.; Woldt, R. *Macromol. Chem., Rapid Commun.* **1983**, *4*, 417.

(9) (a) Kaminsky, W.; Arndt, M. *Applied Homogeneous Catalysis with Organometallic Compounds*; Cornils, B.; Herrmann, W. A., Eds.; VCH: Weinheim, New York, Basel, Cambridge, Tokyo, 1996; Vols. 1 and 2. (b) Alt, H. G.; Köppl, A. *Chem. Rev.* **2000**, *100*, 1205. (c) Brintzinger, H. H.; Fischer, D.; Mülhaupt, R.; Rieger, B.; Waymouth, R. M. *Angew. Chem.* **1995**, *107*, 1255. (d) Shapiro, P. J.; *Coord. Chem. Rev.* **2002**, *231*, 67.

(10) (a) Britovsek, J. P.; Gibson, V. C.; Wass, D. F. *Angew. Chem.* **1999**, *111*, 448; *Angew. Chem., Int. Ed.* **1999**, *38*, 428. (b) Gibson, V. C.; Spitzmesser, K. *Chem. Rev.* **2003**, *103*, 283.

(11) (a) Grocholl, L. P.; Stahl, L.; Staples, R. J. *Chem. Commun.* **1997**, 1465. (b) Moser, D. F., Carrow, C. J.; Stahl, L.; Staples, R. J. *J. Chem. Soc., Dalton Trans.* **2001**, 1246.

(12) (a) Huang, J.; Rempel, G. L. *Prog. Polym. Sci.* **1995**, *20*, 459. (b) Diamond, G. M.; Jordan, R. F.; Petersen, J. L. *J. Am. Chem. Soc.* **1996**, *118*, 8024. (b) Zanella, P.; Mascellani, N.; Cason, A.; Garon, S.; Rossetto, G.; Carta, G. *Appl. Organomet. Chem.* **2001**, *15*, 717.

(13) (a) Cosée, P. *J. Mol. Cat.* **1964**, *3*, 80. (b) Arlman, E. J. *J. Mol. Cat.* **1964**, *3*, 89. (c) Cosée, P.; Arlman, E. J. *J. Mol. Cat.* **1964**, *3*, 99.

(14) (a) For β-hydrogen transfer to monomer: Tsutsui, T.; Mizuno, A.; Kashiwa, N. *Polymer* **1989**, *30*, 428. (b) For β-hydrogen elimination: Burger, B. J.; Thompson, M. E.; Cotter, W. D.; Bercaw, J. E. *J. Am. Chem. Soc.* **1990**, *112*, 1566. Hajela, S.; Bercaw, J. E. *Organometallics* **1994**, *13*, 1147. (c) For chain transfer to aluminum: Resconi, L.; Cavallo, L.; Fait, A.; Piemontesi, F. *Chem. Rev*. **2000**, *100*, 1253.

(15) Scollard, J. D.; McConville, D. H.; Payne, N. C.; Vittal, J. J. *Macromolecules* **1996**, *29*, 5241.

(16) Scollard, J. D.; McConville, D. H. *J. Am. Chem. Soc.* **1996**, *118*, 10008.

(17) Scollard, J. D.; McConville, D. H.; Vittal, J. J.; Payne, N. C. *J. Mol. Cat., Ser. A: Chemical* **1998**, *128*, 201.

(18) Lorber, C.; Donnadieu, B.; Choukroun, R. *Organometallics* **2000**, *19*, 1963.

(19) (a) Ziniuk, Z.; Goldberg, I.; Kol, M. *Inorg. Chem. Comm.* **1999**, *2*, 549. (b) Uozumi, T.; Tsubaki, S.; Jin, J. Z.; Sano, T.; Soga, K. *Macromol. Chem. Phys.* **2001**, *202*, 3279.

(20) (a) Mack, H.; Eisen, M. S. *J. Organomet. Chem.* **1996**, *525*, 81. (b) Tinkler, S.; Deeth, R. J.; Duncalf, D. J.; McCamley, A. *Chem. Commun.* **1996**, 2623. (c) Warren, T. H.; Schrock, R. R.; Davis, W. M. *Organometallics* **1996**, *15*, 562. (d) Warren, T. H.; Schrock, R. R.; Davis, W. M. *Organometallics* **1998**, *17*, 308.

(21) Jäger, F.; Roesky, H. W.; Dorn, H.; Shah, S.; Noltemeyer, M.; Schmidt, H. G. *Chem. Ber.* **1997**, *130,* 399.

(22) Patton, J. T.; Feng, S. G.; Abboud, K. A. *Organometallics,* **2001** *20*, 3399.

(23) (a) Lee, C. H.; La, Y.-H.; Park, S. J.; Park, J. W. *Organometallics* **1998**, *17*, 3648. (b) Lee, C. H.; La, Y.-H.; Park, J. W. *Organometallics,* **2000**, *19*, 344.

(24) Nomura, K.; Naga, N.; Takaoki, K.; Imai, A. *J. Mol. Cat., Ser. A: Chemical* **1998**, *130*, L209.

(25) (a) Westmoreland, I.; Munslow, I. J.; O'Shaughnessy, P. N.; Scott, P. *Organometallics* **2003**, *22*, 2972. (b) Gountchev, T. I.; Tilley, T. D.; *Inorg. Chim. Acta* **2003**, *345*, 81.

(26) Daniele, S.; Hitchcock, P. B.; Lappert, M. F. *Chem. Commun.* **1999**, 1909.

(27) Shafir, A.; Power, M. P.; Whitener, G. D.; Arnold, J. *Organometallics,* **2001**, *20*, 1365.

(28) (a) Guérin, F.; McConville, D. H.; Vittal, J. J. *Organometallics,* **1996**, *15*, 5586. (b) Guérin, F.; McConville, D. H.; Vittal, J. J.; Yap, G. A. P. *Organometallics,* **1998**, *17*, 5172.

(29) Guérin, F.; McConville, D. H.; Payne, N. C. *Organometallics,* **1996**, *15*, 5085.

(30) Schrock, R. R.; Schattenmann, F.; Aizenberg, M.; Davis, W. M. *Chem. Commun.* **1998**, 199.

(31) Horton, A. D.; de With, J.; van der Linden, A. J.; van de Weg, H. *Organometallics,* **1996**, *15*, 2672.

(32) Schrock, R. R.; Casado, A. L.; Goodman, J. T.; Liang, L.-C.; Bonitatebus Jr., P. J.; Davis, W. M. *Organometallics,* **2000**, *19*, 5325.

(33) Liang, L.-C.; Schrock, R. R.; Davis, W. M.; McConville, D. H. *J. Am. Chem. Soc.,* **1999**, *121*, 5797.

(34) (a) Schrodi, Y.; Schrock, R. R.; Bonitatebus Jr., P. J. *Organometallics,* **2001**, *20*, 3560. (b) Schrock, R. R.; Bonitatebus Jr., P. J.; Schrodi, Y. *Organometallics,* **2001**, *20*, 1056.

(35) (a) Mehrkhodavandi, P.; Schrock, R. R. *J. Am. Chem. Soc.,* **2001**, *123*, 10746. (b) Schrock, R. R.; Adamchuk, J.; Ruhland, K.; Lopez, L. P. H. *Organometallics,* **2005**, *24*, 857.

(36) Mehrkhodavandi, P.; Schrock, R. R.; Bonitatebus Jr., P. J. *Organometallics,* **2002**, *21*, 5785.

(37) Mehrkhodavandi, P.; Schrock, R. R.; Pryor, L. L. *Organometallics,* **2003**, *22*, 4569.

(38) Schrock, R. R.; Adamchuk, J.; Ruhland, K.; Lopez, L. P. H. *Organometallics,* **2003**, *22*, 5079.

(39) Tonzetich, Z. J.; Lu, C. C.; Schrock, R. R.; Hock, A. S.; Bonitatebus Jr., P. J. *Organometallics,* **2004**, *23*, 4362.

(40) Schattenmann, F.; Schrock, R. R.; Davis, W. M. *Organometallics,* **1998**, *17*, 989.

(41) Schrock, R. R.; Baumann, R. WO 9846651 (1998).

(42) Aizenberg, M.; Turculet, L.; Davis, W. M.; Schattenmann, F.; Schrock, R. R. *Organometallics,* **1998**, *17*, 4795.

(43) (a) Baumann, R.; Davis, W. M.; Schrock, R. R. *J. Am. Chem. Soc.,* **1997**, *119*, 3830. (b) Baumann, R.; Schrock, R. R. *J. Organomet. Chem.*, **1998**, *557*, 69. (c) Liang, L.-C.; Schrock, R. R.; Davis, W. M. *Organometallics,* **2000**, *19*, 2526. (d) Goodman, J. T.; Schrock, R. R. *Organometallics,* **2001**, *20*, 5205.

(44) Baumann, R.; Stumpf, R.; Davis, W. M.; Liang, L.-C.; Schrock, R. R. *J. Am. Chem. Soc.,* **1999**, *121*, 7822.

(45) Flores, M. A.; Manzoni, M. R.; Baumann, R.; Davis, W. M.; Schrock, R. R. *Organometallics,* **1999**, *18*, 3220.

(46) Male, N. A. H.; Thornton-Pett, M.; Bochmann, M. *J. Chem. Soc., Dalt. Trans.*, **1997**, 2487.

(47) (a) Sinn, H.; Kaminsky, W.; Hoker, H., Eds. *Aluminoxanes*: Macromolecular Symposia 97; Huthig&Wepf: Heidelberg, Germany, 1995. (b) Srinivasa, R. S.; Sivaram, S. *Prog. Polym. Sci.*, **1995**, *20*, 309.

(48) Chen, E. Y.-X.; Marks, T. J. *Chem. Rev.*, **2000**, *100*, 1391.

(49) Jordan, R. F.; Dasher, W. E.; Echols, S. F. *J. Am. Chem. Soc.,* **1986**, *108*, 1718.

(50) Jordan, R. F.; Bajgur, C. S.; Willet, R.; Scott, B. *J. Am. Chem. Soc.,* **1986**, *108*, 7410.

(51) (a) Jordan, R. F.; LaPointe, R. E.; Bajgur, C. S.; Echols, S. F.; Willet, R. *J. Am. Chem. Soc.,* **1987**, *109*, 4111. (b) Jordan, R. F.; LaPointe, R. E.; Baenziger, N.; Hinch, G. D. *Organometallics,* **1990**, *9*, 1539.

(52) (a) Hlatky, G. G.; Turner, H. W.; Eckman, R. R. *J. Am. Chem. Soc.,* **1989**, *111*, 2728. (b) Crowther, D. J.; Borkowsky, S. L.; Swenson, D.; Meyer, T. Y.; Jordan, R. F. *Organometallics,* **1993**, *12*, 2897.

(53) Yang, X.; Stern, C. L.; Marks, T. J. *Organometallics,* **1991**, *10*, 840.

(54) Chien, J. C. W.; Tsai, W.-M.; Rausch, M. D. *J. Am. Chem. Soc.,* **1991**, *113*, 8570.

(55) Yang, X.; Stern, C. L.; Marks, T. J. *J. Am. Chem. Soc.,* **1991**, *113*, 3623.

(56) Green, M. L. H.; Saßmannshausen, J. *Chem. Commun.* **1999**, 115.

(57) Bochmann, M.; Lancaster, S. J. *Angew. Chem.,* **1994**, *106*, 1715.

(58) Chen, E. Y.-X.; Metz, M. V.; Li, L.; Stern, C. L.; Marks, T. J. *J. Am. Chem. Soc.,* **1998**, *120*, 6287.

(59) Boyd, C. L.; Toupance, T.; Tyrrell, B. R.; Ward, B. D.; Wilson, C. R.; Cowley, A. R.; Mountford, P. *Organometallics,* **2005**, *24*, 309.

(60) Yang, X.; Stern, C. L.; Marks, T. J. *J. Am. Chem. Soc.,* **1994**, *116*, 10015.

(61) Deck, P. A.; Marks, T. J. *J. Am. Chem. Soc.,* **1995**, *117*, 6128.

(62) Deck, P. A.; Beswik, C. L.; Marks, T. J. *J. Am. Chem. Soc.,* **1998**, *120*, 1772.

(63) Beswik, C. L.; Marks, T. J. *J. Am. Chem. Soc.,* **2000**, *122*, 10358.

(64) (a) Beswik, C. L.; Marks, T. J. *Organometallics,* **1999**, *18*, 2410. (b) Chen, M-C.; Roberts, J. A. C.; Marks, T. J. *J. Am. Chem. Soc.,* **2004**, *126*, 4605. (c) Stahl, N. G.; Salata, M. R.; Marks, T. J. *J. Am. Chem. Soc.,* **2005**, *127*, 10898.

(65) (a) Jia, L.; Yang, X.; Ishihara, A.; Marks, T. J. *Organometallics,* **1995**, *14*, 3135. (b) Jia, L.; Yang, X.; Stern, C. L.; Marks, T. J. *Organometallics,* **1997**, *16*, 842.

(66) Scollard, J. D.; McConville, D.H.; Rettig, S. J. *Organometallics,* **1997**, *16*, 1810.

(67) (a) Li, L.; Marks, T. J. *Organometallics,* **1998**, *17*, 3996. (b) Chen, M.-C.; Roberts, J. A. C.; Marks, T. J. *Organometallics,* **2004**, *23*, 932.

(68) Chen, Y.-X.; Marks, T. J. *Organometallics,* **1997**, *16*, 3649.

(69) Horton, A. D.; de With, J. *Chem. Commun.*, **1996**, 1375.

(70) Bochmann, M.; Cuenca, T.; Hardy, D. T. *J. Organomet. Chem.*, **1994**, *484*, C10.

(71) (a) Bertuleit, A.; Fritze, C.; Erker, G.; Frönlich, R. *Organometallics,* **1997**, *16*, 289. (b) Hill, M.; Erker, G.; Kehr, G.; Frönlich, R.; Kataeva, O. *J. Am. Chem. Soc.,* **2004**, *126*, 11046.

(72) Shafir, A.; Arnold, J. *J. Am. Chem. Soc.,* **2001**, *123*, 9212.

(73) Gielens, E. E. C. G.; Tiesnitsch, J. Y.; Hessen, B.; Teuben, J. H. *Organometallics,* **1998**, *17*, 1652.

(74) Bochmann, M.; Jaggar, A. J.; Nichols, J. C. A*ngew. Chem.*, **1990**, *102*, 830.

(75) Horton, A. D.; Frijns, J. H. G. A*ngew. Chem.*, **1991**, *103*, 1181.

(76) (a) Bochmann, M.; Lancaster, S. J. *Organometallics,* **1993**, *12*, 633. (b) Gillis, D. J.; Tudoret, M.-J.; Baird, M. C. *J. Am. Chem. Soc.,* **1993**, *115*, 2543. (c) Gillis, D. J.; Quyoum, R.; Tudoret, M.-J.; Wang, Q.; Jeremic, D.; Roszak, A. W.; Baird, M. C. *Organometallics,* **1996**, *15*, 3600.

(77) Schaper, F.; Geyer, A.; Brintzinger, H. H. *Organometallics,* **2002**, *21*, 473.

(78) Yang, X.; Stern, C. L.; Marks, T. J. *Organometallics,* **1991**, *10*, 840.

(79) Pellecchia, C.; Grassi, A.; Immirzi, A. *J. Am. Chem. Soc.,* **1993**, *115*, 1160.

(80) Pellecchia, C.; Immirzi, A.; Grassi, A.; Zambelli, A. *Organometallics,* **1993**, *12*, 4473.

(81) Pellecchia, C.; Immirzi, A.; Pappalardo, D.; Peluso, A. *Organometallics,* **1994**, *13*, 3773.

(82) Horton, A. D.; de With, J. *Organometallics,* **1997**, *16*, 5424.

(83) Scollard, J. D.; McConville, D.H.; Vittal, J. J. *Organometallics,* **1997**, *16*, 4415.

(84) (a) Shafir, A.; Arnold, J. *Inorg. Chim. Acta*, **2003**, *345*, 216. (b) Shafir, A.; Arnold, J. *Organometallics,* **2003**, *22*, 567.

(85) Schrock, R. R.; Baumann, R.; Reid, S. M.; Goodman, J. T.; Stumpf, R.; Davis, W. M. *Organometallics,* **1999**, *18*, 3649.

(86) Mehrkhodavandi, P.; Schrock, R. R.; Bonitatebus Jr., P. J. *J. Am. Chem. Soc.,* **2000**, *122*, 7841.

(87) (a) Stephan, D. W.; Guerin, F.; Spence, R. E. H.; Koch, L.; Gao, X.; Brown, S. J.; Swabey, J. W.; Wang, Q.; Xu, W.; Zoricak, P.; Harrison, D. G. *Organometallics,* **1999**, *18*, 2046. (b) Guerin, F.; Stewart, J. C.; Beddie, C.; Stephan, D. W. *Organometallics,* **2000**, *19*, 2994.

(88) Guerin, F.; Stephan, D. W. *Angew. Chem. Int. Ed.*, **2000**, *39*, 1298.

(89) (a) Fokken, S.; Reichwald, F.; Spaniol, T. P.; Okuda, J. *J. Organomet. Chem.*, **2002**, *663*, 158. (b) Beckerle, K.; Capacchione, C.; Ebeling, H.; Manivannan, R.; Mülhaupt, R.; Proto,

A.; Spaniol, T. P.; Okuda, J. *J. Organomet. Chem.*, **2004**, *689*, 4636. (c) Tshuva, E. Y.; Groysman, S.; Goldberg, I.; Kol, M. *Organometallics,* **2002**, *21*, 662. (d) Toupance, T.; Dubberley, S. R.; Rees, N. H.; Tyrrell, B. R.; Mountford, P. *Organometallics,* **2002**, *21*, 1367.

(90) (a) Thorn, M. G.; Etheridge, Z. C.; Fanwick, P. E.; Rothwell, I. P. *Organometallics,* **1998**, *17*, 3636. (b) Thorn, M. G.; Etheridge, Z. C.; Fanwick, P. E.; Rothwell, I. P. *J. Organomet. Chem.*, **1999**, *591*, 148.

(91) Shao, P.; Gendron, R. A. L.; Berg, D. J.; Bushnell, G. W. *Organometallics,* **2000**, *19*, 509.

(92) (a) Bei, X.; Swenson, D. C.; Jordan, R. F. *Organometallics,* **1997**, *16*, 3282. (b) Tsukahara, T.; Swenson, D. C.; Jordan, R. F. *Organometallics,* **1997**, *16*, 3303.

(93) Tjaden, E. B.; Swenson, D. C.; Jordan, R. F.; Petersen, J. L. *Organometallics,* **1995**, *14*, 371.

(94) Michaelis, A.; Schroeter, G. *Chem. Ber.*, **1894**, *27*, 490.

(95) (a) Shaw, R. A. *Phosphorus and Sulfur*, **1978**, *4*, 99. (b) Hill, T. G.; Haltiwanger, R. C.; Thompson, M. L.; Katz, S. A.; Norman, A. D. *Inorg. Chem.*, **1994**, *33*, 1770. (c) Davies, A. R.; Dronsfield, A. T.; Haszeldine, R. N.; Taylor, D. R. *J. Chem. Soc., Perkin Trans. I*, **1973**, 379. (d) Bulloch, G.; Keat, R. *J. Chem. Soc., Dalton Trans.*, **1974**, 2010. (e) Keat, R.; Rycroft, D. S.; Thompson, D. G. *J. Chem. Soc., Dalton Trans.*, **1980**, 321. (f) Bulloch, G.; Keat, R. *J. Chem. Soc., Dalton Trans.*, **1977**, 99. (g) Bulloch, G.; Keat, R. *J. Chem. Soc., Dalton Trans.*, **1977**, 1045. (h) Jefferson, R.; Nixon, J. F.; Painter, T. M.; Keat, R.; Stobbs, L. *J. Chem. Soc., Dalton Trans.*, **1973**, 1414. (i) Keat, R.; Rycroft, D. S.; Thompson, D. G. *J. Chem. Soc., Dalton Trans.*, **1979**, 1224.

(96) Silaghi-Dumitrescu, I.; Haiduc, I. *Phosphorus Sulfur Silicon*, **1994**, *91*, 21.

(97) (a) Scherer, O. J.; Andres, K. *Z. Naturforsch.*, **1978**, *33b*, 467. (b) Pohl, S. *Z. Naturforsch.*, **1979**, *34b*, 256. (c) Zeiss, W.; Weis, J. *Z. Naturforsch.*, **1977**, *32b*, 485.

(98) Stahl, L. *Coord. Chem. Rev.*, **2000**, *210*, 203 and references there.

(99) Scherer, O. J.; Klusmann, P. *Angew. Chem. Int. Ed.*, **1969**, *8*, 752.

(100) Moser, D. F.; Grocholl, L.; Stahl, L.; Staples, R. J. *J. Chem. Soc., Dalton Trans.* **2003**, 1402.

(101) (a) Reddy, N. D.; Elias, A. J.; Vij, A. *J. Chem. Soc., Dalton Trans.*, **1997**, 2167. (b) Schranz, I.; Stahl, L.; Staples, R. J. *Inorg. Chem.*, **1998**, *37*, 1493.

(102) Lappert, M. F.; Slade, M. J.; Singh, A. *J. Am. Chem. Soc.*, **1983**, *105*, 302.

(103) Bochmann, M. *Comprehensive Organometallic Chemistry II*, vol. 4, Lappert, M. F., Ed., Pergamon Press, Oxford, UK,**1995**.

(104) Huheey, J. E.; Keiter, E. A.; Keiter, R. L. *InorganicChemistry: Principles of Structure and Reactivity*, HarperCollins College Publishers, New York, 1993.

(105) Structural characteristics of Ti benzyl complexes can be found in: (a) Carpentier, J.-F.; Martin, A.; Swenson, D. C.; Jordan, R. F. *Organometallics*, **2003**, *22*, 4999. (b) Mahanthappa, M. K.; Cole, A. P.; Waymouth, R. M. *Organometallics*, **2004**, *23*, 1405. (c) Minhas, R. K.; Scoles, L.; Wong, S.; Gambarotta, S. *Organometallics*, **1996**, *15*, 1113.

(106) (a) Briand, G. G.; Chivers, T.; Krahn, M. *Coord. Chem. Rev.*, **2002,** *233-234*, 237. (b) Chivers, T.; Krahn, M.; Schatt, G. *Inorg. Chem.*, **2002**, *41*, 4348. (c) Lief, G. R.; Carrow, C. J.; Stahl, L.; Staples, R. J. *Chem. Commun.*, **2001**, 1562. (d) Chivers, T.; Fedorchuk, C.; Krahn, M.; Parvez, M.; Schatt, G. *Inorg. Chem.*, **2001**, *40*, 1936.

(107) (a) Scherer, O. J.; Schnabl, G. *Chem. Ber.*, **1976**, *109*, 2996. (b) Scherer, O. J.; Klusmann, P.; Kuhn, N. *Chem. Ber.*, **1974**, *107*, 552.

(108) Pohl, S.; Krebs, B. *Chem. Ber.*, **1977**, *110*, 3183.

(109) (a) Al-Benna, S.; Sarsfield, M. J.; Thornton-Pett, M.; Ormsby, D. L.; Maddox, P. J.; Bres, P.; Bochmann, M. *J. Chem. Soc., Dalton Trans.* **2000**, 4247. (b) Bochmann, M.; Sarsfield, M. J. US Patent WO 2000047592.

(110) For the information about Brookhart's complexes see: Ittel, S. D.; Johnson, L. K.; Brookhart, M. *Chem. Rev.*, **2000**, *100*, 1169.

(111) For oligomerization of olefins see (a) Vogt, D. *Applied Homogeneous Catalysis with Organometallic Compounds*; Cornils, B.; Herrmann, W. A., Eds.; VCH: Weinheim, New York, Basel, Cambridge, Tokyo, 1996; Vol. 1, p. 245. Dimerization of olefins see (b) Chauvin, Y.; Olivier, H. *Applied Homogeneous Catalysis with Organometallic Compounds*; Cornils, B.; Herrmann, W. A., Eds.; VCH: Weinheim, New York, Basel, Cambridge, Tokyo, 1996; Vol. 1, p. 258 and references there. (c) Pillai, S. M.; Ravindranathan, M.; Sivaram, S. *Chem. Rev.*, **1986**, *86*, 353.

(112)(a) Keim, W. *Fundamental Research in Homogeneous Catalysis;* Graziani, M., Eds.; Plenum: New York, 1984; Vol. 4, p.131. (b) Lutz, E. F. *J. Chem. Educ.*, **1986**, *63*, 202. (c) Baur, S. R.; Chung, H.; Glockner, P. W.; Keim, W.; van Zwet, H. US patent 3635937 (1972). (d) Keim, W. *New J. Chem.*, **1987**, *11*, 531.

(113) (a) Bogärt, S.; Chenal, T.; Mortreux, A.; Nowogorcki, G.; Lehmann, W. C.; Carpentier, J.-F. *Organometallics,* **2001**, *20*, 199. (b) Hungenrg, K.-D.; Kerth, J.; Langhauser, F.; Müller, H.-J.; Müller, P. *Angew. Makromol. Chem.,* **1995**, *227*, 159.

(114) (a) Killian, C. M.; Johnson, L. K.; Brookhart, M. *Organometallics,* **1997**, *16*, 2005. (b) Svejda, S. A.; Brookhart, M. *Organometallics,* **1999**, *18*, 65.

(115) (a) Small, B. L.; Carney, M. J.; Holman, D. M.; O'Rourke, C. E.; Halfen, J. A. *Macromolecules,* **2004**, *37*, 4375. (b) Small, B. L.; Brookhart, M. *J. Am. Chem. Soc.,* **1998**, *120*, 7143. (c) Tellmann, K. P.; Cibson, V. G.; White, A. J. P.; Williams, D. J. *Organometallics,* **2005**, *24*, 280.

(116) (a) Speiser, F.; Braunstein, P. *Organometallics,* **2004**, *23*, 2633. (b) Speiser, F.; Braunstein, P. *Organometallics,* **2004**, *23*, 2625.

(117) Heinicke, J.; Köhler, M.; Peulecke, N.; Keim, W. *J. Cat.*, **2004**, *225*, 16.

(118) For the olefin oligomerization review see Scupiňska, J. *Chem. Rev.*, **1991**, *91*, 613. Parshal, G. W., Ittel, S. D., *Homogeneous Catalysis; The Application and Chemistry of Catalysis by Soluble Transition Metal Complexes*; John Wiley&Sons, Inc.: New York, Chichester, Brisbane, Toronto, Singapore, **1992**; p.12.